UCSF
UC San Francisco Electronic Theses and Dissertations

Title
Genetic regulation of prefrontal cortex development

Permalink
https://escholarship.org/uc/item/87m24694

Author
Cholfin, Jeremy Adam

Publication Date
2007-04-02

Peer reviewed|Thesis/dissertation

eScholarship.org Powered by the California Digital Library
University of California

Genetic regulation of prefrontal cortex development

by

Jeremy A. Cholfin

DISSERTATION

Submitted in partial satisfaction of the requirements for the degree of

DOCTOR OF PHILOSOPHY

in

Neuroscience

in the

GRADUATE DIVISION

of the

Dedication and Acknowledgements

First and foremost, I would like to thank and dedicate my thesis to my family, including my mom and dad, brothers Evan and Zach, and my wonderful wife Tania, who have provided an immeasurable amount of support during what would otherwise have been an insurmountable period of my life.

I thank my advisor John L.R. Rubenstein for challenging me in ways I never thought possible, for supporting my research, and for working closely with me throughout my years in his laboratory. His door was always open to me and his sense of humor often was key to levity during both intense and tense moments.

My thesis committee members have been a great source of support. Peter Ohara, my committee chairman deserves particular credit for many meetings with me over coffee (often at his expense). Ben Cheyette, Sam Pleasure, Patricia Janak, and Andy Peterson have all provided important scientific insight and moral support, helping to guide my work.

Members of the Rubenstein laboratory both past and present deserve special credit for their invaluable scientific and technical expertise, discussions, and friendships: Andrea Faedo, Bei Wang, Carol Kim, Cathy Dye, Christian Wong, Cindy Yee, Dianna Kahn, Greg Potter, Inma Cobos, Jason Long, Juhee Jeong, Kelly Huffman, Magda Petryniak, Mario Maira, Oscar Marin, Pierre Fladin-Blety, Renee Hoch, Sonia Garel, Ugo Borello, Yanling Wang, and Youlin Ruan. Additionally, I would like to thank members of the Tecott lab, Miles Berger and Gerard Honig, for insightful discussions and moral support.

I would like to thank my collaborators, who added a very important dimension to my research and facilitated my interest in the neurobiology of behavior: Kimberly Scearce-Levie, Erik Roberson, Lennart Mucke, Nirao Shah, Irene Merzlyak, and Patricia Janak.

Bruce Miller has provided a level of mentorship, support and encouragement that has inspired me to pursue my interests and taught me the importance of being an inspiration to others.

Finally, I would like to thank Pat Veitch, Jana Toutolmin, and Catherine Norton for making sure that I stayed afloat while navigating the stormy ocean that is the academic world.

This work was supported by the Medical Scientist Training Program and Neuroscience Graduate Program, School of Medicine, University of California, San Francisco.

Genetic Regulation of Prefrontal Cortex Development

Jeremy A. Cholfin

The prefrontal cortex (PFC) has been called "the organ of civilization" (Luria). The most anterior part of cerebral cortex, the PFC consists of multiple areas that mediate a wide range of higher-order behaviors in mammals. Despite years of intensive neuroanatomical and functional studies, little is known about the genetic mechanisms that pattern this structure during development. It has been recognized that fibroblast growth factor (FGF) signaling from the rostral patterning center could have a central role in regulating rostral telencephalic development. A subset of FGF genes are expressed in the rostral patterning center in the embryonic telencephalon. Recent evidence shows that FGFs regulate the graded expression of regulatory genes (i.e. *Emx2*) in the cortical neuroepithelium, which may specify the initial distribution of PFC regional subdivisions and ultimately mature areas. I have devised a novel panel of gene expression markers to study the roles of *Fgf17* and *Fgf8*, and genetic interactions between *Fgf17* and *Emx2* in patterning the frontal cortex. In addition, I have identified signaling mechanisms and genetic interactions during early forebrain development that may contribute to the postnatal regionalization phenotypes. Finally, I have initiated behavioral studies through collaborations with other laboratories to investigate higher-order behaviors that are dependent on intact PFC function. I have found that *Fgf17*, *Fgf8* and *Emx2* each play unique roles in the early regionalization of the PFC, and that *Fgf17* and *Emx2* specifically interact on the genetic level to regulate this process. In addition, *Fgf17* mutant mice exhibit circumscribed deficits in social behavior and associated selective hypo-activation

of the dorsal PFC. These studies reveal that the organization of subdivisions within a higher-order cortical area is partially under genetic control, and suggest that mispatterning of the PFC via genetic mutation may contribute to abnormal behavior.

Table of Contents

1) Introduction……. p. 1

2) Patterning of frontal cortex subdivisions by *Fgf17*……. p. 15

3) *Fgf17* and *Emx2* antagonistic interactions pattern frontal cortex subdivisions... p. 55

4) Conclusion……... p. 104

5) Appendix: Behavioral and neural activation studies in *Fgf17*$^{-/-}$ mutants.....……p. 106

Chapter 1

Introduction: FGF signaling and the prefrontal cortex

The cerebral cortex is a highly ordered brain structure consisting of a sheet of over a billion neurons that mediates cognition and behavior. Along its longitudinal dimension, the cortical sheet is organized into histologically discrete areas that emerge gradually during embryonic and postnatal development. The process of cortical arealization has been an area of intense investigation over the past two decades. Two models that are now largely viewed as complementary have arisen to account for this process. The protomap model explains arealization in terms of the early specification of neural precursors in the neuroepithelium that give rise to the cerebral cortex (Rakic, 1988). By contrast, the protocortex model suggests that extrinsic (i.e. thalamocortical) input imparts areal characteristics onto an otherwise "blank slate" cortex (O'Leary, 1989). Accumulating evidence within the last several years has identified key genetic and non-genetic factors that regulate cortical arealization, suggesting that complex interactions between intrinsic and extrinsic mechanisms regulate this process (O'Leary and Nakagawa, 2002; Grove and Fukuchi-Shimogori, 2003; Sur and Rubenstein, 2005).

Prior to and after the arrival of thalamocortical afferents, the main source of input to the cortex, a subset of genes are expressed in graded and coarse areal patterns within the cortical progenitor zone and emergent cortical plate (Nakagawa et al., 1999; Rubenstein et al., 1999). Genetic removal of thalamocortical input results in the establishment and maintenance of normal patterns of areal gene expression, providing

strong evidence that early regionalization of the cortex occurs independent of thalamic input (Miyashita-Lin et al., 1999; Nakagawa et al., 1999). Therefore, research over the last several years has been focused on identifying genes that specify regional identity of neural progenitors and thereby contribute to cortical arealization.

FGF signaling and cortical patterning

A current model of forebrain patterning suggests that FGF signaling from a rostral source (the rostral patterning center), imparts positional information onto the adjacent neuroepithelium by regulating the expression of transcription factors and other regulatory molecules (O'Leary and Nakagawa, 2002; Grove and Fukuchi-Shimogori, 2003; Sur and Rubenstein, 2005). The initial forebrain pattern is regulated by interactions between FGFs (in particular Fgf8) from the rostral patterning center and two other centers: the dorsal midline, which expresses members of the bone morphogenic protein (*BMP*) and *Wnt* family of genes, and the ventral midline, which expresses Shh (Shimamura et al., 1997; Shimamura and Rubenstein, 1997; Crossley et al., 2001; Shimogori et al., 2004; Sur and Rubenstein, 2005; Storm et al., 2006). *Fgf8* exhibits dosage-dependent functions in early forebrain patterning through regulation of neural specification, progenitor proliferation and cell death (Storm et al., 2003; Storm et al., 2006). *Fgf8* has similar functions in zebrafish (Shanmugalingam et al., 2000). It is unclear from these studies to what extent the neural specification function is dissociable from proliferative and apoptotic mechanisms, and whether these functions can be attributed directly to reduced *FGF* signaling, versus indirect interactions with the other patterning centers.

A nested set of FGF genes are expressed in and around the rostral patterning center: *Fgf8*, *Fgf18*, *Fgf17* and *Fgf15* (Crossley and Martin, 1995; Maruoka et al., 1998; Xu et al., 1999; Bachler and Neubuser, 2001). The nested expression patterns may indicate that FGFs operate hierarchically by regulating the expression of other FGFs in an adjacent zone. However, the regulatory relationships among the rostral patterning center-expressed FGFs are unknown. We have been examining the requirements of these FGFs for the expression of the others using loss-of-function mutant mice for *Fgf8*, *Fgf17* and *Fgf15*. We have found that *Fgf8* expression does not depend on *Fgf17*, while *Fgf17* expression is regulated by *Fgf8* in a dosage-dependent manner (Cholfin, Borello and Rubenstein, unpublished data).

FGF receptors (FGFRs) are receptor tyrosine kinases that are expressed in the cortical neuroepithelium and lead to the activation of the mitogen-activated protein kinase (MAPK) and phosphotidylinositol-3-kinase (PI3K) signaling pathways (Orr-Urtreger et al., 1991; Peters et al., 1992; Peters et al., 1993; Cobb and Goldsmith, 1995; Klint and Claesson-Welsh, 1999; Ornitz, 2000; Shinya et al., 2001; Hebert et al., 2003). This suggests that rostral patterning center FGFs may signal to cortical progenitors directly. FGFRs participate in patterning the telencephalon, including the olfactory bulb and ventral forebrain (Hebert et al., 2003; Gutin et al., 2006). Attenuated forebrain FGFRI signaling has been reported to result in loss of glutamateric pyramidal neurons in the frontal and temporal cortex (Shin et al., 2004). Microarray analysis of the *FgfR1* mutant cortical primordium suggests that FGFRI may be the key receptor that mediates Fgf8 signaling in the telencephalon *in vivo* (Sansom et al., 2005). We and other groups have recently demonstrated that the MAPK pathway is a target of Fgf8 signaling in the

dorsal forebrain (E. Grove laboratory and Borello, Cholfin and Rubenstein, unpublished data). Evidence in zebrafish indicates that the MAPK pathway participates in patterning the subpallial telencephalon (Shinya et al., 2001), but the functional contribution of the MAPK signaling pathway to cortical patterning remains to be tested.

Fgf8 signaling induces the expression of several genes, including those that encode the ETS transcription factors Erm, Er81 and Pea3 (Fukuchi-Shimogori and Grove, 2003). FGF signaling through Erm and Pea3 has been found to regulate tendon progenitor specification in somite development (Brent and Tabin, 2004), suggesting that this genetic pathway plays a role in cell-type specification. *Erm* knockout mice fail to maintain a niche for sperm stem cells leading to progressive germ-cell depletion (Chen et al., 2005), indicating that *Erm* could be important for stem cell maintenance. We have found that *Erm* and *Pea3* are highly expressed in the frontal cortex neuroepithelium and that *Fgf17* regulates their expression (Cholfin and Rubenstein, unpublished data), suggesting that these transcription factors play a role in regionalization of the frontal cortex. Fgf8 also positively regulates the expression of the general receptor tyrosine kinase signaling inhibitors Sprouty1 and 2 (Fukuchi-Shimogori and Grove, 2001, 2003; Storm et al., 2003), which suggests that negative feedback may regulate the extent of FGF signaling. It appears that *Fgf8* and *Fgf17* have a differential ability to regulate Sprouty expression in the forebrain (Cholfin and Rubenstein, unpublished data), consistent with previous studies of *Fgf8* and *Fgf17* in the mid-hindbrain patterning center (Liu et al., 2003).

By contrast, Fgf8 represses expression of *Emx2* and *COUP-TF1* in the cortical neuroepithelium (Crossley et al., 2001; Fukuchi-Shimogori and Grove, 2003; Garel et al.,

2003), two transcription factors with important roles in cortical patterning and arealization (Bishop et al., 2000; Mallamaci et al., 2000; Zhou et al., 2001; O'Leary and Rubenstein, unpublished data). Unlike *Fgf8*, *Fgf17* appears not to have a major effect on gradients of these factors (Cholfin and Rubenstein, unpublished data), suggesting that *Fgf17* may act more selectively to control regional properties of the frontal cortex.

Complementary gain and loss-of-function experiments point to a critical role for *Fgf8* in neocortical patterning and arealization (Fukuchi-Shimogori and Grove, 2001, 2003; Garel et al., 2003). For example, $Fgf8^{neo/neo}$ mild hypomorphic mutants exhibit rostral shifts in gradients of *Emx2* and *COUP-TF1* in the cortical neuroepithelium that correlate with reduced frontal cortex size and expanded caudal cortical regions (Garel et al., 2003). Ectopic expression of *Fgf8* in the caudal cortical primordium results in partial duplications of the somatosensory cortex, suggesting that *Fgf8* acts as a true neocortical patterning signal (Fukuchi-Shimogori and Grove, 2001). Although the initial pattern of thalamocortical connectivity is not affected in newborn $Fgf8^{neo/neo}$ mutants (Garel et al., 2003), *Fgf8* can regulate neocortical cues that guide area-specific thalamic innervation postnatally (Shimogori and Grove, 2005). *Fgf8* appears to regulate the early intracortical wiring pattern, another aspect of cortical arealization (Huffman et al., 2004). Finally, FGF signaling is essential for the crossing of dorsal telencephalic midline commissures (Shanmugalingam et al., 2000; Huffman et al., 2004; Smith et al., 2006).

Emx2, which is expressed in a high-caudomedial to low rostrolateral gradient in the cortical primordium (Simeone et al., 1992; Gulisano et al., 1996), regulates neocortical arealization in a direction opposite of *Fgf8*. *Emx2* mutant mice ($Emx2^{-/-}$) have reduced caudal and expanded rostral cortical areas (Bishop et al., 2000; Mallamaci et al.,

2000; Bishop et al., 2002), defects that were rescued by reducing FGF signaling (Fukuchi-Shimogori and Grove, 2003). By contrast, over-expression of *Emx2* in neural progenitors results in expanded caudal and reduced rostral areas, despite normal *Fgf8* expression (Hamasaki et al., 2004). Therefore, *Emx2* may regulate cortical arealization both by repressing *Fgf8* expression and by direct specification of neural progenitors (Fukuchi-Shimogori and Grove, 2003; Hamasaki et al., 2004). However, genetic interactions between endogenous FGF signaling and *Emx2* in cortical patterning have not yet been explored.

Much less is known about the roles of other FGFs that are expressed in the rostral patterning center in cortical arealization. Although *Fgf17* over-expression was reported to have effects similar to *Fgf8* in neocortical patterning (Fukuchi-Shimogori and Grove, 2003), the role of endogenous *Fgf17* in cortical development has not been studied. *Fgf17* mutant mice (*Fgf17*-/-) have a small anterior cerebellar vermis and inferior colliculus, but no reported forebrain phenotype (Xu et al., 2000). *Fgf8* and *Fgf17* have different effects on mid-hindbrain patterning, which may result from differences in their spatiotemporal expression patterns, ligand-receptor affinity and/or ability to regulate downstream gene expression (Xu et al., 2000; Liu et al., 2003; Olsen et al., 2006). Therefore, it is reasonable to hypothesize that *Fgf8* and *Fgf17* may have overlapping, but distinct roles in neocortical development.

Focusing on the PFC

Virtually all of the previous work in cortical arealization has focused on relatively large territories within the cerebral cortex (i.e. frontal, parietal, occipital), mainly due to a lack of early markers that distinguish subdivisions within a given cortical region. Do such markers exist? How are individual subdivisions of an area altered in the context of mutations in genes involved in cortical patterning? Here, I focus on subdivisions of the frontal cortex (FC), in particular the prefrontal cortex (PFC) (Chapter 2), because of its involvement in a range of important higher cognitive, motor and behavioral functions, largely unexplored development, and possible relevance to neurodevelopmental disorders.

In adult rodents, the PFC was originally described as the projection zone of the thalamic mediodorsal nucleus (Krettek and Price, 1977; Guldin et al., 1981) and can be divided into medial and orbital regions that are thought to have homologs in primate species (Uylings and van Eden, 1990; Zilles and Wree, 1995; Ongur and Price, 2000; Heidbreder and Groenewegen, 2003; Uylings et al., 2003; Dalley et al., 2004). The medial PFC is subdivided into dorsal (frontal association, anterior cingulate and prelimbic) and ventral (infralimbic and medial orbital) areas, while the orbital cortex is subdivided into ventral, lateral, dorsolateral and ventrolateral orbital areas.

The connectivity of the PFC follows most of the same general organizational principles as the six-layer neocortex: intracortical projections arise from layers II/III; subcortical projections to the striatum, brainstem and spinal cord layer arise from layer V; and thalamic efferents arise from layer VI. The notable exception is that the rodent PFC lacks a well-developed granular layer (layer IV), which normally receives afferents fibers

from the thalamus. Instead, in the PFC thalamocortical axons terminate principally in layer III (Krettek and Price, 1977; Zilles and Wree, 1995).

The PFC as a whole is involved in higher order regulation of cognition and behavior (Fuster, 2001; Miller and Cohen, 2001). However, accumulating evidence indicates that dorsal and ventral PFC each mediates distinct functions. The dorsal PFC is involved in working memory, executive function, response selection, temporal processing of information, effort-related decision making and social valuation, while ventral and orbital PFC is implicated in behavioral flexibility, emotional regulation, delay-related decision making, evaluation of rewards and autonomic control (Goldman-Rakic, 1996; Heidbreder and Groenewegen, 2003; Uylings et al., 2003; Dalley et al., 2004; Amodio and Frith, 2006; Kellendonk et al., 2006; Mitchell et al., 2006; Price, 2006; Rudebeck et al., 2006a; Rudebeck et al., 2006b). Defining how unique territories within the rodent PFC contribute to behavior is an area of intense investigation (Kolb and Robbins, 2003). Currently, there is a lack of genetic mouse models that have selective dysfunction of PFC subdivisions.

The accepted anatomical subdivisions of the PFC are based on relatively subtle cytoarchitectonic characteristics (Krettek and Price, 1977; Zilles and Wree, 1995) that emerge gradually during postnatal development. Therefore, it is difficult to distinguish subdivisions earlier in development, which would be required to interpret regionalization in the context of patterning mutants that die perinatally. It is currently unknown whether a subset of genes, which could be used to demarcate subdivisions, is regionally expressed within the early FC.

Therefore, I initially focused on defining a novel panel of gene expression markers in the newborn (postnatal day 0 – P0) mouse brain (Chapter 2). None of the genes were expressed exclusively in only one PFC subdivision (note – our analysis also includes motor cortex and rostral parts of the somatosensory cortex). However, all of them were expressed in regional patterns. A subset had sharp expression borders, which were useful in mapping genetically-defined boundaries that we propose delineate PFC subdivisions. Subsequent comparison with anatomically-defined subdivisions (Zilles and Wree, 1995) indicated a remarkable correlation with mature PFC areas. These results provide evidence for a genetic partitioning of the PFC that precedes overt cytoarchitectonic differentiation.

I then used this gene expression panel to determine how individual PFC subdivisions are altered in *Fgf17*$^{-/-}$ mice, in addition to studying effects on caudal cortical regions and connectivity (Chapter 2). Unexpectedly, I found that *Fgf17*$^{-/-}$ mice have reduced size and medially-shifted positions of dorsal PFC subdivisions, while ventral PFC subdivisions are normal. The reduced dorsal PFC is complemented by a rostral shift of caudal cortical areas, suggesting that the phenotype may be due to a defect in patterning. These regionalization changes persisted into adulthood. Although no qualitative changes in the pathfinding properties of PFC axons were apparent, we found evidence for a quantitative reduction in projections to the dorsolateral striatum and ventral midbrain, consistent with the reduced dorsal PFC.

To gain further insight into genetic control of PFC regionalization, I studied *Fgf8* hypomorphic (*Fgf8*$^{n/n}$), *Fgf17* null (*Fgf17*$^{-/-}$), *Emx2* null (*Emx2*$^{-/-}$) and *Emx2-Fgf17* double mutants (*Emx2*$^{-/-}$*;Fgf17*$^{-/-}$) (Chapter 3). I found that *Fgf8*, *Fgf17*, and *Emx2* differentially

regulate gene expression in the cortical primordium and PFC regionalization. These results suggest that *Fgf17* and *Emx2* may control PFC regionalization by antagonistically regulating the expression of transcription factors *Erm*, *Pea3* and *Er81* in the rostral cortical primordium.

What are the functional consequences of abnormal frontal cortex patterning? Recently, mutations in a G-protein coupled receptor (GPR56) were identified in human patients with bilateral fronto-parietal polymicrogyria (BFPP), a cortical malformation disorder that selectively affects the frontal lobes (Piao et al., 2004). Patients with BFPP exhibit cognitive and motor dysfunction, consistent with abnormal frontal cortex function (Chang et al., 2003). Mouse *Gpr56* is expressed in the cortical progenitor zones, but not in the cortical plate, suggesting abnormal specification as a potential mechanism for the regionally-selective defects (Piao et al., 2004).

It has been hypothesized that a mouse with frontal cortex hypoplasia due to a weakened FGF signaling center may exhibit 'hypofrontal' behaviors (Sur and Rubenstein, 2005). Therefore I have initiated collaborations to examine behaviors that are associated with decreased frontal cortex function, ranging from motor function to higher order cognitive and social behaviors (Appendix). We have identified a set of social deficits and an associated reduction in dorsal PFC activation in *Fgf17*$^{-/-}$ mice (Scearce-Levie, Roberson, Cholfin, Shah, Rubenstein and Mucke, unpublished data), providing evidence for functional consequences of reduced rostral patterning center FGF signaling during development.

REFERENCES

Amodio DM, Frith CD (2006) Meeting of minds: the medial frontal cortex and social cognition. Nat Rev Neurosci 7:268-277.

Bachler M, Neubuser A (2001) Expression of members of the Fgf family and their receptors during midfacial development. Mech Dev 100:313-316.

Bishop KM, Goudreau G, O'Leary DD (2000) Regulation of area identity in the mammalian neocortex by Emx2 and Pax6. Science 288:344-349.

Bishop KM, Rubenstein JL, O'Leary DD (2002) Distinct actions of Emx1, Emx2, and Pax6 in regulating the specification of areas in the developing neocortex. J Neurosci 22:7627-7638.

Brent AE, Tabin CJ (2004) FGF acts directly on the somitic tendon progenitors through the Ets transcription factors Pea3 and Erm to regulate scleraxis expression. Development 131:3885-3896.

Chang BS, Piao X, Bodell A, Basel-Vanagaite L, Straussberg R, Dobyns WB, Qasrawi B, Winter RM, Innes AM, Voit T, Grant PE, Barkovich AJ, Walsh CA (2003) Bilateral frontoparietal polymicrogyria: clinical and radiological features in 10 families with linkage to chromosome 16. Ann Neurol 53:596-606.

Chen C, Ouyang W, Grigura V, Zhou Q, Carnes K, Lim H, Zhao GQ, Arber S, Kurpios N, Murphy TL, Cheng AM, Hassell JA, Chandrashekar V, Hofmann MC, Hess RA, Murphy KM (2005) ERM is required for transcriptional control of the spermatogonial stem cell niche. Nature 436:1030-1034.

Cobb MH, Goldsmith EJ (1995) How MAP kinases are regulated. J Biol Chem 270:14843-14846.

Crossley PH, Martin GR (1995) The mouse Fgf8 gene encodes a family of polypeptides and is expressed in regions that direct outgrowth and patterning in the developing embryo. Development 121:439-451.

Crossley PH, Martinez S, Ohkubo Y, Rubenstein JL (2001) Coordinate expression of Fgf8, Otx2, Bmp4, and Shh in the rostral prosencephalon during development of the telencephalic and optic vesicles. Neuroscience 108:183-206.

Dalley JW, Cardinal RN, Robbins TW (2004) Prefrontal executive and cognitive functions in rodents: neural and neurochemical substrates. Neurosci Biobehav Rev 28:771-784.

Fukuchi-Shimogori T, Grove EA (2001) Neocortex patterning by the secreted signaling molecule FGF8. Science 294:1071-1074.

Fukuchi-Shimogori T, Grove EA (2003) Emx2 patterns the neocortex by regulating FGF positional signaling. Nat Neurosci 6:825-831.

Fuster JM (2001) The prefrontal cortex--an update: time is of the essence. Neuron 30:319-333.

Garel S, Huffman KJ, Rubenstein JL (2003) Molecular regionalization of the neocortex is disrupted in Fgf8 hypomorphic mutants. Development 130:1903-1914.

Goldman-Rakic PS (1996) Regional and cellular fractionation of working memory. Proc Natl Acad Sci U S A 93:13473-13480.

Grove EA, Fukuchi-Shimogori T (2003) Generating the cerebral cortical area map. Annu Rev Neurosci 26:355-380.

Guldin WO, Pritzel M, Markowitsch HJ (1981) Prefrontal cortex of the mouse defined as cortical projection area of the thalamic mediodorsal nucleus. Brain Behav Evol 19:93-107.
Gulisano M, Broccoli V, Pardini C, Boncinelli E (1996) Emx1 and Emx2 show different patterns of expression during proliferation and differentiation of the developing cerebral cortex in the mouse. Eur J Neurosci 8:1037-1050.
Gutin G, Fernandes M, Palazzolo L, Paek H, Yu K, Ornitz DM, McConnell SK, Hebert JM (2006) FGF signalling generates ventral telencephalic cells independently of SHH. Development 133:2937-2946.
Hamasaki T, Leingartner A, Ringstedt T, O'Leary DD (2004) EMX2 regulates sizes and positioning of the primary sensory and motor areas in neocortex by direct specification of cortical progenitors. Neuron 43:359-372.
Hebert JM, Lin M, Partanen J, Rossant J, McConnell SK (2003) FGF signaling through FGFR1 is required for olfactory bulb morphogenesis. Development 130:1101-1111.
Heidbreder CA, Groenewegen HJ (2003) The medial prefrontal cortex in the rat: evidence for a dorso-ventral distinction based upon functional and anatomical characteristics. Neurosci Biobehav Rev 27:555-579.
Huffman KJ, Garel S, Rubenstein JL (2004) Fgf8 regulates the development of intra-neocortical projections. J Neurosci 24:8917-8923.
Kellendonk C, Simpson EH, Polan HJ, Malleret G, Vronskaya S, Winiger V, Moore H, Kandel ER (2006) Transient and selective overexpression of dopamine D2 receptors in the striatum causes persistent abnormalities in prefrontal cortex functioning. Neuron 49:603-615.
Klint P, Claesson-Welsh L (1999) Signal transduction by fibroblast growth factor receptors. Front Biosci 4:D165-177.
Kolb B, Robbins T (2003) The rodent prefrontal cortex. Behav Brain Res 146:1-2.
Krettek JE, Price JL (1977) The cortical projections of the mediodorsal nucleus and adjacent thalamic nuclei in the rat. J Comp Neurol 171:157-191.
Liu A, Li JY, Bromleigh C, Lao Z, Niswander LA, Joyner AL (2003) FGF17b and FGF18 have different midbrain regulatory properties from FGF8b or activated FGF receptors. Development 130:6175-6185.
Mallamaci A, Muzio L, Chan CH, Parnavelas J, Boncinelli E (2000) Area identity shifts in the early cerebral cortex of Emx2-/- mutant mice. Nat Neurosci 3:679-686.
Maruoka Y, Ohbayashi N, Hoshikawa M, Itoh N, Hogan BL, Furuta Y (1998) Comparison of the expression of three highly related genes, Fgf8, Fgf17 and Fgf18, in the mouse embryo. Mech Dev 74:175-177.
Miller EK, Cohen JD (2001) An integrative theory of prefrontal cortex function. Annu Rev Neurosci 24:167-202.
Mitchell JP, Macrae CN, Banaji MR (2006) Dissociable medial prefrontal contributions to judgments of similar and dissimilar others. Neuron 50:655-663.
Miyashita-Lin EM, Hevner R, Wassarman KM, Martinez S, Rubenstein JL (1999) Early neocortical regionalization in the absence of thalamic innervation. Science 285:906-909.

Nakagawa Y, Johnson JE, O'Leary DD (1999) Graded and areal expression patterns of regulatory genes and cadherins in embryonic neocortex independent of thalamocortical input. J Neurosci 19:10877-10885.
O'Leary DD (1989) Do cortical areas emerge from a protocortex? Trends Neurosci 12:400-406.
O'Leary DD, Nakagawa Y (2002) Patterning centers, regulatory genes and extrinsic mechanisms controlling arealization of the neocortex. Curr Opin Neurobiol 12:14-25.
Olsen SK, Li JY, Bromleigh C, Eliseenkova AV, Ibrahimi OA, Lao Z, Zhang F, Linhardt RJ, Joyner AL, Mohammadi M (2006) Structural basis by which alternative splicing modulates the organizer activity of FGF8 in the brain. Genes Dev 20:185-198.
Ongur D, Price JL (2000) The organization of networks within the orbital and medial prefrontal cortex of rats, monkeys and humans. Cereb Cortex 10:206-219.
Ornitz DM (2000) FGFs, heparan sulfate and FGFRs: complex interactions essential for development. Bioessays 22:108-112.
Orr-Urtreger A, Givol D, Yayon A, Yarden Y, Lonai P (1991) Developmental expression of two murine fibroblast growth factor receptors, flg and bek. Development 113:1419-1434.
Peters K, Ornitz D, Werner S, Williams L (1993) Unique expression pattern of the FGF receptor 3 gene during mouse organogenesis. Dev Biol 155:423-430.
Peters KG, Werner S, Chen G, Williams LT (1992) Two FGF receptor genes are differentially expressed in epithelial and mesenchymal tissues during limb formation and organogenesis in the mouse. Development 114:233-243.
Piao X, Hill RS, Bodell A, Chang BS, Basel-Vanagaite L, Straussberg R, Dobyns WB, Qasrawi B, Winter RM, Innes AM, Voit T, Ross ME, Michaud JL, Descarie JC, Barkovich AJ, Walsh CA (2004) G protein-coupled receptor-dependent development of human frontal cortex. Science 303:2033-2036.
Price JL (2006) Prefrontal cortex. Boca Raton: CRC Press.
Rakic P (1988) Specification of cerebral cortical areas. Science 241:170-176.
Rubenstein JL, Anderson S, Shi L, Miyashita-Lin E, Bulfone A, Hevner R (1999) Genetic control of cortical regionalization and connectivity. Cereb Cortex 9:524-532.
Rudebeck PH, Buckley MJ, Walton ME, Rushworth MF (2006a) A role for the macaque anterior cingulate gyrus in social valuation. Science 313:1310-1312.
Rudebeck PH, Walton ME, Smyth AN, Bannerman DM, Rushworth MF (2006b) Separate neural pathways process different decision costs. Nat Neurosci 9:1161-1168.
Sansom SN, Hebert JM, Thammongkol U, Smith J, Nisbet G, Surani MA, McConnell SK, Livesey FJ (2005) Genomic characterisation of a Fgf-regulated gradient-based neocortical protomap. Development 132:3947-3961.
Shanmugalingam S, Houart C, Picker A, Reifers F, Macdonald R, Barth A, Griffin K, Brand M, Wilson SW (2000) Ace/Fgf8 is required for forebrain commissure formation and patterning of the telencephalon. Development 127:2549-2561.
Shimamura K, Rubenstein JL (1997) Inductive interactions direct early regionalization of the mouse forebrain. Development 124:2709-2718.

Shimamura K, Martinez S, Puelles L, Rubenstein JL (1997) Patterns of gene expression in the neural plate and neural tube subdivide the embryonic forebrain into transverse and longitudinal domains. Dev Neurosci 19:88-96.
Shimogori T, Grove EA (2005) Fibroblast growth factor 8 regulates neocortical guidance of area-specific thalamic innervation. J Neurosci 25:6550-6560.
Shimogori T, Banuchi V, Ng HY, Strauss JB, Grove EA (2004) Embryonic signaling centers expressing BMP, WNT and FGF proteins interact to pattern the cerebral cortex. Development 131:5639-5647.
Shin DM, Korada S, Raballo R, Shashikant CS, Simeone A, Taylor JR, Vaccarino F (2004) Loss of glutamatergic pyramidal neurons in frontal and temporal cortex resulting from attenuation of FGFR1 signaling is associated with spontaneous hyperactivity in mice. J Neurosci 24:2247-2258.
Shinya M, Koshida S, Sawada A, Kuroiwa A, Takeda H (2001) Fgf signalling through MAPK cascade is required for development of the subpallial telencephalon in zebrafish embryos. Development 128:4153-4164.
Simeone A, Gulisano M, Acampora D, Stornaiuolo A, Rambaldi M, Boncinelli E (1992) Two vertebrate homeobox genes related to the Drosophila empty spiracles gene are expressed in the embryonic cerebral cortex. Embo J 11:2541-2550.
Smith KM, Ohkubo Y, Maragnoli ME, Rasin MR, Schwartz ML, Sestan N, Vaccarino FM (2006) Midline radial glia translocation and corpus callosum formation require FGF signaling. Nat Neurosci 9:787-797.
Storm EE, Rubenstein JL, Martin GR (2003) Dosage of Fgf8 determines whether cell survival is positively or negatively regulated in the developing forebrain. Proc Natl Acad Sci U S A 100:1757-1762.
Storm EE, Garel S, Borello U, Hebert JM, Martinez S, McConnell SK, Martin GR, Rubenstein JL (2006) Dose-dependent functions of Fgf8 in regulating telencephalic patterning centers. Development 133:1831-1844.
Sur M, Rubenstein JL (2005) Patterning and plasticity of the cerebral cortex. Science 310:805-810.
Uylings HB, van Eden CG (1990) Qualitative and quantitative comparison of the prefrontal cortex in rat and in primates, including humans. Prog Brain Res 85:31-62.
Uylings HB, Groenewegen HJ, Kolb B (2003) Do rats have a prefrontal cortex? Behav Brain Res 146:3-17.
Xu J, Liu Z, Ornitz DM (2000) Temporal and spatial gradients of Fgf8 and Fgf17 regulate proliferation and differentiation of midline cerebellar structures. Development 127:1833-1843.
Xu J, Lawshe A, MacArthur CA, Ornitz DM (1999) Genomic structure, mapping, activity and expression of fibroblast growth factor 17. Mech Dev 83:165-178.
Zhou C, Tsai SY, Tsai MJ (2001) COUP-TFI: an intrinsic factor for early regionalization of the neocortex. Genes Dev 15:2054-2059.
Zilles K, Wree A (1995) Cortex: areal and laminar structure. San Diego: Academic Press.

Chapter 2

Patterning of frontal cortex subdivisions by *Fgf17*

ABSTRACT

The frontal cortex (FC) is the seat of higher cognition. The genetic mechanisms that control formation of the functionally distinct subdivisions of the FC are unknown. Using a novel set of gene expression markers that distinguish subdivisions of the newborn mouse FC, we show that loss of *Fgf17* selectively reduces the size of the dorsal FC, while ventral/orbital FC appears normal. These changes are complemented by a rostral shift of sensory cortical areas. Thus, *Fgf17* functions similar to *Fgf8* in patterning the overall neocortical map, but has a more selective role in regulating the properties of the dorsal but not ventral FC.

INTRODUCTION

The frontal cortex (FC) consists of prefrontal, premotor and motor areas that play a central role in cognition, movement and behavior (1). The adult rodent prefrontal cortex (PFC) can be divided into medial and orbital regions that are thought to have homologues in primates (2). The medial PFC (mPFC) can be further subdivided into the dorsal mPFC that includes frontal association, anterior cingulate, and dorsal prelimbic areas, and the ventral mPFC that consists of ventral prelimbic, infralimbic and medial orbital areas (3). The developmental mechanisms that generate FC subdivisions are unknown, due in part

to the lack of markers that distinguish these regions. In addition, most known mouse mutants that affect cortical patterning die at birth, precluding later analysis, when individual areas are distinguishable by classical histological methods.

Current evidence shows that neocortical areas are presaged by regionalized expression of transcription factors and other regulatory genes in the cortical neuroepithelium and cortical plate, supporting the protomap model (4-7). Members of the fibroblast growth factor (*Fgf*) family of genes have been implicated in controlling neocortical regionalization. *Fgf8* and *Fgf17* encode secreted signaling proteins and are expressed in a partially overlapping pattern in the rostral forebrain patterning center immediately adjacent to the developing FC (Fig. 1A, Supporting material Fig. S1) (8-11). *Fgf8* patterns the neocortex in part by regulating the expression of transcription factor gradients in the cortical neuroepithelium (7, 12-16). Although ectopic expression of *Fgf17* has been reported to have effects similar to that of *Fgf8* in mediating overall patterning of the neocortical map (13), the role of endogenous *Fgf17* in forebrain development is unknown.

In this study, we devised a novel panel of gene expression markers to examine the role of *Fgf17* in regionalization of the rodent FC using *Fgf17* null mice (*Fgf17*$^{-/-}$) (17). We report that the dorsal FC of *Fgf17*$^{-/-}$ mice was reduced in size, whereas ventral and orbital FC regions appeared normal. The reduction in dorsal FC area was complemented by a rostromedial shift of caudal cortical areas. These changes in regionalization persisted into adulthood and were accompanied by a reduction in FC projections to subcortical targets. Thus, in addition to an overall effect on neocortical patterning, *Fgf17* has an unexpectedly selective role in regulating dorsal FC development.

RESULTS

We examined *Fgf8* expression in the rostral patterning center of *Fgf17*$^{-/-}$ mutants, given *Fgf8's* important function in telencephalic patterning (12, 14-16). At embryonic day (E)10.5, telencephalic expression of *Fgf8* appeared the same in wild-type and *Fgf17*$^{-/-}$ littermate embryos (Fig. 1C-C'), suggesting that *Fgf17* does not affect cortical development by regulating *Fgf8* expression.

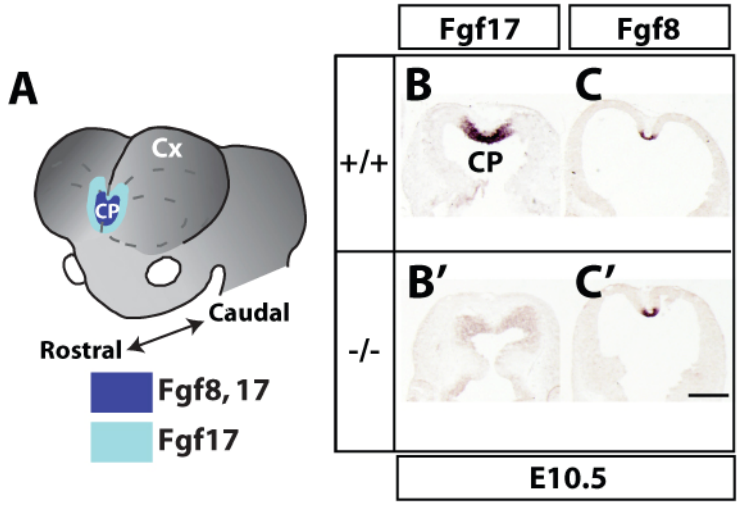

Fig. 1. *Fgf8* and *Fgf17* expression overlap in the forebrain rostral patterning center and *Fgf8* expression is maintained in the *Fgf17*$^{-/-}$ mutant. (A) *Fgf17* and *Fgf8* RNA expression in the rostral forebrain patterning center. CP, commissural plate; Cx, cortex. **(B-C')** *Fgf17* and *Fgf8 in situ* hybridization (ISH) on horizontal sections from E10.5 *Fgf17*$^{+/+}$ (B, C) and *Fgf17*$^{-/-}$ (B', C') forebrain. Top = rostral. Scale bar = 0.5mm.

The *Fgf17*$^{-/-}$ forebrain lacked overt morphological defects (Fig. S2A-B'). Although we found no significant difference in cortical surface area in postnatal day 0 (P0) brains (Fig. S2C), adult cortical surface area was slightly (~7%) reduced (Fig. S2D). In addition, the olfactory bulbs and basal ganglia, which are severely reduced in *Fgf8*$^{neo/neo}$ and *Fgf8*$^{neo/null}$ hypomorphic mutants, respectively (14, 16), are roughly normal in size and exhibited no differences in histology or gene expression in *Fgf17*$^{-/-}$ mutants

(Fig. S3). This suggests that compared to *Fgf8*, *Fgf17* has only a minor role in regulating the overall growth of the telencephalon.

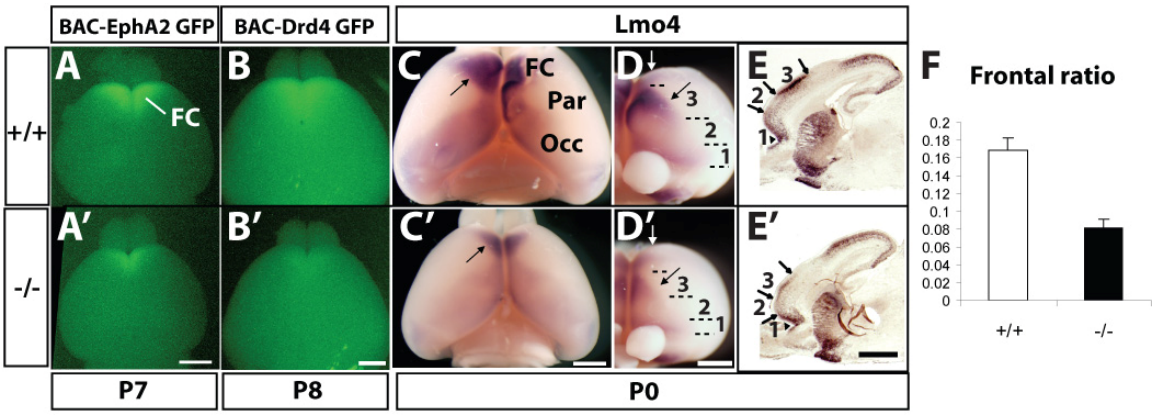

Fig. 2. Reduced frontal cortex (FC) size in *Fgf17*$^{-/-}$ mice. Arrows signify shifted boundaries and arrowheads signify maintained boundaries. **(A-A')** Dorsal views of P7 *Fgf17*$^{+/+}$ and *Fgf17*$^{-/-}$ brains positive for the BAC-EphA2 GFP transgene. The GFP+ domain that marks the FC was reduced in *Fgf17*$^{-/-}$ mutants. **(B-B')** Dorsal views of P8 *Fgf17*$^{+/+}$ and *Fgf17*$^{-/-}$ brains positive for the BAC-Drd4 GFP transgene. **(C-C')** Dorsal views of *Lmo4* wholemount ISH on P0 *Fgf17*$^{+/+}$ and *Fgf17*$^{-/-}$ brains. FC, frontal cortex; Par, parietal cortex; Occ, occipital cortex. **(D-D')** Frontal views of the same brains in (C-C') reveal gene expression boundaries that distinguish three early FC subdivisions that we have labeled #1-3. **(E-E')** Sagittal sections processed for *Lmo4* ISH on P0 *Fgf17*$^{+/+}$ and *Fgf17*$^{-/-}$ brains reveal sharp gene expression boundaries within the FC. White arrows in (D-D') indicate the approximate plane of section in (E-E'). **(F)** Ratio of *Lmo4*+ dorsal frontal cortex area to total cortex area in *Fgf17*$^{+/+}$ (n=4) and *Fgf17*$^{-/-}$ (n=4) P0 hemispheres (Student's t-test; $t = 5.21$, $p < 0.01$). Scale bars = 1mm.

To assess whether the *Fgf17*$^{-/-}$ mutation altered rostral parts of the telencephalon, we focused on the FC. To this end, we introduced BAC-EphA2 and BAC-Drd4 alleles, which express green fluorescent protein (GFP) in specific FC domains (18). *Fgf17*$^{-/-}$ mice at postnatal day (P)0, P7 and P8 had a smaller domain of FC GFP fluorescence (Fig. 2A-B' and data not shown), suggesting a decrease in FC size. We similarly observed reduced dorsal FC *Lmo4* RNA expression in *Fgf17*$^{-/-}$ wholemount brains at P0 (Fig. 2C-D'), providing evidence that the small FC is not due to the BAC transgene. *Lmo4*+ dorsal FC area was reduced by 52% after correcting for overall cortex size (Fig. 2F). Interestingly, *Lmo4* expression in the medial and orbital FC was not overtly affected (Fig. 2D-D'), suggesting that *Fgf17* has a selective role in patterning FC subdivisions.

To distinguish between a reduction in expression levels versus a shift in area properties, we examined *Lmo4* expression in sagittal sections. We observed no change in the level of *Lmo4* RNA or in the layer-specific pattern, but rather a rostral shift of the sharp borders that approximate neocortical areal subdivisions (Fig. 2E-E'). In the sagittal view, the dorsal FC domain was rostrally shifted (#3, Fig. 2E-E'), while the ventral domain was less affected (#1, Fig. 2E-E'). Other brain structures such as the striatum, olfactory tubercle and hippocampus displayed normal *Lmo4* expression.

We explored the possibility that *Fgf17* has a selective role in dorsal FC patterning using a novel panel of gene expression markers on series of coronal sections that span the FC at P0 (Figs. 3, S4-5). Based on the expression domains and complementary borders of BAC-Drd4 GFP, *Lmo4*, *Cad8*, *Nt3*, *Steel*, *Ngn2*, *Rzr-β*, *Cad6*, *Lmo3*, *EphrinA5* and *Id2*, we distinguished subdivisions in the rostral cortex that correlate with presumptive anatomical cortical areas (Figs. 3A, S4, Tables 1, S1). In the dorsal cortex, we defined three FC subdivisions, dorsomedial (dM), dorsal (D) and dorsolateral (dL), and a single parietal cortex (Par) subdivision, while the ventral FC consisted of orbital subdivisions (MO, VO, LO, dLO), and more caudally the agranular insular (AI) and infralimbic (IL) areas (Figs. 3A, S4, Tables 1, S1).

Table 1: Frontal cortex subdivision definitions

	Anatomical areas	
Gene-defined region	**Zilles & Wree, 1995**	**Krettek & Price, 1977**
Dorsolateral (dL)	Fr1, Fr3	PrCl
dorsal (D)	Fr1, Fr2	PrCl, PrCm
dorsomedial (dM)	Cg1, Cg2, Cg3	ACd, ACv, PL
infralimbic (IL)	IL	IL
medial orbital (MO)	MO	MO
ventral orbital (VO)	VO	VO
lateral orbital (LO)	LO	LO
Dorsolateral orbital (dlO)	DLO	DLO
agranular insular (AI)	AID/AIV	AId/AIv
Parietal (Par)	Par1	S1

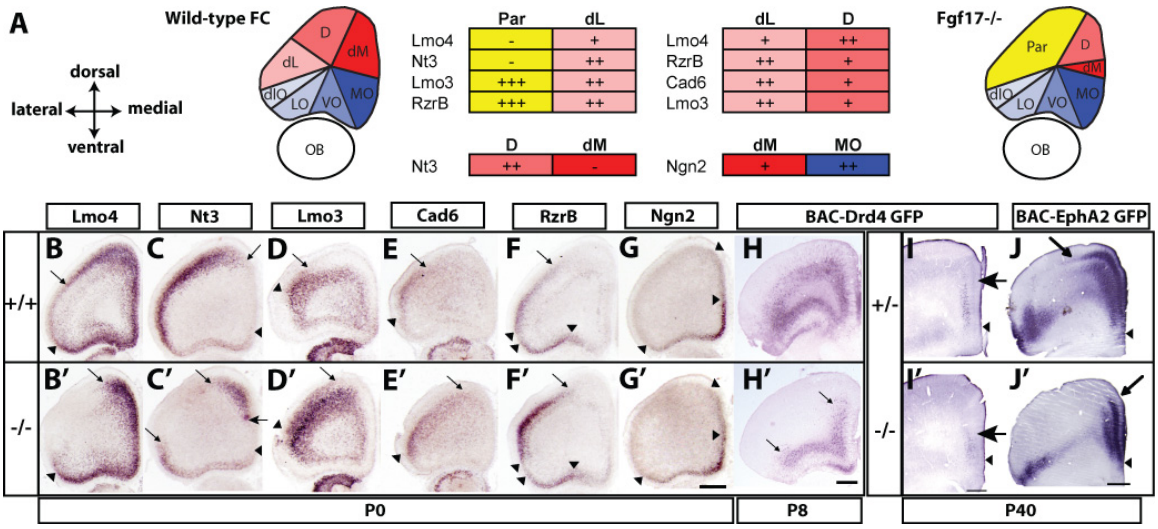

Fig. 3. Selective changes in dorsal FC molecular properties revealed by a novel panel of gene expression markers. Arrows signify shifted boundaries and arrowheads signify maintained boundaries. **(A)** Schema of wild-type and *Fgf17*$^{-/-}$ mutant FC subdivisions based on a panel of gene expression markers at P0. Dorsal and ventral FC subdivisions are shaded in red and blue, respectively. The parietal cortex is shaded in yellow. The table focuses on key wild-type subdivision distinctions with levels of expression for each gene: +++, strong expression; ++, moderate expression; +, weak expression; -, no detectable expression. See Table 1 for corresponding anatomical areas and Supporting Tables 1 and 2 for more detailed analysis. **(B-G')** ISH for *Lmo4*, *Nt3, Lmo3, Cad6, Rzr-β* and *Ngn2* on *Fgf17*$^{+/+}$ and *Fgf17*$^{-/-}$ littermate P0 coronal sections. Note the shift in dorsal expression borders (arrows) but maintenance of ventral borders (arrowheads). **(H-I')** Anti-GFP immunohistochemistry on coronal sections from P8 (H-H') and P40 (I-I') mice containing the BAC-Drd4 GFP transgene. Note that the expression is much broader in the FC at P8, but restricted in the medial prefrontal cortex at P40. **(J-J')** Anti-GFP immunohistochemistry on coronal sections from P40 mice containing the BAC-EphA2 GFP transgene. Abbreviations: D, dorsal FC; dlO, dorsolateral orbital cortex; dM, dorsomedial FC; LO, lateral orbital cortex; MO, medial orbital cortex; Par, parietal cortex; VO, ventral orbital cortex. Scale bars = 0.5mm.

We used this gene expression panel to determine how individual regional FC subdivisions were altered in P0 *Fgf17*$^{-/-}$ mutants. In this analysis, we compared matched coronal sections (Fig. 3) and whole series of coronal sections (Fig. S4-5). We focused on some key subdivision distinctions which showed the most obvious changes in gene expression (Fig. 3A, Table S2). *Fgf17*$^{-/-}$ mice had medially shifted dorsal FC expression borders of *Lmo4*, *Nt3*, BAC-Drd4 GFP and *Cad8* (Figs. 3B-C', S4-5), while Par markers *Lmo3*, *Cad6*, *Rzr-β* and *EphrinA5* showed a complementary expansion from more caudal cortex into this region (Figs. 3D-F', S4-5). By contrast, the ventral FC showed no

changes in gene expression (Figs. 3, S4-5). Together, the pattern of changes suggests that subdivisions of the dorsal FC (regions dL, D and dM) are reduced, parietal cortex expands into the FC and ventral FC subdivisions are not affected (Figs. 3A, S5). This provides strong evidence that *Fgf17* has a selective role in regulating the regional properties of the dorsal but not ventral FC.

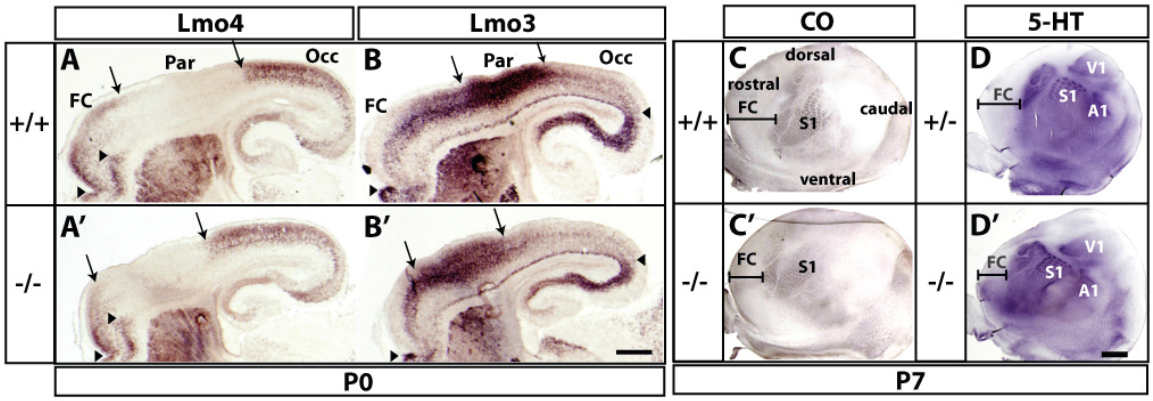

Fig. 4. Rostral shift of the neocortical map in *Fgf17*$^{-/-}$ mutants. Rostral is to the left. Arrows signify shifted boundaries and arrowheads signify maintained boundaries. **(A-B')** *Lmo4* and *Lmo3* ISH on sagittal sections from *Fgf17*$^{+/+}$ and *Fgf17*$^{-/-}$ P0 brains mark complementary cortical domains: frontal/occipital (FC/Occ) and parietal (Par) cortex, respectively. Scale bar = 0.5mm. **(C-D')** Cytochrome oxidase (CO) and anti-serotonin (5-HT) immunohistochemistry on tangential sections of flattened P7 cortices reveal a rostrodorsal shift of primary sensory areas (S1, somatosensory; V1, visual; A1, auditory). Scale bar = 1mm.

To explore further whether there is a rostral shift of caudal cortical regions, we examined gene expression in P0 sagittal sections. This revealed a rostral shift of parietal and occipital domains delimited by *Lmo4* and *Lmo3* expression (Figs. 4A-B', S6). These observations were confirmed at P7 based on a rostral shift of the somatosensory and visual cortex in flat-mount preparations stained for cytochrome oxidase (CO) and 5-hydroxytryptamine (5-HT, serotonin) (Fig. 4C-D') (19). Therefore, in addition to regulating the size of dorsal FC areas, *Fgf17* controls the position of sensory neocortical areas along the rostral-caudal axis.

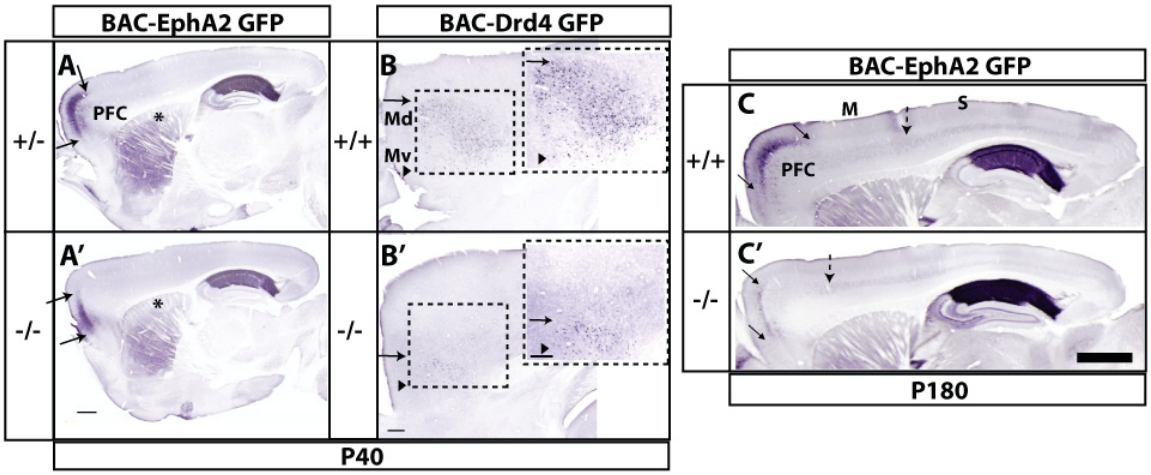

Fig. 5. Persistence of changes in FC molecular regionalization in mature *Fgf17*$^{-/-}$ mice. Arrows signify shifted boundaries and arrowheads signify maintained boundaries. **(A-B')** Sagittal sections of brains from P40 mice carrying either the BAC-EphA2 GFP or BAC-Drd4 GFP transgene processed for anti-GFP immunohistochemistry. Fiber staining in the dorsal striatum in BAC-EphA2 GFP+ mice corresponds to projections from the FC (asterisks in A-A'). Boxed areas, consisting of dorsomedial (Md) and ventromedial (Mv) subdivisions of the prefrontal cortex (PFC), are shown in magnified view (right insets in B-B'). Scale bars = 0.5mm. **(C-C')** Sagittal sections of cortex from adult (P180) BAC-EphA2+, *Fgf17*$^{+/+}$ and *Fgf17*$^{-/-}$ mice processed for anti-GFP immunohistochemistry. The dotted arrow approximates the sensory (S)-motor (M) boundary. Scale bar = 1mm.

Next, we assessed whether these early postnatal alterations in cortical areas were observed in the mature brain, by examining expression of BAC-Drd4 GFP and BAC-EphA2 GFP in P40 and 6-month-old mice. At P40, BAC-Drd4 GFP labeled a discrete domain of cells in the medial FC that correlates with the prelimbic area (Figs. 3I, 5B) (20). While the position of the ventral border and layer-specificity of GFP+ cells was maintained, the extent of this domain was reduced in the *Fgf17*$^{-/-}$ brain (Figs. 3I', 5B'), suggesting that the prelimbic cortical area (ventral part of dM) is reduced in size. At P40 and in 6-month-old mice, BAC-EphA2 GFP labels the prefrontal cortex (including frontal association, anterior cingulate, prelimbic and infralimbic areas) (Figs. 3J, 5A,C, S7-8). In the *Fgf17*$^{-/-}$ mutant, the dorsal expression border was shifted medially, while the ventral border was maintained (Figs. 3J', 5A',C', S7-8), confirming that the prefrontal cortex is smaller.

The dorsal FC sends projections through the dorsal striatum, which can be visualized in mice expressing BAC-EphA2 GFP (3, 18). In *Fgf17*$^{+/-}$ BAC-EphA2 GFP+ mice, GFP+ fiber staining is apparent throughout most of the dorsal striatum (Figs. 5A, S7). However, in *Fgf17*$^{-/-}$ mice, GFP+ fiber labeling in the dorsolateral striatum appeared reduced, consistent with the smaller domain of BAC-EphA2 GFP+ labeled cells in the dorsal FC (Figs. 5A', S7).

BAC-EphA2 GFP is expressed at higher levels in the somatosensory cortex and lower levels in motor cortex at P180 (Fig. 5C). The sensory-motor boundary was shifted to a more rostral position in the *Fgf17*$^{-/-}$ cortex (dashed arrows in Fig. 5C-C'). Consistent with this gene expression shift, CO staining of adjacent sections revealed that the somatosensory barrels were shifted rostrally in the *Fgf17*$^{-/-}$ mutant (Fig. S8). Together, these findings suggest that the early pattern of changes in regional molecular properties (Figs. 2-4) result in a permanent change in the distribution of adult cortical areas.

A subset of FC projections extend to the substantia nigra pars compacta and adjacent ventral tegmental area (SNc/VTA) (3). These projections can be visualized in mice expressing the BAC-Drd4 GFP transgene (Fig. 6A and S9) (18). Staining of these projections was reduced in the *Fgf17*$^{-/-}$ mutant (Fig. 6A'), consistent with the reduction of BAC-Drd4 GFP+ cells in the FC (Figs. 3H', S5). This suggests that the *Fgf17*$^{-/-}$ mutation has a quantitative effect on dorsal FC cell number, but does not have an overt qualitative effect on the pathfinding properties of the remaining BAC-Drd4 GFP^{+} axons. Furthermore, despite the reduction in BAC-Drd4 GFP^{+} FC axons, staining for tyrosine hydroxylase (TH), a marker of midbrain dopamine neurons, did not show a discernable

change (Fig. 6B-B'), suggesting that the *Fgf17*$^{-/-}$ mutation does not overtly affect midbrain dopamine cell number.

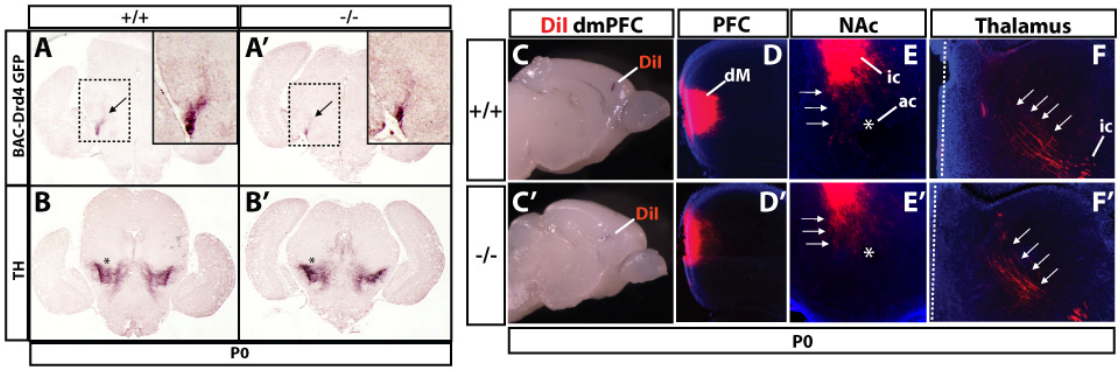

Fig. 6. FC connectivity in *Fgf17*$^{-/-}$ mice. (A-A') Reduction in FC projections to the ventral midbrain revealed by anti-GFP immunohistochemistry on P0 coronal sections from *Fgf17*$^{+/+}$ and *Fgf17*$^{-/-}$ mice containing the BAC-Drd4 GFP transgene. Note the reduced staining of fibers emanating from the cerebral peduncle (arrows). Insets show magnified views of the boxed areas. **(B-B')** Anti-tyrosine hydroxylase (TH) immunohistochemistry on sections adjacent to those shown in (A-A'). Staining of the substantia nigra pars compacta and ventral tegmental area (asterisks) was similar between genotypes. **(C-C')** DiI crystal placements in the dorsomedial FC of P3 *Fgf17*$^{+/+}$ and *Fgf17*$^{-/-}$ brains viewed from the medial side. **(D-D')** Restricted DiI labeled field in the dorsomedial (dM) prefrontal cortex (PFC) in coronal section rostral to the crystal placement. Medial is to the left. **(E-E')** Projections to the nucleus accumbens (NAc) (arrows). Anterograde labeled fibers in the internal capsule (ic) restricted to the ventromedial striatum are also present. The anterior commisure provides a landmark (asterisk). Medial is to the left. **(F-F')** Cortico-thalamic fibers (arrows) emanate from the internal capsule (ic) and are present in similar locations in both genotypes. A dashed line designates the thalamic midline.

Finally, we examined immature FC connectivity in P0 and P3 *Fgf17*$^{+/+}$ and *Fgf17*$^{-/-}$ mutant brains using the lipophilic dye diI (Figs. 6, S10). Placement of diI crystals in the medial prefrontal cortex (Figs. 6C, S10) (regions dM and vM) labeled cells and fibers in restricted domains within the medial prefrontal cortex and did not back-label cells or fibers in other parts of the cortex (Figs. 6D, S10). We observed a subset of projections oriented toward the nucleus accumbens (Figs. 6E, S10), other fibers tightly localized within the internal capsule in the medial striatum (Figs. 6E, S10), and labeling in the medial thalamus (Figs. 6F, S10). We did not observe major differences between genotypes in these labeling patterns (Figs. 6C'-F', S10).

DISCUSSION

We provide evidence that *Fgf17* has a selective function in the regionalization of FC subdivisions. Our analysis required identifying a novel panel of gene expression markers that distinguish dorsal and ventral subdivisions of the newborn rodent FC (Figs. 3, S4 and Tables 1, S1-2). In addition, we have characterized two lines of BAC transgenic mice that provide specific GFP labeling of the FC, and show that they can be used as read-outs of cortical regionalization and projections patterns from the FC (Figs. 2, 3, 5, S4, S7, S8). The expression pattern of many of these genes revealed distinct borders within the FC at birth, suggesting a genetic partitioning of this cortical region prior to overt cytoarchitectonic differentiation. Although expression of none of the genes was limited to a single cortical region, combinations of genes were useful in defining regional subdivisions that correlated with histologically-defined cortical areas (Table 1).

The lack of overt forebrain morphologic defects in *Fgf17*$^{-/-}$ mutants, and the mildly reduced cortical surface area in the adult (Fig. S2), shows that *Fgf17* does not have a major effect on forebrain growth. Rather the results suggest that *Fgf17* has a more specific function in regulating regional specification, particularly within the FC. By contrast, severe reductions in *Fgf8* levels result in gross forebrain morphologic defects that are likely due to a combination of abnormal regional specification, decreased proliferation and increased apoptosis (15, 16). In addition to spatiotemporal differences in *Fgf8* and *Fgf17* expression (17) (Fig. 1), differences in ligand affinity for FGF receptors and ability to regulate gene expression may explain the differences in phenotypic effects (21, 22).

The *Fgf17*$^{-/-}$ mutant displays a rostral shift of caudal cortical areas (Fig. 4, S6) that is less severe than in *Fgf8*$^{neo/neo}$ mildly hypomorphic mutants (14), suggesting that *Fgf17* has a more subtle role than *Fgf8* in patterning the neocortical areal map. Our postnatal analyses do not clarify whether the rostral shift in sensory cortices is only due to hypoplasia of the frontal cortex and/or due to respecification of the rostral progenitor domain to develop as more caudal cortex. Ongoing studies are aimed at distinguishing these mechanisms.

Analysis of FC subdivisions unexpectedly identified that *Fgf17* selectively regulates the sizes and positions of dorsal, but not ventral FC subdivisions (Figs. 3, S4-5). In *Fgf8*$^{neo/neo}$ mutants, both the dorsal and ventral FC are reduced (Garel et al., 2003; Cholfin and Rubenstein, unpublished). These phenotypic differences may be explained in part by the observations that 1) *Fgf17* was expressed in a broader domain in the rostral patterning center than *Fgf8* (particularly in its dorsal extent) and 2) *Fgf8* expression was normal in the *Fgf17*$^{-/-}$ embryonic brain (Fig. 1). We propose that reduced FGF signaling specifically in the dorsal part of the rostral patterning center could selectively affect dorsal FC regionalization, while preserving the ventral FC. Current evidence, which is consistent with the protomap model, suggests that FGFs produced by the rostral patterning center regulate the regional expression of transcription factors in the neuroepithelium to specify cortical areal identity (4-7). Ongoing studies aim to elucidate how *Fgf17* differentially regulates the expression of these transcription factors.

The neocortex of *Fgf17*$^{-/-}$ mutants shows correct area-specific thalamic innervation, as exemplified by the presence of somatosensory barrels, detected by both cytochrome oxidase staining and 5-HT immunohistochemistry at P7 (Fig. 4). However,

the position of the somatosensory barrel fields is shifted rostrally, showing that thalamocortical innervation shifts in concert with the shift in areal molecular markers. In both the the *Fgf17*$^{-/-}$ and *Fgf8*$^{neo/neo}$ mutants, there was no detectable difference in thalamocortical innervation at P0 (14) (Fig. S10 and data not shown). Ectopic *Fgf8* expression experiments, that result in viable animals, suggest that re-routing of thalamocortical axons to area-specific targets occurs postnatally within the cortex (23). This could account for the rostral shift of the innervation of somatosensory barrel fields in the *Fgf17*$^{-/-}$ mutant.

Recent evidence suggests that *Fgf8* plays a role in regulating patterns of intracortical connectivity (24). Unlike in the *Fgf8*$^{neo/neo}$ mutant, we found no evidence for ectopic rostral projections of caudally located cortical neurons in the *Fgf17*$^{-/-}$ brain (data not shown), consistent with the subtler phenotype of the *Fgf17*$^{-/-}$ mutants.

Although *Fgf17*$^{-/-}$ mutants did not show an overt qualitative defect in dorsomedial FC connectivity/projections (Figs. 6, S10), there was evidence for a quantitative reduction in its subcortical projections based on BAC-EphA2 and BAC-Drd4 GFP expression in the striatum and ventral midbrain, respectively (Figs. 5, 6, S7, S9). We propose that this is secondary to a reduction in the number of FC-specified neurons. Reduced prefrontal cortex output to striatal or midbrain dopaminergic neurons may have important physiologic ramifications for the regulation of neural pathways involved in reward, cognition and social behavior (25-29).

Dorsal and ventral FC subdivisions have distinct roles in regulating cognition and behavior in rodents (3, 26) and primates including humans (25, 30, 31). For example, subdivisions of the dorsal prefrontal cortex are implicated in working memory, attention,

response selection, temporal processing of information, effort-related decision making and social valuation, while ventromedial and orbital subdivisions are implicated in behavioral flexibility, emotional regulation, delay-related decision making, evaluation of rewards and autonomic control (1, 3, 25, 26, 29, 30, 32-34). Therefore, the *Fgf17*$^{-/-}$ mutant provides a unique opportunity to examine the behavioral and neurophysiologic consequences of an early developmental genetic lesion that selectively affects the dorsal FC. Ongoing studies have identified circumscribed behavioral deficits in *Fgf17*$^{-/-}$ mutants that affect social interactions (Scearce-Levie, Roberson, Cholfin, Rubenstein, and Mucke, unpublished). We propose that elucidating the signaling pathways downstream of *Fgf17* will provide important insights into the genetic pathways that regulate frontal cortex development, and that may be disrupted in disorders that affect cognition, emotion and social interactions.

METHODS

Supporting Material contains a more detailed description of methods.

Animals and tissue preparation

All mice were housed and handled in accordance with the Institutional Animal Care and Use Committee of the University of California, San Francisco. *Fgf17*$^{-/-}$ mice and embryos were generated by mating male and female heterozygotes (*Fgf17*$^{+/-}$) (17). BAC transgenic lines BAC-Drd4 GFP and BAC-EphA2 GFP (18) were mated to *Fgf17*$^{-/-}$ mice to generate double heterozygotes, which were then crossed to *Fgf17*$^{+/-}$ mice to generate *Fgf17*$^{+/+}$ and *Fgf17*$^{-/-}$ BAC transgene-positive littermates. All tissue was harvested, fixed and cryopreserved according to standard methods. Sections were cut on either a cryostat or freezing microtome.

In situ hybridization and immunohistochemistry

Digoxigenin (DIG)-labeled riboprobes were generated for the following genes: *Cadherin-6*, *Cadherin-8* (35), *Fgf8* (36), *Fgf17* (10), *Id-2* (35), *Lmo3* and *Lmo4* (37), *Neurogenin-2* (38), *Neurotrophin-3* (gift from L. Ma), *RZR-β* (35) and *Steel* (gift from E. Grove). Section and wholemount *in situ* hybridization were performed as described previously in (35) and (19), respectively.

Immunohistochemistry was performed using standard protocols (35) with the following antibodies: rabbit anti-GFP (1:1000; Molecular Probes, Eugene, OR), rabbit anti-tyrosine hydroxylase (1:500; Chemicon, Temecula, CA), rabbit anti-serotonin

(1:50,000; Immunostar, Hudson, WI), and detected with goat anti-rabbit biotinylated secondary antibody (1:200-1:400; Vector Laboratories, Burlingame, CA) and ABC kit (Vector).

Axon tracing

P0-3 brains were stored in 4% PFA in PBS at 4°C. Single crystals of the fluorescent carbocyanide dye DiI (1,1'-dioctadecyl 3,3,3',3'-tetramethylindocarbocyanine perchlorate; Molecular Probes) were placed in various cortical locations (39). After diffusion, sections were cut on a vibratome and immediately mounted on slides using Vectashield mounting medium with DAPI (Vector).

Digital imaging and Quantification of cortical areas

Whole brains and sections were photographed using SPOT (Diagnostic Instruments) and Olympus digital cameras and imaging software. Areas were determined using photos of dorsally-viewed whole mount brains in Scion Image (Scion Corp). Excel (Microsoft) was used for calculations and statistical analysis.

REFERENCES

1. **Fuster, J. M. (2001) *Neuron* 30, 319-33.**
2. **Uylings, H. B., Groenewegen, H. J. & Kolb, B. (2003) *Behav Brain Res* 146, 3-17.**
3. **Heidbreder, C. A. & Groenewegen, H. J. (2003) *Neurosci Biobehav Rev* 27, 555-79.**
4. **Rakic, P. (1988) *Science* 241, 170-6.**
5. **O'Leary, D. D. & Nakagawa, Y. (2002) *Curr Opin Neurobiol* 12, 14-25.**
6. **Grove, E. A. & Fukuchi-Shimogori, T. (2003) *Annu Rev Neurosci* 26, 355-80.**
7. **Sur, M. & Rubenstein, J. L. (2005) *Science* 310, 805-10.**
8. **Maruoka, Y., Ohbayashi, N., Hoshikawa, M., Itoh, N., Hogan, B. L. & Furuta, Y. (1998) *Mech Dev* 74, 175-7.**
9. **Hoshikawa, M., Ohbayashi, N., Yonamine, A., Konishi, M., Ozaki, K., Fukui, S. & Itoh, N. (1998) *Biochem Biophys Res Commun* 244, 187-91.**
10. **Xu, J., Lawshe, A., MacArthur, C. A. & Ornitz, D. M. (1999) *Mech Dev* 83, 165-78.**
11. **Bachler, M. & Neubuser, A. (2001) *Mech Dev* 100, 313-6.**
12. **Fukuchi-Shimogori, T. & Grove, E. A. (2001) *Science* 294, 1071-4.**
13. **Fukuchi-Shimogori, T. & Grove, E. A. (2003) *Nat Neurosci* 6, 825-31.**
14. **Garel, S., Huffman, K. J. & Rubenstein, J. L. (2003) *Development* 130, 1903-14.**
15. **Storm, E. E., Rubenstein, J. L. & Martin, G. R. (2003) *Proc Natl Acad Sci U S A* 100, 1757-62.**
16. **Storm, E. E., Garel, S., Borello, U., Hebert, J. M., Martinez, S., McConnell, S. K., Martin, G. R. & Rubenstein, J. L. (2006) *Development* 133, 1831-44.**
17. **Xu, J., Liu, Z. & Ornitz, D. M. (2000) *Development* 127, 1833-43.**
18. **Gong, S., Zheng, C., Doughty, M. L., Losos, K., Didkovsky, N., Schambra, U. B., Nowak, N. J., Joyner, A., Leblanc, G., Hatten, M. E. & Heintz, N. (2003) *Nature* 425, 917-25.**
19. **Hamasaki, T., Leingartner, A., Ringstedt, T. & O'Leary, D. D. (2004) *Neuron* 43, 359-72.**
20. **Noain, D., Avale, M. E., Wedemeyer, C., Calvo, D., Peper, M. & Rubinstein, M. (2006) *Eur J Neurosci* 24, 2429-38.**
21. **Olsen, S. K., Li, J. Y., Bromleigh, C., Eliseenkova, A. V., Ibrahimi, O. A., Lao, Z., Zhang, F., Linhardt, R. J., Joyner, A. L. & Mohammadi, M. (2006) *Genes Dev* 20, 185-98.**
22. **Liu, A., Li, J. Y., Bromleigh, C., Lao, Z., Niswander, L. A. & Joyner, A. L. (2003) *Development* 130, 6175-85.**
23. **Shimogori, T. & Grove, E. A. (2005) *J Neurosci* 25, 6550-60.**
24. **Huffman, K. J., Garel, S. & Rubenstein, J. L. (2004) *J Neurosci* 24, 8917-23.**
25. **Goldman-Rakic, P. S. (1996) *Proc Natl Acad Sci U S A* 93, 13473-80.**

26. Dalley, J. W., Cardinal, R. N. & Robbins, T. W. (2004) *Neurosci Biobehav Rev* 28, 771-84.
27. Young, L. J. & Wang, Z. (2004) *Nat Neurosci* 7, 1048-54.
28. Meyer-Lindenberg, A., Kohn, P. D., Kolachana, B., Kippenhan, S., McInerney-Leo, A., Nussbaum, R., Weinberger, D. R. & Berman, K. F. (2005) *Nat Neurosci* 8, 594-6.
29. Kellendonk, C., Simpson, E. H., Polan, H. J., Malleret, G., Vronskaya, S., Winiger, V., Moore, H. & Kandel, E. R. (2006) *Neuron* 49, 603-15.
30. Price, J. L. (2006) *Prefrontal cortex* (CRC Press, Boca Raton).
31. Amodio, D. M. & Frith, C. D. (2006) *Nat Rev Neurosci* 7, 268-77.
32. Rudebeck, P. H., Buckley, M. J., Walton, M. E. & Rushworth, M. F. (2006) *Science* 313, 1310-2.
33. Rudebeck, P. H., Walton, M. E., Smyth, A. N., Bannerman, D. M. & Rushworth, M. F. (2006) *Nat Neurosci* 9, 1161-8.
34. Mitchell, J. P., Macrae, C. N. & Banaji, M. R. (2006) *Neuron* 50, 655-63.
35. Rubenstein, J. L., Anderson, S., Shi, L., Miyashita-Lin, E., Bulfone, A. & Hevner, R. (1999) *Cereb Cortex* 9, 524-32.
36. Crossley, P. H. & Martin, G. R. (1995) *Development* 121, 439-51.
37. Bulchand, S., Subramanian, L. & Tole, S. (2003) *Dev Dyn* 226, 460-9.
38. Fode, C., Gradwohl, G., Morin, X., Dierich, A., LeMeur, M., Goridis, C. & Guillemot, F. (1998) *Neuron* 20, 483-94.
39. Godement, P., Vanselow, J., Thanos, S. & Bonhoeffer, F. (1987) *Development* 101, 697-713.

ACKNOWLEDGEMENTS

We thank Kimberly Scearce-Levie, Erik Roberson, Lennart Mucke and members of the Rubenstein laboratory for insightful discussion and valuable comments regarding this manuscript. We also thank Dianna Kahn for technical assistance. This work was supported by the UCSF Medical Scientist Training Program (J.A.C.), Nina Ireland (J.L.R.R.), Larry L. Hillblom Foundation (J.L.R.R.), and NIH grants: NS34661-01A1 (J.L.R.R.) and K05 MH065670 (J.L.R.R.).

SUPPORTING TABLES

Table S2: Gene expression-defined subdivisions of the newborn mouse frontal cortex

Section 1 — Rostral FC

	Lmo4	Cad8	Id2	Steel (sup)	Steel (deep)	Nt3	BAC-Drd4	Ngn2	RzrB	Cad6	Lmo3	EphrinA5
D	++	++	+++	++	-	++	++	-	+	+	+	+
dM	++	++	++	++	-	-	++	+	+	-	+	+
MO	+++	++	++	++	-	-	++	++	++	-	+	-
VO	+++	++	++	++	-	+	++	++	++	-	+	-
LO	+++	++	+++	++	-	+	++	+	++	+	+	-
DLO	++	++	+++	++	-	++	++	-	++	+	+	-

Section 2

	Lmo4	Cad8	Id2	Steel (sup)	Steel (deep)	Nt3	BAC-Drd4	Ngn2	RzrB	Cad6	Lmo3	EphrinA5
dL	+	+	++	+	+	++	+	-	++	++	++	+
D	++	++	+++	++	++	++	+	-	+	+	+	+
dM	++	++	++	++	+	-	+	+	+	-	+	+
MO	+++	++	+	++	-	-	++	++	+	-	+	-
VO	+++	++	++	++	-	+	++	++	+	-	+	-
LO	+++	++	+++	++	-	+	++	+	++	-	+	-
DLO	++	++	+++	++	-	++	++	+	++	+	+	-

Section 3

	Lmo4	Cad8	Id2	Steel (sup)	Steel (deep)	Nt3	BAC-Drd4	Ngn2	RzrB	Cad6	Lmo3	EphrinA5
dL	+	+	++	+	+	+	+	-	++	++	++	+
D	++	++	+++	++	++	++	+	-	+	+	+	+
dM	++	++	++	++	+	-	+	+	+	+	+	+
MO	++	+	+	++	-	-	+++	+	+	+	+	-
VO	++	+	++	+	-	+	+++	+	+	+	+	-
LO	++	+	+++	++	-	+	+++	+	++	+	+	-
AI	++	+	+++	++	-	++	+++	+/s	++	+	+	-
DP	++	s/-	+	+	n/a	+	-	-	++	-	++	-
TT	-	s/-	+	+	n/a	-	-	-	-	+/s	++	+/s

Section 4 — Caudal FC

	Lmo4	Cad8	Id2	Steel (sup)	Steel (deep)	Nt3	BAC-Drd4	Ngn2	RzrB	Cad6	Lmo3	EphrinA5
Par	-	+ (bi)	+	+/s	+	-	-	-	+++	++	+++	+++
D	++	++	+++	+/s	++	++	+	-	+	+	+	+
dM	++	++	++	+/s	+	-	+	+	+	+	+	+
IL	++	-	+	++	-	-	+	-	++	+	++	+/s
LO	++	+/s	+++	++	-	+	+++	+	++	+	+	-
AI	++	+	+++	++	-	++	+++	+	++	+	+	-
DP	++	+/s	+	+	n/a	+	-	-	++	-	++	-
TT	-	+/s	+	+	n/a	-	-	-	-	-	++	+/s

+++	very strong expression
++	moderate expression
+	weak expression
+/s	scattered cells
s/-	very weak/scattered cells
-	no expression
bi	bilaminar distribution

Assignments are internally consistent for a given gene.

Table S2: Key FC subdivision distinctions

	Par	**dL**
Lmo4	-	+
Id2	+	++
Nt3	-	++
Lmo3	+++	++
EphrinA5	+++	+

	dL	**D**
Lmo4	+	++
Cad8	+	++
Id2	++	+++
Steel sup	+	++
Steel deep	+	++
RzrB	++	+
Cad6	++	+
Lmo3	++	+

	D	**dM**
Steel deep	++	+
Nt3	++	-

	dM	**MO**
Lmo4	++	+++
Id2	++	+/s
Steel deep	+	-
Ngn2	+	++

+++	very strong expression
++	moderate expression
+	weak expression
+/s	scattered cells
-	no detectable expression

SUPPORTING FIGURES

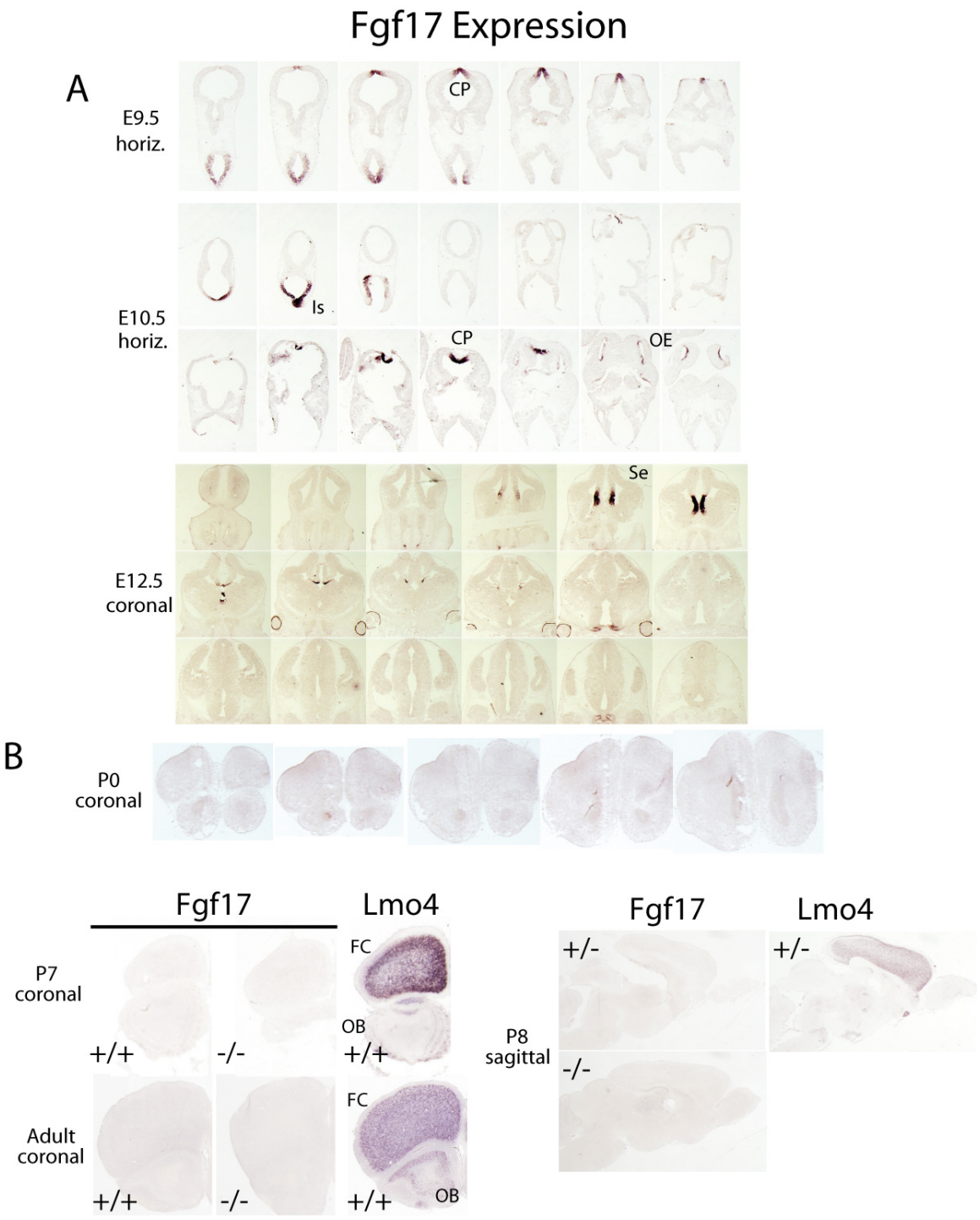

Fig. S1. *Fgf17* expression in the developing and adult brain. (A) Prenatal *Fgf17* expression by RNA *in situ* hybridization at the timepoints and in plane of section indicated. At E9.5-12.5, sites of expression included the commissural plate/rostral patterning center (CP), the isthmic mid/hindbrain patterning center (Is), dorsal diencephalon, optic chiasm, and olfactory epithelium (OE). In the forebrain, *Fgf17* expression was down-regulated, but maintained in the septum at E14.5 and E16.5 and was not expressed in the neocortex (data not shown). **(B)** Postnatal *Fgf17* expression by RNA *in situ* hybridization at the timepoints

and in plane of section indicated. *Lmo4* was used as a positive control probe for tissue RNA quality. At P0, P7, P8 and in the adult, *Fgf17* expression was not detected in the frontal cortex (FC) or olfactory bulb (OB). At P0 and P7-8 a low level of *Fgf17* expression was detected in a sparse subset of cells in the septum (not shown). In the adult, expression was not detected in any brain structures, consistent with the Allen Brain Atlas (http://www.brainatlas.org/).

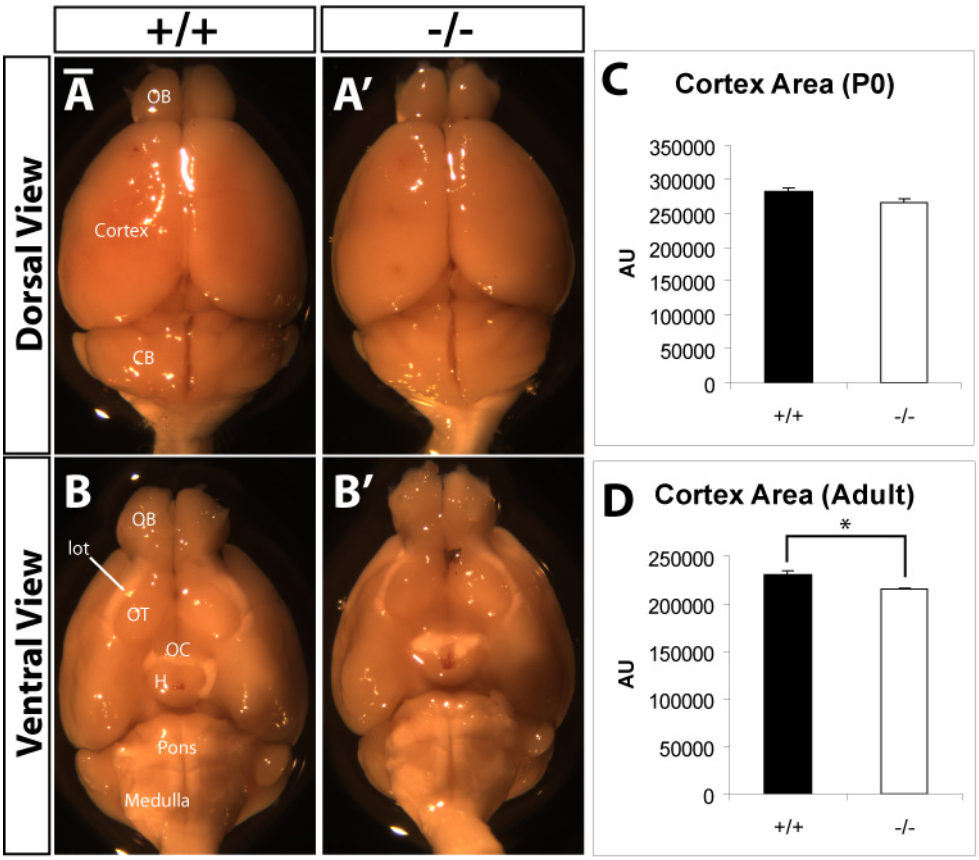

Fig. S2. Normal gross forebrain morphology, but slightly reduced cortical area in *Fgf17*$^{-/-}$ mice. (A) Dorsal view of representative adult *Fgf17*$^{+/+}$ and *Fgf17*$^{-/-}$ brains. **(B)** Ventral views of same brains as in (A). **(C)** Quantification of P0 cerebral cortex hemisphere area from dorsal views yielded a non-significant trend (P = 0.09, *t* test) between *Fgf17*$^{+/+}$ (n = 5) and *Fgf17*$^{-/-}$ (n = 3). AU = arbitrary units. **(D)** Quantification of adult cerebral cortex hemisphere area from dorsal views revealed a small (~7%) but significant (P = 0.0498, *t* test) difference between *Fgf17*$^{+/+}$ (n = 3) and *Fgf17*$^{-/-}$ (n = 3). Adult brains were collected from two litters. AU = arbitrary units. Abbreviations: CB, cerebellum; H, hypothalamus; lot, lateral olfactory tract; OB, olfactory bulb; OC, optic chiasm; OT, olfactory tubercle. Scale bar = 1mm.

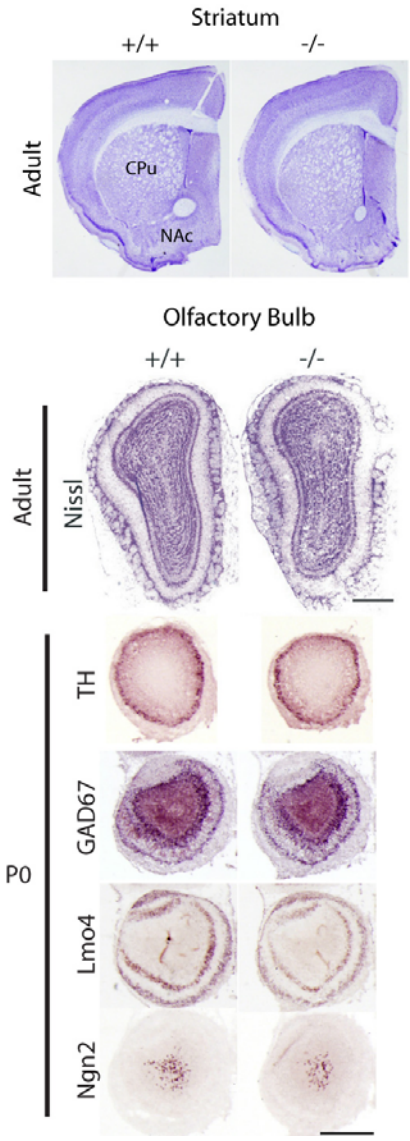

Fig. S3. No evidence of abnormal olfactory bulb histology or gene expression in *Fgf17*$^{-/-}$ mice. Cytoarchitecture of adult OB by Nissl stain of coronal sections and expression of tyrosine hydroxylase (TH), glutamic acid decarboxylase (*Gad67*), *Lmo4*, and *Ngn2* in P0 OB coronal sections. Scale bar = 0.5 mm.

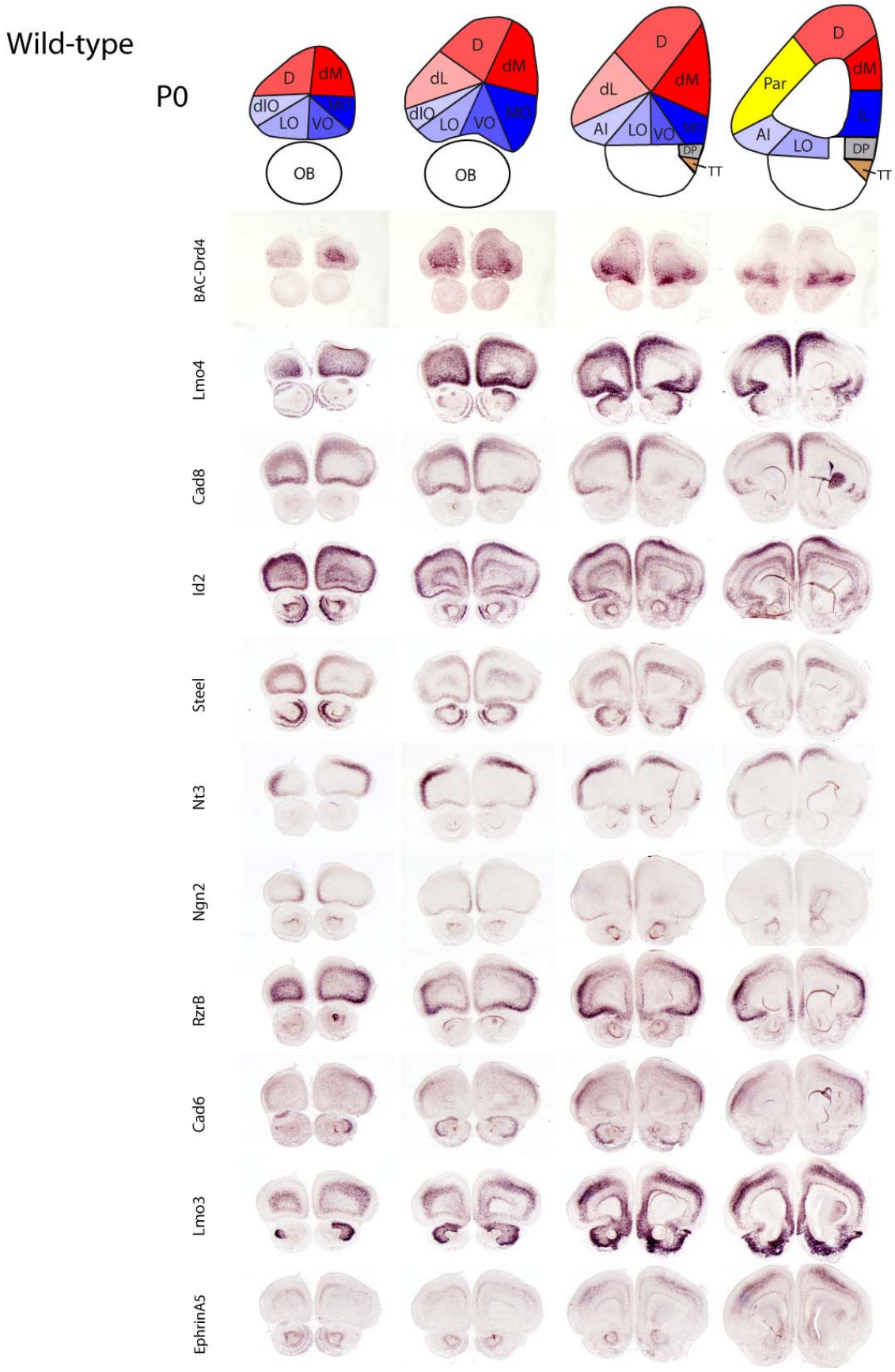
Wild-type
P0
D
dM
dIO
LO
VO
MO
OB
dL
AI
DP
TT
Par
IL
BAC-Drd4
Lmo4
Cad8
Id2
Steel
Nt3
Ngn2
RzrB
Cad6
Lmo3
EphrinA5

Fig. S4. Gene expression map of wild-type newborn frontal cortex (FC). The top row displays a schema of gene expression-derived subdivisions at 4 rostral-caudal levels (left to right). Red and blue colors demarcate dorsal and ventral FC subdivisions, respectively. Parietal cortex is in yellow. The row labeled BAC-Drd4 is a rostral to caudal series of coronal sections from a P0 *Fgf17*$^{+/+}$;BAC-Drd4 GFP+ brain processed for anti-GFP immunohistochemistry. The rows below show rostral to caudal series of coronal sections from a representative P0 wild-type brain processed for *in situ* hybridization for *Lmo4*, *Cadherin-8* (*Cad8*), *Id2*, *Steel*, *Neurotrophin-3* (*Nt3*), *Neurogenin-2* (*Ngn2*), *Rzr-β*, *Cadherin-6* (*Cad6*), *Lmo3* and *EphrinA5*. Abbreviations are as defined in Table 1.

Fgf17-/-

P0

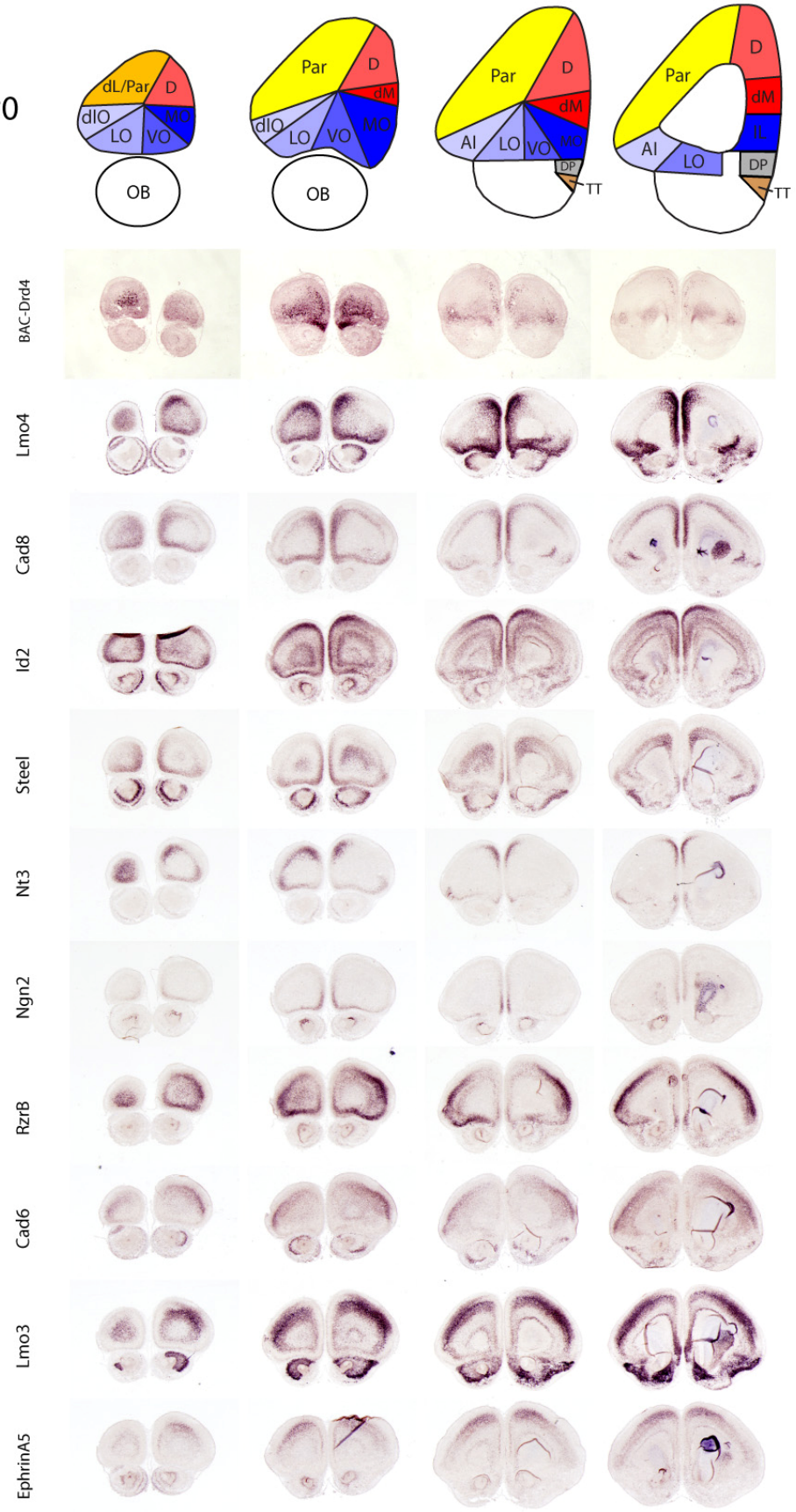
dL/Par
D
dlO
MO
LO
VO
OB
Par
D
dM
dlO
LO
VO
MO
OB
Par
D
dM
AI
LO
VO
MO
DP
TT
Par
D
dM
AI
LO
DP
TT
BAC-Drd4
Lmo4
Cad8
Id2
Steel
Nt3
Ngn2
RzrB
Cad6
Lmo3
EphrinA5

Fig. S5. Changes in dorsal FC regionalization in a representative *Fgf17*$^{-/-}$ mutant brain. The schema (top row) displays a summary of the BAC-transgenic GFP and *in situ* hybridization data: contraction and medial shift of dorsal FC subdivisions (red), with a complementary rostromedial expansion of parietal cortex (yellow). Ventral FC regions are preserved (blue). The row labeled BAC-Drd4 is a rostral to caudal series of coronal sections from a P0 *Fgf17*$^{-/-}$;BAC-Drd4 GFP+ brain processed for anti-GFP immunohistochemistry. The rows below show rostral to caudal series of coronal sections from a representative P0 *Fgf17*$^{-/-}$ brain processed for *in situ* hybridization for *Lmo4*, *Cadherin-8* (*Cad8*), *Id2*, *Steel*, *Neurotrophin-3* (*Nt3*), *Neurogenin-2* (*Ngn2*), *Rzr-β*, *Cadherin-6* (*Cad6*), *Lmo3* and *EphrinA5*. Abbreviations are as defined in Table 1.

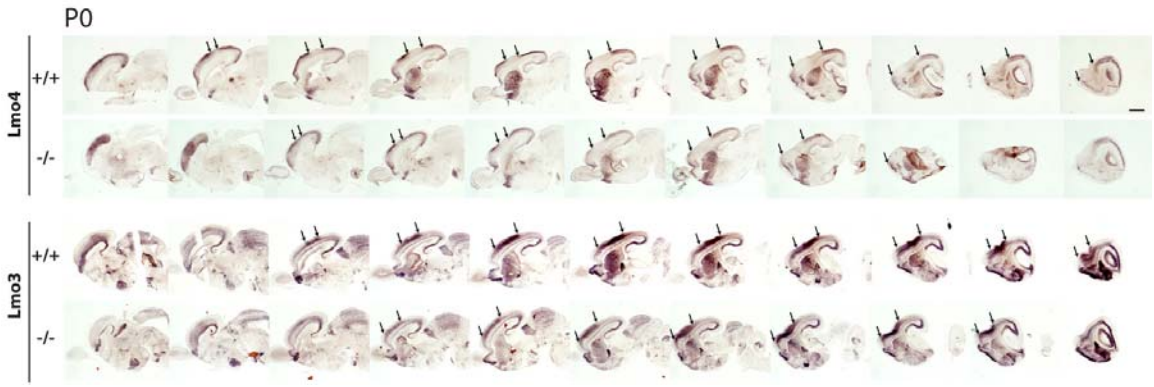

Fig. S6. Rostral shift of regional cortical markers at P0. Medial to lateral (left to right) sagittal section series from *Fgf17*$^{+/+}$ and *Fgf17*$^{-/-}$ brains processed by *in situ* hybridization for *Lmo4* and *Lmo3*. Arrows indicate shifted borders. Scale bar = 1mm.

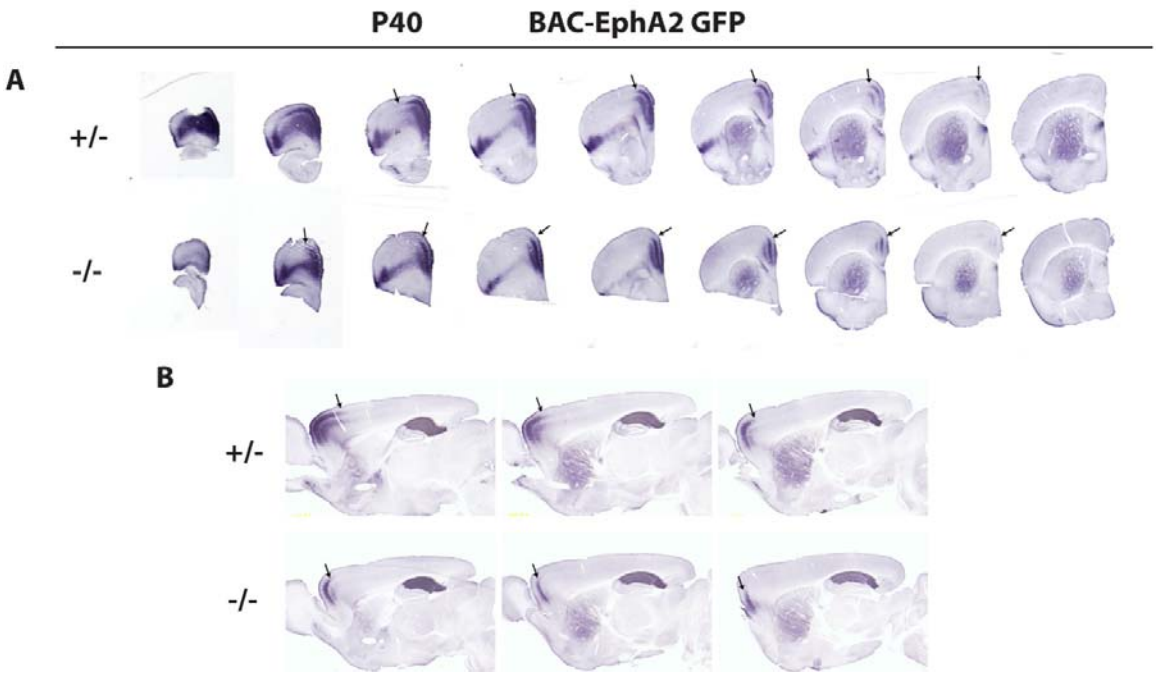

Fig. S7. Comparison of BAC-EphA2 GFP expression in *Fgf17*$^{+/-}$ and *Fgf17*$^{-/-}$ P40 brains in coronal (A) and sagittal (B) views. *Fgf17*$^{-/-}$ mice had a reduced and rostromedially shifted FC GFP expression domain (arrows). Note the maintenance of strong GFP expression in CA1 of the hippocampus.

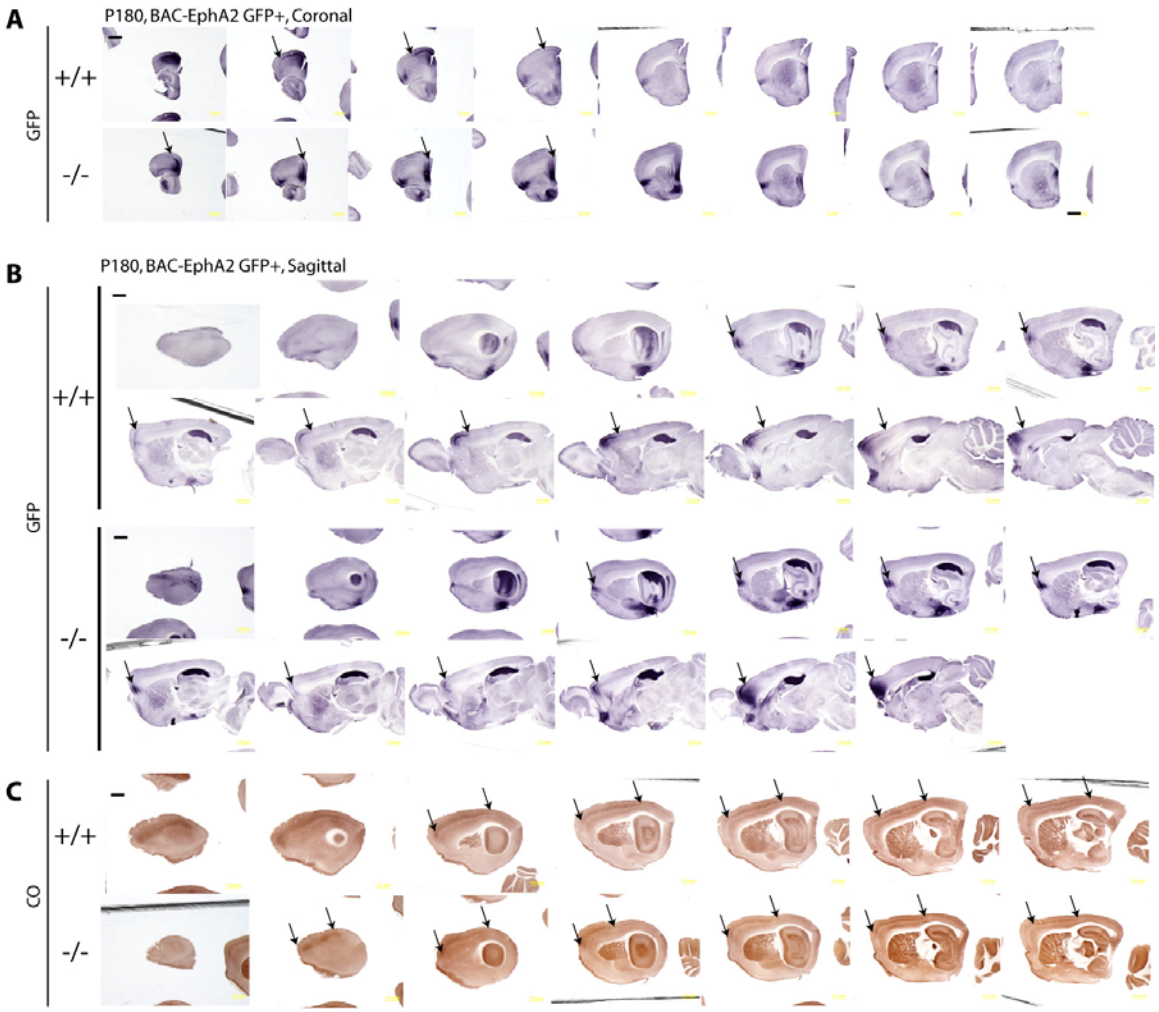

Fig. S8. Reduced FC and complementary rostral shift of caudal cortical features are maintained in the adult *Fgf17*$^{-/-}$ brain. Arrows and arrowheads indicate shifted and maintained borders, respectively. **(A)** Coronal sections of brains from P180 *Fgf17*$^{+/+}$ and *Fgf17*$^{-/-}$ animals containing the BAC-EphA2 transgene, processed for anti-GFP immunohistochemistry (GFP). Left to right: rostral to caudal. **(B)** Sagittal section series from P180 *Fgf17*$^{+/+}$ and *Fgf17*$^{-/-}$ brains containing the BAC-EphA2 transgene, processed as in (A). Left to right: lateral to medial. **(C)** Sagittal section series (adjacent to series in [B]) processed for cytochrome oxidase histochemistry (CO). Scale bars = 1mm.

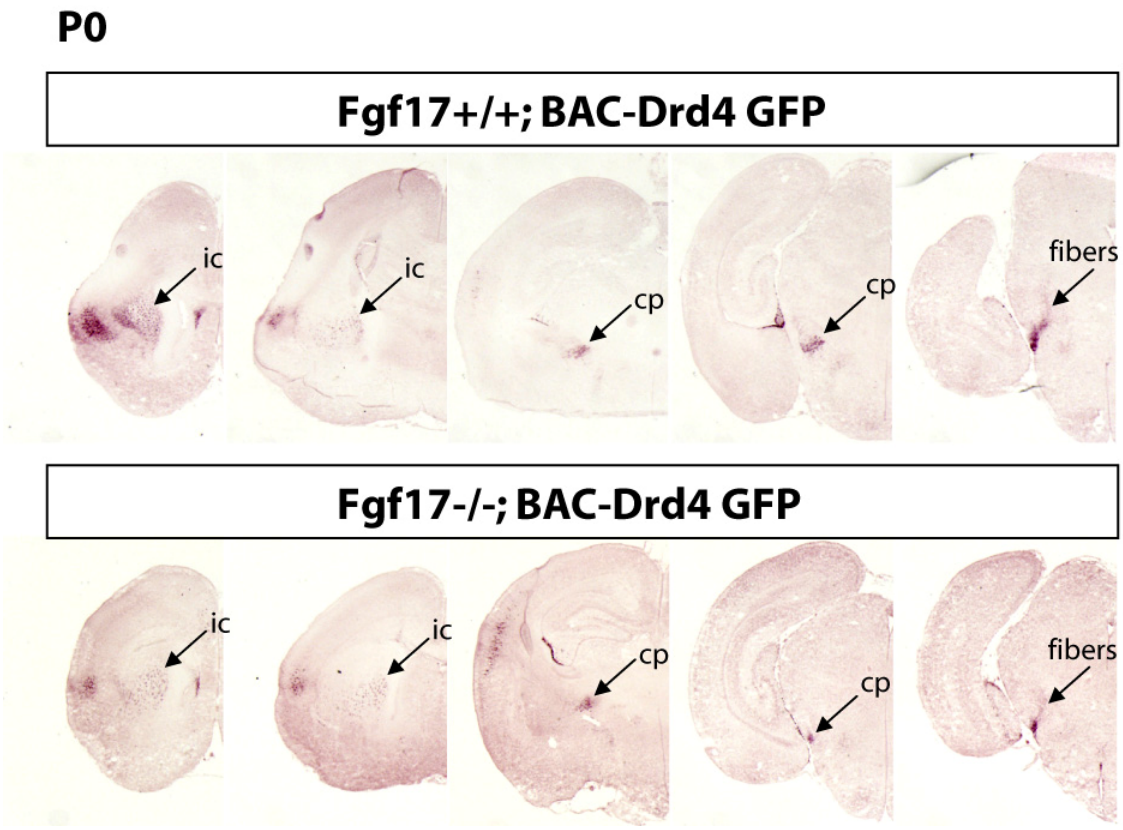

Fig. S9. Anti-GFP immunohistochemistry marks prefrontal cortex efferent projections in *Fgf17*$^{+/+}$ and *Fgf17*$^{-/-}$ P0 brains positive for BAC-Drd4 GFP. Rostral to caudal coronal series shows GFP expression in efferent fibers that project through the internal capsule (ic) to the cerebral peduncle (cp).

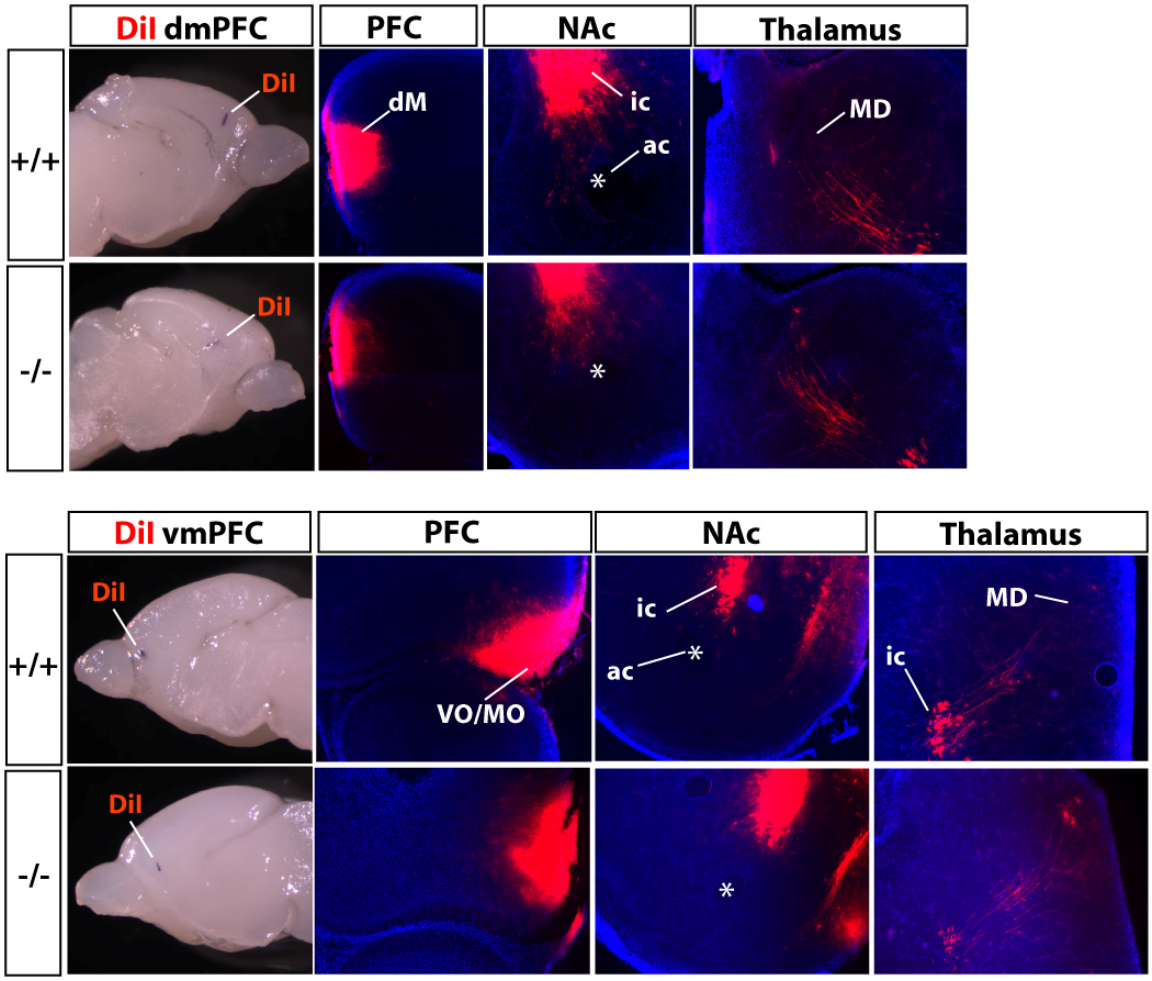

Fig. S10. Medial prefrontal cortex (PFC) connectivity analysis using DiI tracer reveals no major genotype differences. DiI crystals were placed in either the dorsomedial (top two rows) or ventromedial (bottom two rows) PFC of P3 *Fgf17*$^{+/+}$ (n=6) and *Fgf17*$^{-/-}$ (n=4) hemispheres. Coronal sections at the level of the PFC (composite images), nucleus accumbens (NAc), and thalamus showed similar labeling (red) between genotypes. Abbreviations: ac, anterior commissure; dM, dorsomedial FC; ic, internal capsule; MD, mediodorsal thalamus; MO, medial orbital FC; VO, ventral orbital FC.

SUPPORTING MATERIALS AND METHODS

Animals

All mice were housed and handled in accordance with the National Institutes of Health's *Guide for the Care and Use of Laboratory Mice* and the Institutional Animal Care and Use Committee of the University of California, San Francisco. The first 24 hours after birth is considered P0. The *Fgf17* line (1) was maintained on a mixed 129Sv/C57BL/6 background. Homozygous mutants (*Fgf17*$^{-/-}$) were generated using male and female mice heterozygotes (*Fgf17*$^{+/-}$) that had been backcrossed 1 generation to the C57BL/6 background. BAC transgenic lines BAC-Drd4 GFP and BAC-EphA2 GFP (2) were mated to adult *Fgf17*$^{-/-}$ mice to generate double heterozygous mice. Double heterozygous males were then crossed to *Fgf17*$^{+/-}$ females to generate *Fgf17* wild-type (*Fgf17*$^{+/+}$) and *Fgf17*$^{-/-}$ BAC transgene-positive littermates.

Genotyping

Genotyping was performed on genomic DNA obtained from tail clippings using polymerase chain reaction (PCR). Standard reagents were used for all PCR reactions. *Fgf17* primers: (WT allele) 5'-GAAGTTTCTCCAGCGATGGG-3' and 5'-GACAGCAGAGAATCAATAGCTGC-3'; (Mutant allele- Cre) 5'-CCATGAGTGAACGAACCTGG-3' and 5'-TTGGCTTCTCTGGGACTCTAC-3'. Cycle program: 95°C for 10', followed by 35 cycles of 94°C for 45", 58°C for 45", 72°C for 1', then 72°C for 10'. GFP primers: 5'-CCTACGGCGTGCAGTGCTTCAGC-3' and 5'-CGGCGAGCTGCACGCTGCGTCCTC-3'. Cycle program: 95°C for 5', followed by

35 cycles of 95°C for 1', 60°C for 1', 72°C for 1', then 72°C for 10'. Amplified PCR products were electrophoresed on 1% agarose gels and visualized using UV fluorescence.

Tissue Preparation

Embryos were harvested at E10.5 (10 days after vaginal plug date) in cold PBS and transferred to 4% PFA in PBS for overnight fixation at 4°C. Yolk sacs were collected for genotyping. P0 animals were anesthetized on ice and tails collected for genotyping. Brains were dissected in cold PBS and immediately transferred to 4% PFA in PBS for overnight fixation at 4°C. P7 and older animals were deeply anesthetized with 2.5% Avertin and perfusion fixed with fresh 4% PFA in PBS. Brains were removed and post-fixed in 4% PFA for 3-4 hours for immunohistochemistry and overnight for *in situ* hybridization. All fixed tissue was cryoprotected by transferring to 30% sucrose in PBS overnight at 4°C before sectioning. Sections were cut on a freezing cryostat at 16 microns for embryonic, 20 microns for P0-P8 tissue. A freezing microtome was used to cut P7 flattened cortex, P40 and P180 sections in the desired plane at 40 microns. Tissue from adult mice used for behavioral analysis was sectioned on a freezing microtome at 30 microns.

Histology and histochemistry

Cresyl violet (Nissl) staining was performed according to standard methods. Cytochrome oxidase histochemical staining was performed as described previously (3).

In situ hybridization

Digoxigenin (DIG)-labeled riboprobes were generated for the following genes: *Cadherin-6*, *Cadherin-8* (3), *Fgf8* (4), *Fgf17* (5), *Id-2* (3), *Lmo3* and *Lmo4* (6), *Neurogenin-2* (7), *Neurotrophin-3* (gift from L. Ma), *RZR-β* (3) and *Steel* (gift from E. Grove). Section and wholemount *in situ* hybridization were performed as described previously in (3) and (8), respectively.

Immunohistochemistry

Immunohistochemistry was performed using standard protocols (3) with the following antibodies: rabbit anti-GFP (1:1000; Molecular Probes, Eugene, OR), rabbit anti-tyrosine hydroxylase (1:500; Chemicon, Temecula, CA), rabbit anti-serotonin (1:50,000; Immunostar, Hudson, WI), and detected with goat anti-rabbit biotinylated secondary antibody (1:200-1:400; Vector Laboratories, Burlingame, CA) and ABC kit (Vector).

Axon tracing

P0 brains were stored in 4% PFA in PBS at 4°C. Single crystals of the fluorescent carbocyanide dye DiI (1,1'-dioctadecyl 3,3,3',3'-tetramethylindocarbocyanine perchlorate; Molecular Probes) were placed in various rostral cortical locations (9). After storage at room temperature in 4% PFA in PBS for 4 weeks to several months, brains were embedded in 5% agarose and sectioned coronally at 100 μm using a vibratome. Sections were immediately mounted on slides and a coverslip was applied using Vectashield mounting medium with DAPI (Vector). Digital images were taken using a SPOT (Diagnostic Instruments) on a fluorescent microscope.

Digital Imaging

Whole brains and sections were photographed using SPOT (Diagnostic Instruments) and Olympus digital cameras and imaging software. Brains from BAC transgenic-positive litters were imaged by fluorescence microscopy prior to post-fixation. P0 and adult brains were photographed under regular light-microscopy prior to post-fixation.

Quantification of cortical areas

Areas were determined using photos of dorsally-viewed whole mount brains in Scion Image (Scion Corp), and measurements were performed blind to genotype. All photos were taken at identical magnification. Measurements were made in pixels (arbitrary units). Total cortical area for P0 and adult analyses included the neocortex and lateral edge of the hippocampus. To correct for possible cortical size differences, a ratio of *Lmo4*+ dorsal FC area to total cortical area was calculated (frontal ratio). Excel (Microsoft) was used for calculations and statistical analysis.

References

1. Xu, J., Liu, Z. & Ornitz, D. M. (2000) *Development* **127,** 1833-43.
2. Gong, S., Zheng, C., Doughty, M. L., Losos, K., Didkovsky, N., Schambra, U. B., Nowak, N. J., Joyner, A., Leblanc, G., Hatten, M. E. & Heintz, N. (2003) *Nature* **425,** 917-25.
3. Rubenstein, J. L., Anderson, S., Shi, L., Miyashita-Lin, E., Bulfone, A. & Hevner, R. (1999) *Cereb Cortex* **9,** 524-32.
4. Crossley, P. H. & Martin, G. R. (1995) *Development* **121,** 439-51.
5. Xu, J., Lawshe, A., MacArthur, C. A. & Ornitz, D. M. (1999) *Mech Dev* **83,** 165-78.
6. Bulchand, S., Subramanian, L. & Tole, S. (2003) *Dev Dyn* **226,** 460-9.
7. Fode, C., Gradwohl, G., Morin, X., Dierich, A., LeMeur, M., Goridis, C. & Guillemot, F. (1998) *Neuron* **20,** 483-94.
8. Hamasaki, T., Leingartner, A., Ringstedt, T. & O'Leary, D. D. (2004) *Neuron* **43,** 359-72.

9. Godement, P., Vanselow, J., Thanos, S. & Bonhoeffer, F. (1987) *Development* **101,** 697-713.

Chapter 3

Fgf17 and *Emx2* antagonistic interactions pattern frontal cortex subdivisions

ABSTRACT

The frontal cortex (FC) plays a major role in cognition, movement and behavior. However, little is known about the genetic mechanisms that govern its development. We recently described a panel of gene expression markers that delineate neonatal FC subdivisions and identified FC regionalization defects in *Fgf17*$^{-/-}$ mutant mice (Cholfin and Rubenstein, 2007). In the present study, we applied this FC gene expression panel to examine regionalization phenotypes in *Fgf8*$^{n/n}$, *Emx2*$^{-/-}$, and *Emx2*$^{-/-}$*;Fgf17*$^{-/-}$ newborn mice. We report that *Fgf8*, *Fgf17* and *Emx2* play distinct roles in the molecular regionalization of FC subdivisions. The changes in regionalization are presaged by differential effects of rostral patterning center *Fgf8* and *Fgf17* signaling on the rostral cortical neuroepithelium, revealed by altered expression of *Spry1* and *Spry2*, and "rostral" transcription factors *Er81*, *Erm*, *Pea3* and *Sp8*. We used *Emx2*$^{-/-}$;*Fgf17*$^{-/-}$ double mutants to provide direct evidence that *Emx2* and *Fgf17* antagonistically regulate the expression of *Erm*, *Pea3* and *Er81* in the rostral cortical neuroepithelium and FC regionalization. We have integrated our results to propose a model for how FGFs regulate FC patterning through regulation of the transcription factor expression.

INTRODUCTION

The frontal cortex (FC) is an anatomically and functionally heterogeneous brain structure that has a central role in higher cognitive function and behavioral control (Fuster, 2001; Heidbreder and Groenewegen, 2003; Uylings et al., 2003; Dalley et al., 2004; Price, 2006). The FC can be subdivided into a number of histologically distinct areas that differ in function (Zilles and Wree, 1995; Heidbreder and Groenewegen, 2003; Uylings et al., 2003; Dalley et al., 2004). Although adult FC anatomy and function has been well-studied, little is known about how FC subdivisions are patterned during development.

The prevailing model of cortical patterning suggests that members of the fibroblast growth factor (FGF) family, secreted from the rostral patterning center, pattern the neocortex in part by controlling the expression of transcription factors and other regulatory molecules in the cortical neuroepithelium (reviewed in (O'Leary and Nakagawa, 2002; Grove and Fukuchi-Shimogori, 2003; Garel and Rubenstein, 2004; Sur and Rubenstein, 2005)). Currently, four *FGF* genes , *Fgf8, Fgf15*, *Fgf17* and *Fgf18,* are known to be expressed in the rostral patterning center (Crossley and Martin, 1995; Hoshikawa et al., 1998; Maruoka et al., 1998; Xu et al., 1999; Bachler and Neubuser, 2001). Several transcription factors are implicated in cortical patterning, including *COUP-TF1, Emx2, Foxg1, Lhx2* and *Pax6* (Dou et al., 1999; Bishop et al., 2000; Mallamaci et al., 2000; Toresson et al., 2000; Monuki et al., 2001; Zhou et al., 2001; Bishop et al., 2002; Muzio et al., 2002a, 2002b; Bishop et al., 2003; Hamasaki et al., 2004; Shinozaki et al., 2004); among these most information is known about *Emx2*. Both

loss of function and gain of function experiments demonstrate that the level of *Emx2* expression in the cortical neuroepithelium provides positional information that contributes to regional differences in cortical identity (Bishop et al., 2000; Mallamaci et al., 2000; Bishop et al., 2002; Hamasaki et al., 2004).

Previous work has identified functions for the *FGFs* in cortical patterning. Manipulations of Fgf8 and Fgf17 levels *in utero* or in ovo show that they can act as anterior-posterior patterning molecules in the cortex in part through repression of *Emx2* expression (Crossley et al., 2001; Fukuchi-Shimogori and Grove, 2001, 2003). *Fgf8* hypomorphic ($Fgf8^{n/n}$ and $Fgf8^{n/null}$) mice have decreased FC size (including both dorsal and orbital parts) and rostral shifts of caudal cortical areas associated with rostral expansion of *Emx2* expression (Garel et al., 2003; Storm et al., 2006). Conversely, *Emx2* null ($Emx2^{-/-}$) mice have an expanded rostral cortex and reduced caudal cortex (Bishop et al., 2000; Mallamaci et al., 2000; Bishop et al., 2002). *Emx2* can both negatively regulate *Fgf8* signaling and directly specify the identity of neural progenitors (Fukuchi-Shimogori and Grove, 2003; Hamasaki et al., 2004). Thus, *Fgf8* and *Emx2* have reciprocal repressive interactions. Analysis of compound *Fgf;Emx2* mutants would be an effective approach to directly demonstrate their *in vivo* interactions in cortical patterning. Unfortunately, *Fgf8* and *Emx2* are closely linked on mouse chromosome 19, making it difficult to generate the double mutant. We have circumvented this problem by assessing the phenotype of *Emx2;Fgf17* double mutants. Our analysis demonstrated that loss of *Fgf17* rescues a specific subset of cortical defects in *Emx2* mutants.

The analysis of *Emx2;Fgf17* mutants depended on the use of a panel of gene expression markers that delineate neonatal mouse FC subdivisions (Cholfin and

Rubenstein, 2007). Here we demonstrate that *Fgf8, Fgf17* and *Emx2* have distinct roles in FC patterning. At birth, $Fgf8^{n/n}$ brains display reduced dorsal and orbital FC, $Fgf17^{-/-}$ mutants have a selective loss of dorsal FC molecular properties (Cholfin and Rubenstein, 2007), whereas $Emx2^{-/-}$ mutants have an expansion of dorsal and orbital FC molecular subdivisions. By examining changes in regionally-expressed transcription factors (*COUP-TFI*, *Emx2*, *Er81*, *Erm*, *Pea3* and *Sp8*) and other FGF-responsive genes (*Spry1* and *Spry2*), we provide evidence for the mechanisms through which *Fgf8* and *Fgf17* regulate FC patterning.

METHODS

Mouse lines and genotyping

Fgf17 (Xu et al., 2000), *Fgf8* (Meyers et al., 1998) and *Emx2* (Pellegrini et al., 1996) alleles were maintained on a mixed 129Sv/C57BL/6 background. Heterozygotes were crossed to generate homozygous mutants. For the $Emx2^{-/-};Fgf17^{-/-}$ genotype, double heterozygous mice were generated by an intercross of $Fgf17^{+/-};Emx2^{+/-}$ mice, which are viable and fertile. PCR genotyping was performed as described (Pellegrini et al., 1996; Garel et al., 2003). For embryo staging, noon on the day of the vaginal plug was considered embryonic day 0.5 (E0.5).

In situ hybridization, immunohistochemistry and TUNEL

Embryos and brains were fixed overnight in 4% paraformaldehyde in PBS at 4°C. In situ hybridization was performed on 10-20 μm cryostat sections as described previously (Rubenstein et al., 1999). Digoxigenin (DIG)-labeled riboprobes were generated for the following genes: *Cadherin-6*, *Cadherin-8* (Rubenstein et al., 1999), *COUP-TF1* (gift from M. Tsai), *Emx2* (gift from A. Simeone), *EphrinA5* (Bishop et al., 2002), *Er81* (gift from T. Jessell), *Erm* (gift from A. Chotteau-Lelievre), *Fgf8* (Crossley and Martin, 1995), *Fgf15* (Gimeno et al., 2003), *Fgf17* (Xu et al., 1999), *Fgf18* (Maruoka et al., 1998), *Id-2* (Rubenstein et al., 1999), *Lmo3* and *Lmo4* (Bulchand et al., 2003), *Neurogenin-2* (Fode et al., 1998), *Neurotrophin-3* (gift from L. Ma), *Pea3* (gift from A. Chotteau-Lelievre), *RZR-β* (Rubenstein et al., 1999), *Sp8* (gift from J.C. Belmonte), *Sprouty (Spry) 1* and *2* (gift from G. Martin), and *Steel* (gift from E. Grove).

Immunohistochemistry was performed on 10-16 μm cryostat sections as described previously (Rubenstein et al., 1999). Rabbit anti-phosphohistone-3 (PH3) (Upstate) and rabbit anti-phosphorylated Erk (Cell Signaling) were used as primary antibodies. TUNEL was performed on 16 μm cryostat sections using the ApopTag Plus Peroxidase kit (Chemicon). Images were acquired using an Olympus digital camera system and imaging software.

RESULTS

Abnormal FC molecular properties in cortical patterning mutants

We have developed a panel of gene expression markers to define immature FC subdivisions in the neonatal mouse (Cholfin and Rubenstein, 2007). These markers demonstrated that *Fgf17*$^{-/-}$ mutants show a selective deficit in the dorsal FC (Cholfin and Rubenstein, 2007). Here, we applied the same panel to *Fgf8*$^{n/n}$ and *Emx2*$^{-/-}$ postnatal day 0 (P0) mutants. For purposes of comparison, we also show the wild-type (Figs. 1A-F, S1) and *Fgf17*$^{-/-}$ mutant (Figs. 1A"-F", S2).

Fig. 1.

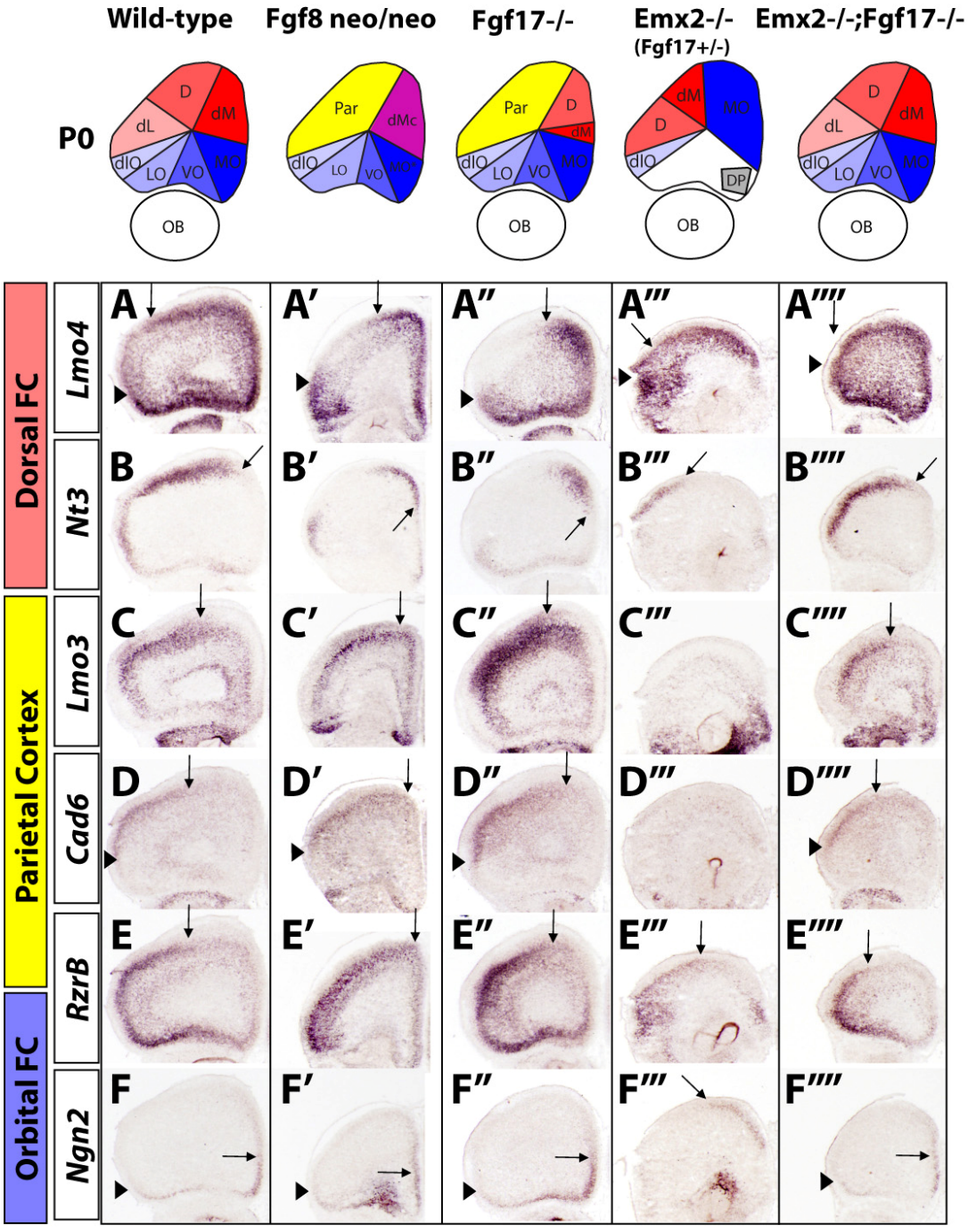

Fig. 1. *Fgf8/17* and *Emx2* antagonistically regulate FC regionalization. Top row: schema showing a summary of changes in P0 FC molecular subdivisions. Dorsal FC is in red, ventral/orbital FC is in blue, and parietal cortex is in yellow. In situ hybridization (ISH) on P0 wild-type (A-F), $Fgf8^{n/n}$ (A'-F'), $Fgf17^{-/-}$ (A"-F"), $Emx2^{-/-};Fgf17^{+/-}$ (A'''-F''') and $Emx2^{-/-};Fgf17^{-/-}$ (A''''-F'''') coronal sections for the following genes: *Lmo4, Nt3, Lmo3, Cad6, Rzr-β,* and *Ngn2*. The wild-type and $Fgf17^{-/-}$ series were published previously (Cholfin and Rubenstein, 2007) and are shown here with permission for purposes of comparison. FC phenotypes of $Emx2^{-/-}$ and $Emx2^{-/-};Fgf17^{+/-}$ mutants were comparable; sections from a $Emx2^{-/-};Fgf17^{+/-}$ brain are shown. Arrows signify shifted borders, while arrowheads indicate maintained borders.

Abbreviations: D, dorsal FC; DP, dorsal peduncular cortex; dlO, dorsolateral orbital cortex; dM, dorsomedial FC; dMc, caudal dorsomedial FC; LO, lateral orbital cortex; MO, medial orbital cortex; OB, olfactory bulb, Par, parietal cortex; VO, ventral orbital cortex.

Fgf8$^{n/n}$ mutants were described previously to have a small FC based on changes in *Id2* and *Cad6* expression (Garel et al., 2003); at that time we did not have the tools to define region-specific defects within the FC. Here we characterized the FC regionalization defects by examining expression of: *Lmo4*, *Cad8*, *Id2*, *Steel*, *Nt3*, *Ngn2*, *Rzr-β*, *Cad6*, *Lmo3* and *EphrinA5* (Figs. 1A'-F', S3). *Fgf8*$^{n/n}$ mutants displayed medially (dorsally) shifted dorsal expression borders of *Lmo4*, *Cad8*, *Id2*, *Steel* and *Nt3* (Figs. 1A'-B', S3). These changes were complemented by a rostromedial expansion of *Lmo3*, *Cad6*, *Rzr-β* and *EphrinA5* expression in the parietal cortex (Figs. 1C'-E', S3). The medial aspect of the FC (formerly regions dM and MO) had molecular and histological features that resemble more caudal structures (caudal dorsomedial FC; dMc) – we postulate that much of this region is transformed into dorsal and ventral anterior cingulate cortex.

Fgf8$^{n/n}$ mutants maintain expression of orbital cortex markers (*Lmo4*, *Cad8*, *Id2*, *Steel*, *Nt3*, *Lmo3*, *Rzr-β* and *Ngn2*), although this region is much smaller than in wild-type brains (see column 1 in Fig. S3). Thus, reduction in Fgf8 dosage reduces the overall size of the FC, and leads to caudalization of the dorsal and dorsomedial FC.

Previous studies have established that in *Emx2*$^{-/-}$ mutants the rostral cortex expands caudally at the expense of a reduced occipital (visual) cortex (Bishop et al., 2000; Mallamaci et al., 2000; Bishop et al., 2002); an analysis of FC patterning has not been performed in these mutants. The *Emx2*$^{-/-}$ FC showed expanded dorsal expression of *Lmo4*, *Cad8*, *Id2*, and *Steel* and laterally (ventrally) shifted dorsal *Nt3* expression (Figs. 1A'''-B''', S4)(note: *Emx2*$^{-/-}$ and *Emx2*$^{-/-}$*;Fgf17*$^{+/-}$ mutants were indistinguishable; data

not shown). This suggests that dorsal FC subdivisions (regions dM, D and dL) were expanded and/or shifted caudolaterally. Strong expression of *Lmo3*, *Cad6* and *EphrinA5* (parietal cortex markers) was located more caudally (Figs. 1C'''-D''', S4), consistent with the known caudal shift of the parietal cortex that is complementary to the expansion/shift of the dorsal FC.

Surprisingly, *Emx2*$^{-/-}$ mutants lose orbital FC expression of *Lmo4*, *Cad8*, *Id2*, *Steel*, *Nt3*, *Lmo3*, *Rzr-β*, and *Ngn2* (Figs. 1A'''-F''', S4). Although this initially suggested a loss of orbital cortex, more detailed analysis provided evidence for an alternative explanation. Strong *Ngn2* expression is normally limited to the ventromedial FC (orbital cortex) (Figs. 1F, S1). However, in the mutants, this strong expression was present in a more dorsal location (Figs. 1F''', S4). This suggests that the medial orbital cortex is shifted to a more dorsal position. We are uncertain about the identity of the tissue that remains in the position of the orbital cortex.

Given the complementary FC phenotypes between the *Fgf* and *Emx2* mutants, we tested whether the genetic programs downstream of these genes interact. To do this, we generated *Emx2*$^{-/-}$*;Fgf17*$^{-/-}$ double mutants. Indeed, *Emx2*$^{-/-}$*;Fgf17*$^{-/-}$ P0 mutants had FC regionalization phenotypes intermediate to *Fgf17*$^{-/-}$ and *Emx2*$^{-/-}$ single mutants for all FC markers examined (Figs. 1A''''-F'''', S5-6), demonstrating that loss of *Fgf17* can partially rescue the *Emx2*$^{-/-}$ FC regionalization defects (and vice-versa). Together, these results provide strong evidence that *Fgf17* and *Emx2* antagonistically regulate regionalization of FC subdivisions *in vivo*.

Rostral patterning center signaling is differentially regulated by *Fgf8*, *Fgf17* and *Emx2*

To investigate the mechanisms by which *Fgf8*, *Fgf17* and *Emx2* regulate FC regionalization, we first expanded on previous findings (Maruoka et al., 1998; Bachler and Neubuser, 2001; Gimeno et al., 2003) by examining the expression domains of *Fgf8*, *Fgf17*, *Fgf15* and *Fgf18* mRNA in the rostral telencephalon of embryonic day (E) 10.5 and E12.5 embryos. Furthermore, we assessed FGF signaling in the rostral neuroepithelium by examining the expression of *FGF*-induced signaling antagonists *Spry1* and *Spry2* (Fukuchi-Shimogori and Grove, 2001; Zhang et al., 2001; Fukuchi-Shimogori and Grove, 2003; Storm et al., 2003).

Fig. 2

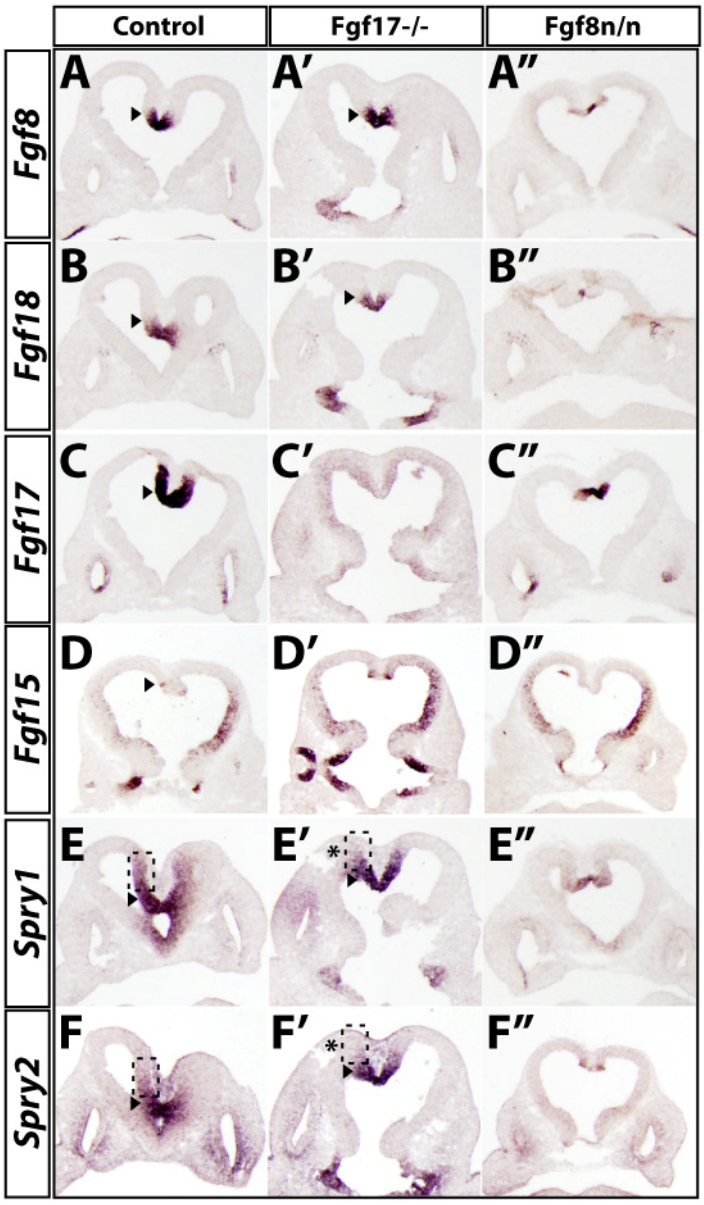

Fig. 2. Differential regulation of rostral patterning center signaling by Fgf8 and Fgf17 at E10.5. In situ hybridization on wild-type (A-F), *Fgf17*$^{-/-}$ (A'-F') and *Fgf8*$^{n/n}$ (A"-F") horizontal sections for *Fgf8*, *Fgf18*, *Fgf17*, *Fgf15*, *Spry1* and *Spry2*. Arrowheads point to the limit of the core *Fgf8* expression domain. Boxed areas of adjacent neuroepithelium are shown. Asterisks indicate reduced *Spry1* and *Spry2* expression in the *Fgf17*$^{-/-}$ mutant neuroepithelium.

At E10.5, *Fgf8* and *Fgf18* were expressed in similar domains in the commissural plate (Fig. 2A-B). By contrast, *Fgf17* was expressed in a broader domain, particularly in

the dorsal dimension (Fig. 2C). *Fgf15* was also expressed more broadly than *Fgf8* and *Fgf18*; unlike *Fgf17, Fgf15* expression extends ventrally (Fig. 2D). *Spry1* and *Spry2* expression correlated with *Fgf8, Fgf17* and *Fgf18* expression, but not with the ventral domain of *Fgf15*, and was strongest at the midline and slightly weaker dorsally (Fig. 2E-F). Thus, *Spry1* and *Spry2* are expressed at the highest levels where there is overlap with *Fgf8/Fgf18* expression, and at slightly lower levels in neuroepithelium that is positive for *Fgf17* and negative for *Fgf8* mRNA.

Fig. 3

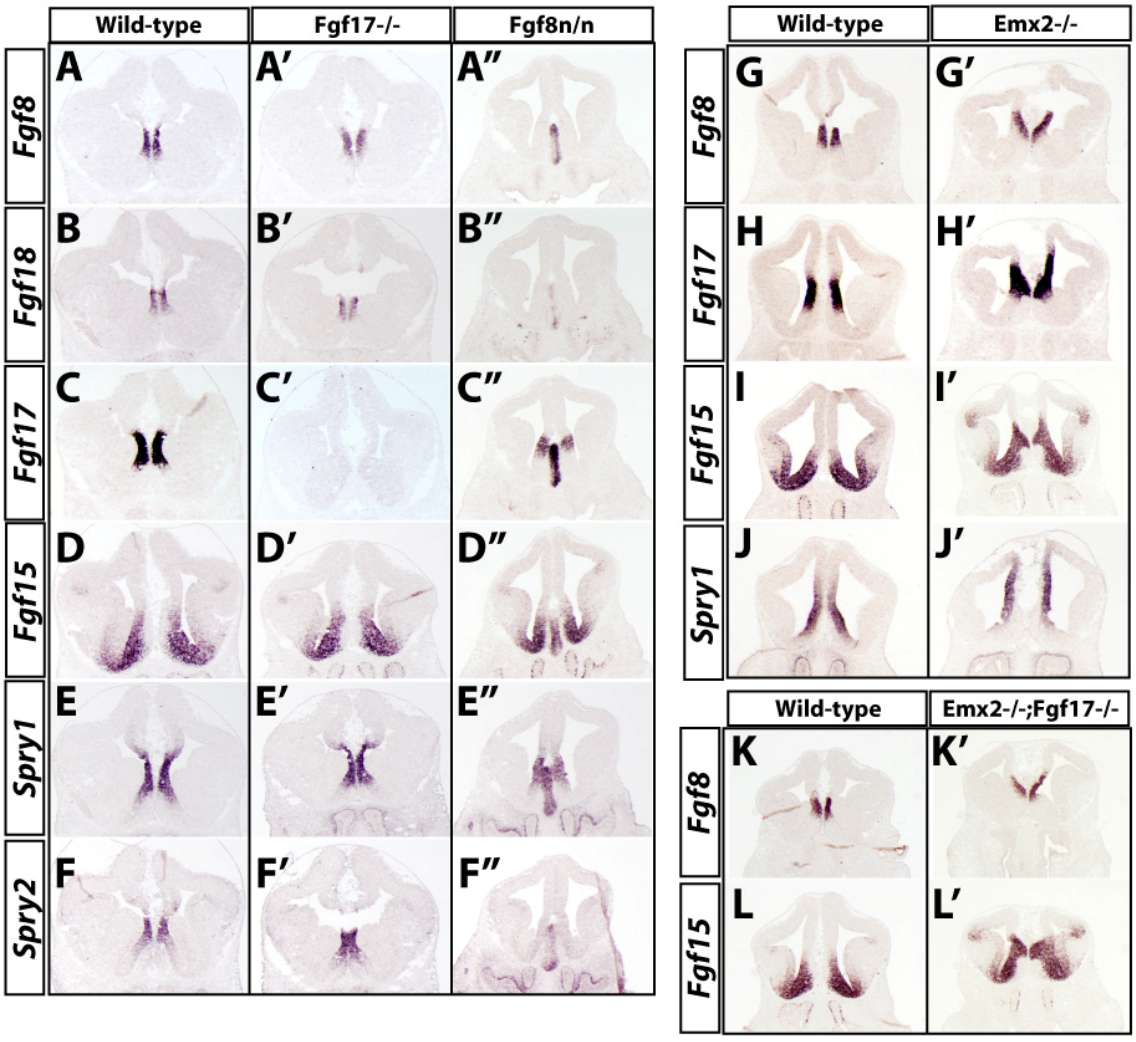

Fig. 3. Differential regulation of rostral patterning center signaling by *Fgf8*, *Fgf17* and *Emx2* at E12.5.

(A-F") ISH on coronal sections from wild-type (A-F), *Fgf17*$^{-/-}$ (A'-F'), and *Fgf8*$^{n/n}$ (A"-F") brains for *Fgf8*, *Fgf18*, *Fgf17*, *Fgf15*, *Spry1* and *Spry2*.
(G-J') ISH on coronal sections from wild-type (G-J) and *Emx2*$^{-/-}$ (G'-J') brains for *Fgf8*, *Fgf17*, *Fgf15* and *Spry1*.
(K-L') ISH on coronal sections from wild-type (K-L) and *Emx2*$^{-/-}$*;Fgf17*$^{-/-}$ (K'-L') brains for *Fgf8* and *Fgf15*.

At E12.5, *Fgf8* and *Fgf18* were expressed in very similar domains in the presumptive septum (Figs. 3A-B, S7). *Fgf17* expression overlapped with *Fgf8* and *Fgf18*, but extended into regions that were ~200μm more rostral than *Fgf8* (Figs. 3C, S7, S12). *Fgf15* expression overlapped with the other FGFs in a small region of the septum, and extended into a distinct domain in the rostroventral telencephalon that appears to include the olfactory bulb rudiment (Figs. 3D, S7). *Fgf15* was also expressed in small domains at the pallial/subpallial and the lateral ganglionic eminence/medial ganglionic eminence boundaries (Figs. 3D, S7). *Spry1* and *Spry2* expression overlapped with *Fgf8*, *Fgf17* and *Fgf18* expression and extended more broadly into the rostrodorsal neuroepithelium than these FGFs (Figs. 3E-F, S7). Therefore, *Fgf8* and *Fgf18* are expressed in a core domain within the septum, from which *Fgf17* expression extends rostrodorsally and *Fgf15* extends rostroventrally. Based on *Spry1/2* expression, FGF signaling is highest within the core domain and extends outward into the rostral telencephalon.

We examined *FGF* expression and signaling in *Fgf17*$^{-/-}$ and *Fgf8*$^{n/n}$ E10.5 and E12.5 mutants. In *Fgf17*$^{-/-}$ mutants, we found no overt change in *Fgf8, Fgf15 and Fgf18* expression. (Figs. 2A'-D', 3A'-D', S8). However, we found a reduction in *Spry1* and *Spry2* expression selectively in the rostrodorsal neuroepithelium, but not in the core (Figs. 2E'-F', 3E'-F', S8). Therefore, *Fgf17*$^{-/-}$ mutants retain the core domain FGF signaling, while the more rostral and dorsal neuroepithelia have decreased FGF signaling.

By contrast, E10.5 and E12.5 *Fgf8*$^{n/n}$ mutants had a severe reduction of *Fgf18* expression and a reduction in the size of the *Fgf17* expression domain; we did not detect a change in *Fgf15* expression (Figs. 2B"-D", 3B"-D", S9). At E10.5, the *Fgf17* expression domain was reduced to approximately the size of the wild-type *Fgf8* domain (compare Fig. 2A, C and C"); correspondingly, *Spry1* and *Spry2* expression was reduced (Fig. 2E"-F"). At E12.5, both *Spry1* and *Spry2* were reduced in the rostrodorsal neuroepithelium (Figs. S9, S12). Thus, *Fgf8*$^{n/n}$ mutants have both a shrunken FGF core domain and smaller rostro-dorsal penumbra of *Fgf17* expression and signaling.

Previously, *Emx2* was found to repress *Fgf8* and *Fgf17* expression in experiments that studied wholemount embryos and tissue explants (Fukuchi-Shimogori and Grove, 2003). We examined the precise spatial relationships of *Fgf8*, *Fgf15*, *Fgf17* and *Spry1* expression in adjacent coronal sections from E12.5 *Emx2*$^{-/-}$ mutants (Figs. 3G'-J', S10). *Fgf8* and *Fgf17* expression appeared more intense and extended more dorsally (Figs. 3G'-H', S10). *Fgf15* expression was clearly increased in intensity, and expanded dorsally into the rostral cortex (Figs. 3I', S10). More caudally, *Fgf15* expression in the pallial/sub-pallial boundary was greatly increased and extended farther dorsally into the cortical neuroepithelium (Fig. S10). The expanded *FGF* expression was correlated with increased *Spry1* expression, suggesting an increase in FGF signaling (Figs. 3J', S10).

Finally, we found that the expanded *Fgf8* and *Fgf15* expression domains were not rescued in E12.5 *Emx2*$^{-/-}$;*Fgf17*$^{-/-}$ double mutants (Figs. 3K'-L', S11), suggesting that *Fgf17* expression is selectively lost without affecting the increase/expansion of *Fgf8* and *Fgf15* expression.

Fgf8, *Fgf17*, and *Emx2* differentially regulate transcription factor expression in the the presumptive frontal cortex neuroepithelium

To explore how changes in *FGF* expression and signaling transduce changes in FC fate and growth, we studied the expression of transcription factors that have been previously implicated in cortical patterning and arealization (*Emx2*, *COUP-TF1*) (Bishop et al., 2000; Mallamaci et al., 2000; Zhou et al., 2001; Bishop et al., 2002; Hamasaki et al., 2004) in coronal sections of E12.5 brains. In parallel, we examined the expression of genes that respond to FGF-signaling (*Sp8*, *Erm*, *Pea3*, *Er81*) (Bell et al., 2003; Fukuchi-Shimogori and Grove, 2003; Kawakami et al., 2004; Storm et al., 2006), but whose functions in cortical patterning are unknown.

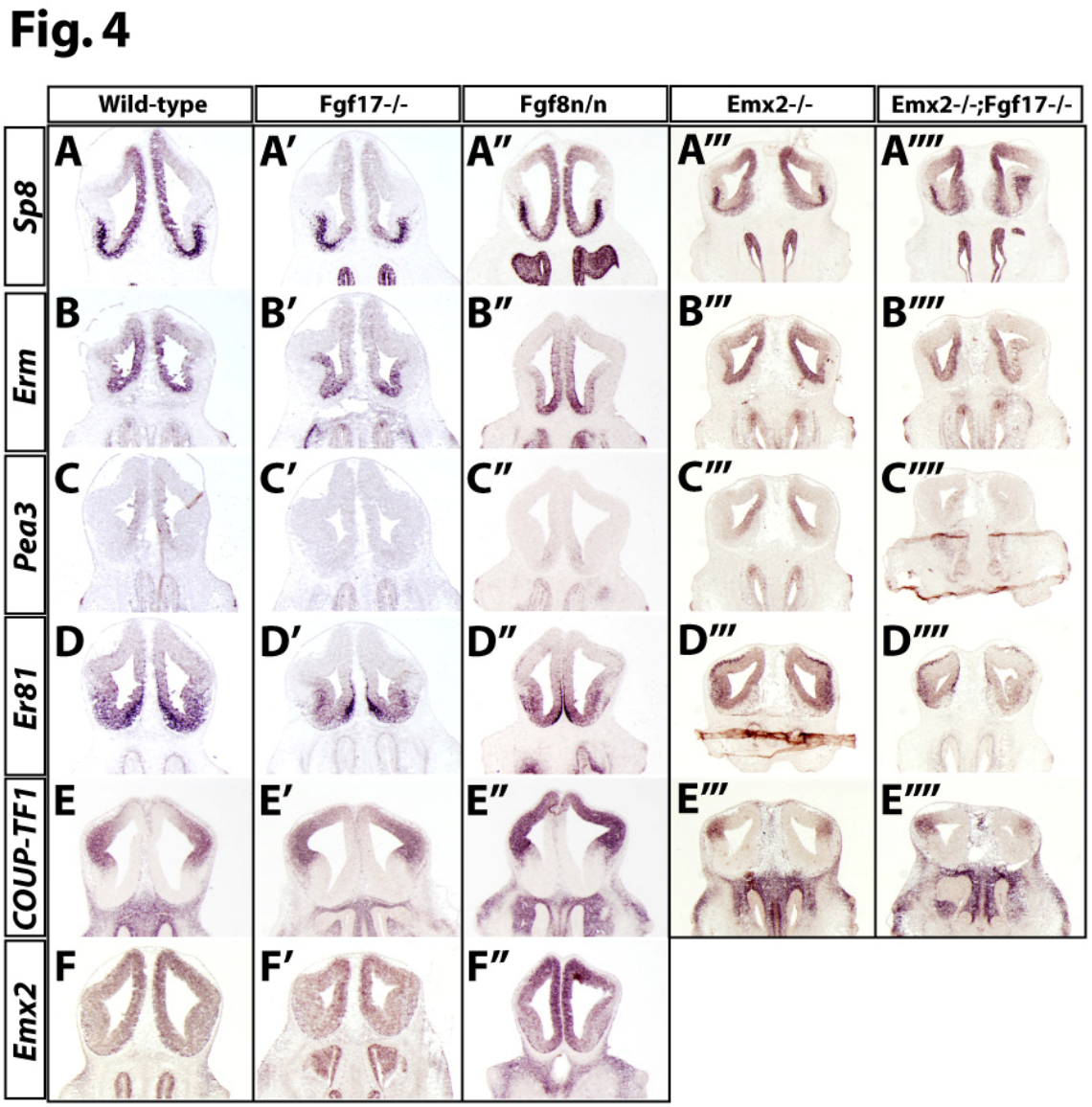

Fig. 4. *Fgf8*, *Fgf17* and *Emx2* differentially control expression of transcription factors in the rostral cortical primordium. ISH on E12.5 wild-type (A-F), *Fgf17*$^{-/-}$ (A'-F'), *Fgf8*$^{n/n}$ (A"-F"), *Emx2*$^{-/-}$ (A'''-E'''), *Emx2*$^{-/-}$*;Fgf17*$^{-/-}$ (A''''-E'''') coronal sections for *Sp8*, *Erm*, *Pea3*, *Er81*, *COUP-TF1* and *Emx2*.

In wild-type E12.5 embryos, *Sp8*, *Erm* and *Pea3* were expressed in high-rostromedial to low-caudolateral gradients in the medial wall of the rostral telencephalic neuroepithelium (Figs. 4A-C, S7). *Sp8* was the most broadly expressed of these "rostral" transcription factors; in addition to its expression in the medial wall of the FC, its dorsal expression extended caudally throughout the entire dorsomedial wall including the

anlagae of the cingulate cortex and hippocampus (Fig. S7). The expression of *Erm* and *Pea3* was more localized to the rostral neuroepithelium (Fig. S7). *Sp8*, *Erm* and *Pea3* were also expressed in overlapping domains within the subpallial telencephalon (Fig. S7). *Er81* was expressed in a high-ventral to low-dorsal gradient in the medial cortical progenitor zone (similar to *Fgf15*), in a discrete layer of cells in the cortical mantle, and in the ventricular zone and mantle of the rostral subpallial telencephalon (Figs. 4D, S7).

The expression of *Emx2* and *COUP-TF1* differed in the rostral cortical neuroepithelium. *Emx2* was expressed in a high-dorsomedial to low-ventrolateral gradient, while *COUP-TF1* was expressed in an opposing high-ventrolateral to low-dorsomedial gradient (Figs. 4E-F, S7). Consistent with previous observations, (Bishop et al., 2000; O'Leary and Nakagawa, 2002; Garel et al., 2003), both *Emx2* and *COUP-TF1* were expressed in high-caudal to low-rostral gradients that extended to the rostral pole (Fig. S7).

Fgf17$^{-/-}$ brains displayed a selective reduction in the dorsomedial expression of *Sp8*, *Erm, Pea3* and *Er81*, which was most evident in the most rostral sections (Figs. 4A'-D', S8). Expression of these genes appeared unaltered in subpallial telencephalic regions that overlap with the maintained *Fgf15* expression (Figs. 3D', S8). On the other hand, *COUP-TF1* expression was stronger in the most rostral sections (Figs. 4E', S8). We did not detect an overt difference in *Emx2* expression (Figs. 4F', S8).

Fgf8$^{n/n}$ mutants exhibited related but distinct changes in transcription factor expression in the rostral cortical primordium. Unlike in the *Fgf17*$^{-/-}$ mutants, *Sp8* expression was not appreciably altered (Figs. 4A", S9). *Erm* and *Er81* expression were strongly reduced in the dorsal FC ventricular zone, whereas their expression in the

dorsomedial wall was preserved (unlike in *Fgf17*$^{-/-}$ mutants) (Figs. 4B", D", S9). *Pea3* expression was reduced in the medial ventricular zone (Fig. 4C", S9). Compared to *Fgf17*$^{-/-}$ mutants, the *Emx2* gradient in *Fgf8*$^{n/n}$ mutants was more strongly shifted rostrally, with increased expression in the dorsomedial ventricular zone (Figs. 4E"-F", S9), consistent with previous findings in *Fgf8*$^{n/n}$ and *Fgf8*$^{null/n}$ mutants (Garel et al., 2003; Storm et al., 2006).

Emx2$^{-/-}$ mutants showed increased dorsomedial ventricular zone expression of *Sp8*, *Erm*, and *Pea3* (Figs. 4A'''-C''', S10). *Er81* expression was upregulated in the lateral, dorsal and medial cortical ventricular zone and was ectopically expressed in the dorsolateral cortical preplate (Figs. 4D''', S10). Conversely, *COUP-TF1* displayed complementary reduced expression in the dorsomedial cortical progenitor zone (Figs. 4E''', S10), consistent with a caudolateral shift in its gradient described previously (Muzio and Mallamaci, 2003).

Finally, we examined *Sp8*, *Erm*, *Pea3*, *Er81* and *COUP-TF1* expression in E12.5 *Emx2*$^{-/-}$*;Fgf17*$^{-/-}$ double mutants to test whether *Emx2* and *Fgf17* have opposing functions in cortical patterning. *Erm*, *Pea3* and *Er81* expression in the rostral cortical progenitor zone was more similar to the wild type brain than either the *Emx2*$^{-/-}$ or *Fgf17*$^{-/-}$ mutants (Figs. 4B''''-D'''', S11). By contrast, *Sp8* and *COUP-TF1* expression was not overtly rescued; nor was the ectopic expression of *Er81* in the cortical preplate (Figs. 4A'''', D'''', E'''', S11). These results provide strong evidence for genetic antagonism between *Fgf17* and *Emx2* in regulating *Erm*, *Pea3* and *Er81* expression in FC progenitors.

Cell proliferation, apoptosis and MAP kinase activation are not overtly affected in *Fgf17*$^{-/-}$ mutants

Previous work has found that *Fgf8* has a dosage-dependent role in regulating cell proliferation and death in the rostral patterning center and cortical neuroepithelium (Storm et al., 2003; Storm et al., 2006).

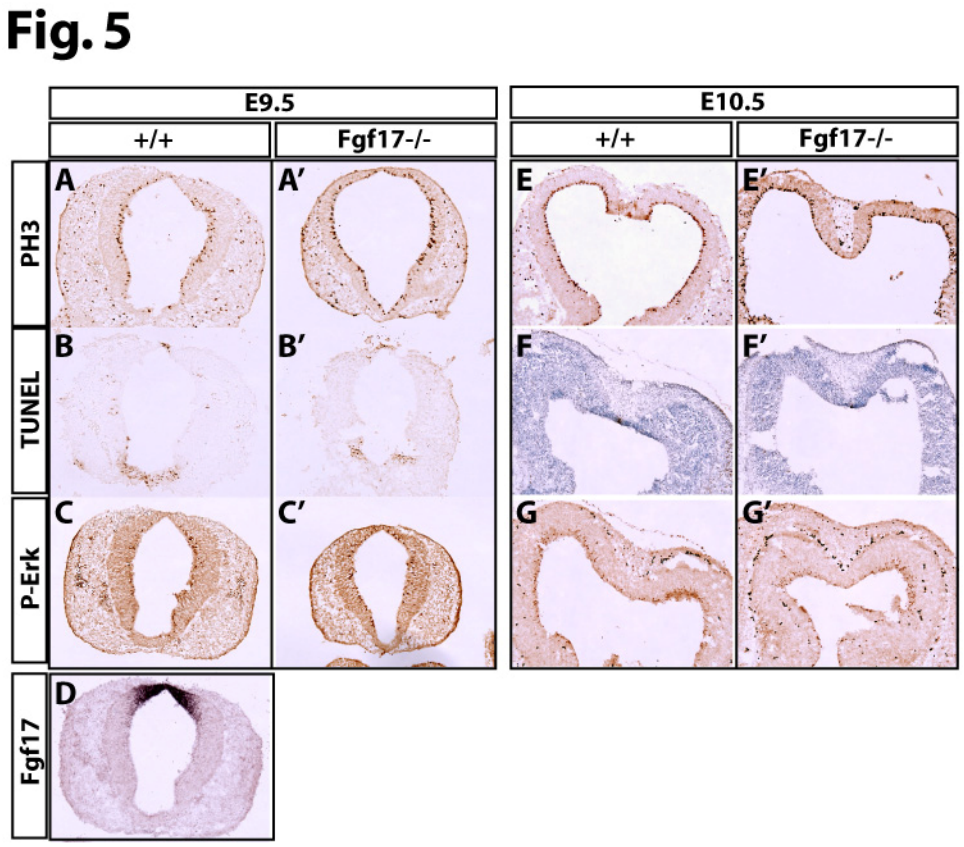

Fig. 5. Normal proliferation, apoptosis and MAP-kinase signaling in E9.5 and E10.5 *Fgf17*$^{-/-}$ mutant neuroepithelium.
(A-D) E9.5 horizontal wild-type (A-D) and *Fgf17*$^{-/-}$ (A'-C') adjacent sections processed for phosphorylated histone H3 (PH3) immunohistochemistry (A-A'), TUNEL (B-B'), phosphorylated ERK immunohistochemistry, or ISH for *Fgf17* (D).
(E-G') E10.5 horizontal wild-type (E-G) and *Fgf17*$^{-/-}$ (E'-G') adjacent sections processed for PH3 immunohistochemistry (A-A'), TUNEL (B-B') or P-Erk immunohistochemistry.

To examine whether smaller reductions in *FGF* signaling have an overt affect on proliferation or apoptosis, we studied E9.5 and E10.5 *Fgf17*$^{-/-}$ embryos using

phosphohistone H3 (PH3) immunohistochemistry and TUNEL. No genotype difference in either PH3 or TUNEL staining was observed (Fig. 5A-B', E-F'), suggesting that proliferative and apoptotic mechanisms are not overtly sensitive to small perturbations in rostral patterning center *FGF* signaling.

FGF signaling leads to activation of the mitogen-activated protein kinase (MAPK) signaling pathway in the telencephalon (Shinya et al., 2001). To determine whether activation of the MAPK pathway is affected by loss of *Fgf17*, we performed phosphorylated-Erk immunohistochemistry on sections from E9.5 and E10.5 *Fgf17*$^{-/-}$ embryos. Although cells along the ventricle were labeled strongly, suggesting that they are mitotic, there was no discernable difference between genotypes in P-Erk staining (Fig. 5C-C', G-G').

DISCUSSION

We have found that *Fgf8*, *Fgf17* and *Emx2* each make unique contributions to patterning FC subdivisions (Fig. 1, S1-6). By applying a panel of *in situ* hybridization probes that selectively marks expression in distinct combinations of FC subdivisions, we have determined which parts of the neonatal FC depend upon *Fgf8*, *Fgf17* and *Emx2* function.

Whereas $Fgf17^{-/-}$ mutants have a selective reduction of the dorsal FC (Cholfin and Rubenstein, 2007), $Fgf8^{n/n}$ mutants have features consistent with a transformation of the medial FC into a cingulate cortex-like structure. Both *FGF* mutants show a rostral expansion of parietal cortex markers; this phenotype is more severe in the $Fgf8^{n/n}$ mutants. On the other hand, in the $Emx2^{-/-}$ mutants there is evidence that the dorsal FC is ventralized; markers of both the ventromedial orbital cortex (*Erm, Pea3, Ngn2*) ventrolateral FC (*Er81*) expand dorsally. Remarkably, many of these severe phenotypes are rescued in $Emx2^{-/-};Fgf17^{-/-}$ mutants. To identify the mechanisms that cause the phenotypes in the neonatal single and compound mutants, we have investigated the molecular and cellular changes in the FC embryonic neuroepithelium.

Fig. 6

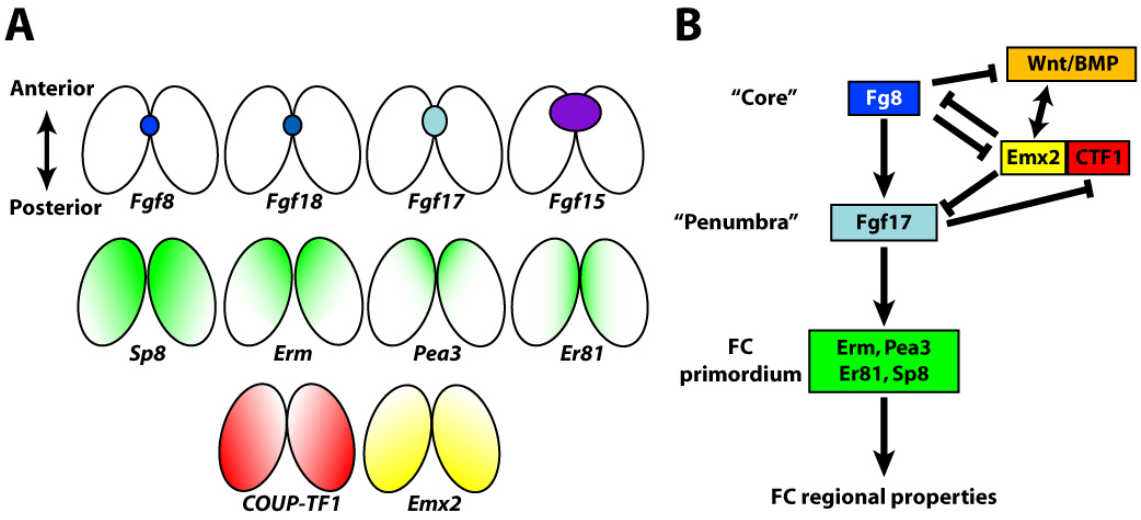

Fig. 6. Model of *FGF-Emx2* genetic interactions in FC patterning.
(A) Dorsal views of embryonic brains showing spatial relationships of rostral patterning center FGFs and transcription factors gradients. Rostral/anterior is to the top. FGF ligands (*Fgf8, Fgf18, Fgf17* and *Fgf15*) are expressed in a nested pattern in the rostral patterning center that parcellates the center into a central "core" (*Fgf8/17/18+*) and surrounding "penumbra" (dorsal: *Fgf17+*, ventral: *Fgf15+*) that have high and low levels of FGF signaling, respectively. Transcription factor gradients of *Sp8, Erm, Pea3, Er81, COUP-TF1* and *Emx2* in the cortical primordium are shown.
(B) Schematic of proposed genetic interactions between rostral patterning center FGFs and transcription factors relevant for global cortical patterning and local FC patterning. Acting more globally, *Fgf8* has a repressive function (lines with bars) on "caudalizing" transcription factors *Emx2* and *COUP-TF1* that may regulate the allocation of anterior and posterior cortical regions. As a subset of its functions, *Fgf8* positively regulates *Fgf17* expression (arrows). Locally in the FC primordium, *Fgf17* induces *Er81, Erm, Pea3* and *Sp8* expression (arrows) and represses *COUP-TF1*, which together may promote frontal cortex regional properties.

Fgf8 Is Upstream of *Fgf17* and *Fgf18*

We propose that *Fgf8* promotes the nested expression of *Fgf17 and Fgf18* in the rostral patterning center (Fig. 6). Reduced expression of *Fgf8* in the $Fgf8^{n/n}$ hypomorph resulted in decreased expression of *Fgf17* and *Fgf18. Fgf15* expression is not strongly affected in $Fgf8^{n/n}$ hypomorphs; we are currently investigating the effect of further reducing *Fgf8* dosage on *Fgf15* expression. While *Fgf17* expression was reduced ~200 microns rostral to the patterning center, its expression remained robust within ~100 microns of the *Fgf8+* core domain (Fig. S12). We propose that the residual *Fgf17*

expression has a key role in maintaining aspects of rostral identity in the *Fgf8*$^{n/n}$ mutant (see below). Unlike in the *Fgf8*$^{n/n}$ hypomorph, we did not detect an overt change in *Fgf8, Fgf15* and *Fgf18* expression in the *Fgf17*$^{-/-}$ mutant, showing that these genes are not strongly regulated by the *Fgf17*. Thus, our current model is that *Fgf8* lies upstream of the other three *FGFs* expressed in the rostral patterning center.

Fgf8 and *Fgf17* Have Overlapping and Distinct Functions in FC Patterning

Both *Fgf8*$^{n/n}$ and *Fgf17*$^{-/-}$ mutants show reduced FGF-signaling based on decreased expression of two FGF-responsive genes: *Spry1* and *Spry2*. *Fgf8*$^{n/n}$ mutants show a greater reduction in *Spry* expression, showing that this aspect of FGF-signaling is more affected by the ~60% reduction in *Fgf8* expression (in *Fgf8*$^{n/n}$)(Meyers et al., 1998; Garel et al., 2003) than by the loss of *Fgf17* expression. Consistent with this finding is the observation that the FC is smaller in the *Fgf8*$^{n/n}$ mutants than in the *Fgf17*$^{-/-}$ mutants (Garel et al., 2003; Cholfin and Rubenstein, 2007). Further reduction of *Fgf8* expression in *Fgf8*$^{n/null}$ severe hypomorph and in conditional *Fgf8* nulls leads to progressively more severe hypoplasia of the rostral telencephalon, showing that FC size is extremely sensitive to *Fgf8* dosage (Storm et al., 2003; Storm et al., 2006).

Fgf8 is believed to regulate telencephalic patterning through regulating the expression of several transcription factors, including *COUP-TFI, Emx2* and *Sp8* (Crossley et al., 2001; Fukuchi-Shimogori and Grove, 2003; Storm et al., 2003; Storm et al., 2006). Here we compared transcription factor expression in the *Fgf8*$^{n/n}$ and *Fgf17*$^{-/-}$ mutants. Both show rostrodorsal expansion of *COUP-TFI* expression, although the increase in *COUP-TFI* was subtle in the *Fgf17*$^{-/-}$ mutants. Over-expression of *COUP-TFI*

suppresses rostral cortical fate (Faedo and Rubenstein, unpublished), consistent with loss of function analysis (Zhou et al., 2001)(M. Studer, personal communication). Thus, we propose that both *Fgf8* and *Fgf17* contribute to rostral cortical fate through repression of *COUP-TFI,* although *Fgf8* appears to have a more prominent role in this repression (Fig. 6).

Fgf8$^{n/n}$ mutants also have a rostroventral expansion of *Emx2* expression (Figs. 4F", S9)(Garel et al., 2003); we do not detect increased *Emx2* expression in the *Fgf17*$^{-/-}$ mutants (Figs. 4F', S8). Over-expression of *Emx2* suppresses rostral cortical fate (Hamasaki et al., 2004). We propose that an increase of *Emx2* in the rostromedial FC accounts for the rostral expansion of molecular features of the posterior parts of the dorsomedial FC (cingulate cortex Cg1 and Cg2) in the *Fgf8*$^{n/n}$ mutant (Fig. 1). The *Fgf17*$^{-/-}$ mutants do not have this phenotype, perhaps because *Fgf8* expression is preserved, which prevents rostral expansion of *Emx2* into this region. Thus, we propose that *Fgf8* and *Fgf17* have distinct roles in suppressing the caudalizing function of *Emx2* (Fig. 6). Previously, we demonstrated that *Fgf8* represses rostral expression of *Wnt8b* (Storm et al., 2006). Thus, the rostral expansion of *Emx2* in the *Fgf8*$^{n/n}$ mutant could be due to reduced FGF-repression of Wnt expression/signaling, as *Emx2* is known to be Wnt-regulated (Theil et al., 2002).

While *COUP-TFI* and *Emx2* expression is increased more in the *Fgf8*$^{n/n}$ than the *Fgf17*$^{-/-}$ mutant, expression of *Erm, Pea3* and *Sp8* are reduced more in the *Fgf17*$^{-/-}$ than the *Fgf8*$^{n/n}$ mutant (Fig. 4). In the *Fgf8*$^{n/n}$ mutant, *Fgf17* expression remains strong near the regions that express *Er81*, *Erm* and *Pea3*, suggesting that *Fgf17* is responsible for preserving the expression of these transcription factors. Thus, *Fgf17* may regulate local

patterning within dorsomedial parts of the FC through control of "rostral" transcription factors (*Erm, Pea3*, *Sp8*), whereas *Fgf8* function may be responsible for regulating the gradients of more global transcription factors, such as *COUP-TFI* and *Emx2*.

Emx2 represses FGF expression/signaling and FC patterning

Emx2$^{-/-}$ mutants have more intense and expanded expression domains of *Fgf8* and *Fgf17*, supporting previous findings (Fukuchi-Shimogori and Grove, 2003). FGF signaling appears to be increased, because *Spry1* expression was increased rostrodorsally. In addition, *Fgf15* expression is upregulated in several telencephalic structures: septum, rostral subpallium, pallial/sub-pallial boundary, LGE/MGE boundary, and caudoventral cortical primordium. Therefore, *Emx2* has a widespread role in repressing FGF signaling in the telencephalon. The increased expression of *Fgf8, Fgf15* and *Fgf17* then contributes to modifying cortical fate through changes in transcription factor expression.

Emx2 promotes caudodorsal cortical fate (Bishop et al., 2000; Mallamaci et al., 2000; Bishop et al., 2002; Bishop et al., 2003; Muzio and Mallamaci, 2003; Hamasaki et al., 2004; Muzio et al., 2005). Consistent with this, *Emx2*$^{-/-}$ mutants had increased expression of *Er81*, *Erm*, *Pea3* and *Sp8* in the rostrodorsal cortical neuropeithelium. We propose that *Erm*, *Pea3* and *Sp8* promote dorsal FC identity, as *Lmo4*, *Cad8*, *Id2*, and *Steel* expression was expanded in *Emx2*$^{-/-}$ mutants (Figs. 1, S4). Furthermore, we propose that *Er81* and *Pea3* may promote ventrolateral and orbital FC identity, as expression of these genes spread dorsally from the ventral parts of the FC neuroepithelium (Figs. 4C'''-D''', S10); they may contribute to the dorsal shift in *Ngn2* expression (Figs. 1F''', S4).

Furthermore, *Emx2* may also contribute to specifying ventrolateral FC by promoting *COUP-TFI* expression.

Fgf17-Emx2 interactions antagonistically regulate FC patterning

To what extent are the increases in rostral cortical identity mediated by the increased *Fgf17* signaling in the *Emx2*$^{-/-}$ mutant? The expression of transcription factors *Er81*, *Erm* and *Pea3* in progenitor cells is normalized in *Emx2*$^{-/-}$*;Fgf17*$^{-/-}$ double mutants relative to both single mutants, which correlates with the normalization of transcription factor expression in the neonatal dorsal and ventral/orbital FC (Figs. 1, 4B’’’’, 4C’’’’, 4D’’’’, S5, S6, S11). Therefore, we propose that restoration of *Erm*, *Er81 and Pea3* expression accounts at least in part for the rescue of neonatal FC molecular features in the *Emx2*$^{-/-}$*;Fgf17*$^{-/-}$ double mutants (Fig. 1).

Despite the robust rescue of many FC features, some phenotypes of the *Emx2*$^{-/-}$ mutants were not rescued in *Emx2*$^{-/-}$*;Fgf17*$^{-/-}$ double mutants. This includes the elevated expression of *Fgf8* and *Fgf15*; this result underscores the importance of reducing *Fgf17* in the rescue of FC patterning (Figs. 3K’-L’, S5-6). In addition, the double mutants exhibit persistently elevated expression of *Sp8*, reduced expression of *COUP-TFI* and ectopic expression of *Er81* in the cortical preplate. The regulatory mechanisms underlying these phenotypes will require additional studies. It merits comment that the persistent increase in *Sp8* expression in the *Emx2*$^{-/-}$*;Fgf17*$^{-/-}$ double mutants could be due to elevated expression of *Fgf8* and *Fgf15*, as *Sp8* is known to be positively regulated by *Fgf8* (Storm et al., 2006).

In summary, we have shown that *Fgf8*, *Fgf17* and *Emx2* play distinct roles in the control of transcription factor gradients in progenitor cells of the FC primordium; these genes may have fundamental roles in regionalization of the FC. We propose that *Fgf8* has a pivotal role in establishing the expression of the other *FGFs* and in shaping the gradients of transcrition factor expression as the telencephalon forms. Then, the other *FGFs*, including *Fgf17*, have the primary role in shaping the local levels of transcription factor expression that determine the local regional identity. *Emx2* and the *FGF* genes share some reciprocal functions in regulating cortical patterning; in the FC this is accomplished at least in part through controlling the levels of *Erm, Pea3* and *Er81* expression. Further studies will need to establish the functions of these transcription factors in FC development.

REFERENCES

Bachler M, Neubuser A (2001) Expression of members of the Fgf family and their receptors during midfacial development. Mech Dev 100:313-316.

Bell SM, Schreiner CM, Waclaw RR, Campbell K, Potter SS, Scott WJ (2003) Sp8 is crucial for limb outgrowth and neuropore closure. Proc Natl Acad Sci U S A 100:12195-12200.

Bishop KM, Goudreau G, O'Leary DD (2000) Regulation of area identity in the mammalian neocortex by Emx2 and Pax6. Science 288:344-349.

Bishop KM, Rubenstein JL, O'Leary DD (2002) Distinct actions of Emx1, Emx2, and Pax6 in regulating the specification of areas in the developing neocortex. J Neurosci 22:7627-7638.

Bishop KM, Garel S, Nakagawa Y, Rubenstein JL, O'Leary DD (2003) Emx1 and Emx2 cooperate to regulate cortical size, lamination, neuronal differentiation, development of cortical efferents, and thalamocortical pathfinding. J Comp Neurol 457:345-360.

Bulchand S, Subramanian L, Tole S (2003) Dynamic spatiotemporal expression of LIM genes and cofactors in the embryonic and postnatal cerebral cortex. Dev Dyn 226:460-469.

Cholfin JA, Rubenstein JL (2007) Patterning of frontal cortex subdivisions by Fgf17. Proc Natl Acad Sci U S A In press.

Crossley PH, Martin GR (1995) The mouse Fgf8 gene encodes a family of polypeptides and is expressed in regions that direct outgrowth and patterning in the developing embryo. Development 121:439-451.

Crossley PH, Martinez S, Ohkubo Y, Rubenstein JL (2001) Coordinate expression of Fgf8, Otx2, Bmp4, and Shh in the rostral prosencephalon during development of the telencephalic and optic vesicles. Neuroscience 108:183-206.

Dalley JW, Cardinal RN, Robbins TW (2004) Prefrontal executive and cognitive functions in rodents: neural and neurochemical substrates. Neurosci Biobehav Rev 28:771-784.

Dou CL, Li S, Lai E (1999) Dual role of brain factor-1 in regulating growth and patterning of the cerebral hemispheres. Cereb Cortex 9:543-550.

Fode C, Gradwohl G, Morin X, Dierich A, LeMeur M, Goridis C, Guillemot F (1998) The bHLH protein NEUROGENIN 2 is a determination factor for epibranchial placode-derived sensory neurons. Neuron 20:483-494.

Fukuchi-Shimogori T, Grove EA (2001) Neocortex patterning by the secreted signaling molecule FGF8. Science 294:1071-1074.

Fukuchi-Shimogori T, Grove EA (2003) Emx2 patterns the neocortex by regulating FGF positional signaling. Nat Neurosci 6:825-831.

Fuster JM (2001) The prefrontal cortex--an update: time is of the essence. Neuron 30:319-333.

Garel S, Rubenstein JL (2004) Patterning of the cerebral cortex, 3rd Edition. Cambridge: MIT Press.

Garel S, Huffman KJ, Rubenstein JL (2003) Molecular regionalization of the neocortex is disrupted in Fgf8 hypomorphic mutants. Development 130:1903-1914.
Gimeno L, Brulet P, Martinez S (2003) Study of Fgf15 gene expression in developing mouse brain. Gene Expr Patterns 3:473-481.
Grove EA, Fukuchi-Shimogori T (2003) Generating the cerebral cortical area map. Annu Rev Neurosci 26:355-380.
Hamasaki T, Leingartner A, Ringstedt T, O'Leary DD (2004) EMX2 regulates sizes and positioning of the primary sensory and motor areas in neocortex by direct specification of cortical progenitors. Neuron 43:359-372.
Heidbreder CA, Groenewegen HJ (2003) The medial prefrontal cortex in the rat: evidence for a dorso-ventral distinction based upon functional and anatomical characteristics. Neurosci Biobehav Rev 27:555-579.
Hoshikawa M, Ohbayashi N, Yonamine A, Konishi M, Ozaki K, Fukui S, Itoh N (1998) Structure and expression of a novel fibroblast growth factor, FGF-17, preferentially expressed in the embryonic brain. Biochem Biophys Res Commun 244:187-191.
Kawakami Y, Esteban CR, Matsui T, Rodriguez-Leon J, Kato S, Belmonte JC (2004) Sp8 and Sp9, two closely related buttonhead-like transcription factors, regulate Fgf8 expression and limb outgrowth in vertebrate embryos. Development 131:4763-4774.
Mallamaci A, Muzio L, Chan CH, Parnavelas J, Boncinelli E (2000) Area identity shifts in the early cerebral cortex of Emx2-/- mutant mice. Nat Neurosci 3:679-686.
Maruoka Y, Ohbayashi N, Hoshikawa M, Itoh N, Hogan BL, Furuta Y (1998) Comparison of the expression of three highly related genes, Fgf8, Fgf17 and Fgf18, in the mouse embryo. Mech Dev 74:175-177.
Meyers EN, Lewandoski M, Martin GR (1998) An Fgf8 mutant allelic series generated by Cre- and Flp-mediated recombination. Nat Genet 18:136-141.
Monuki ES, Porter FD, Walsh CA (2001) Patterning of the dorsal telencephalon and cerebral cortex by a roof plate-Lhx2 pathway. Neuron 32:591-604.
Muzio L, Mallamaci A (2003) Emx1, emx2 and pax6 in specification, regionalization and arealization of the cerebral cortex. Cereb Cortex 13:641-647.
Muzio L, Soria JM, Pannese M, Piccolo S, Mallamaci A (2005) A mutually stimulating loop involving emx2 and canonical wnt signalling specifically promotes expansion of occipital cortex and hippocampus. Cereb Cortex 15:2021-2028.
Muzio L, DiBenedetto B, Stoykova A, Boncinelli E, Gruss P, Mallamaci A (2002a) Conversion of cerebral cortex into basal ganglia in Emx2(-/-) Pax6(Sey/Sey) double-mutant mice. Nat Neurosci 5:737-745.
Muzio L, DiBenedetto B, Stoykova A, Boncinelli E, Gruss P, Mallamaci A (2002b) Emx2 and Pax6 control regionalization of the pre-neuronogenic cortical primordium. Cereb Cortex 12:129-139.
O'Leary DD, Nakagawa Y (2002) Patterning centers, regulatory genes and extrinsic mechanisms controlling arealization of the neocortex. Curr Opin Neurobiol 12:14-25.
Pellegrini M, Mansouri A, Simeone A, Boncinelli E, Gruss P (1996) Dentate gyrus formation requires Emx2. Development 122:3893-3898.
Price JL (2006) Prefrontal cortex. Boca Raton: CRC Press.

Rubenstein JL, Anderson S, Shi L, Miyashita-Lin E, Bulfone A, Hevner R (1999) Genetic control of cortical regionalization and connectivity. Cereb Cortex 9:524-532.
Shinozaki K, Yoshida M, Nakamura M, Aizawa S, Suda Y (2004) Emx1 and Emx2 cooperate in initial phase of archipallium development. Mech Dev 121:475-489.
Shinya M, Koshida S, Sawada A, Kuroiwa A, Takeda H (2001) Fgf signalling through MAPK cascade is required for development of the subpallial telencephalon in zebrafish embryos. Development 128:4153-4164.
Storm EE, Rubenstein JL, Martin GR (2003) Dosage of Fgf8 determines whether cell survival is positively or negatively regulated in the developing forebrain. Proc Natl Acad Sci U S A 100:1757-1762.
Storm EE, Garel S, Borello U, Hebert JM, Martinez S, McConnell SK, Martin GR, Rubenstein JL (2006) Dose-dependent functions of Fgf8 in regulating telencephalic patterning centers. Development 133:1831-1844.
Sur M, Rubenstein JL (2005) Patterning and plasticity of the cerebral cortex. Science 310:805-810.
Theil T, Aydin S, Koch S, Grotewold L, Ruther U (2002) Wnt and Bmp signalling cooperatively regulate graded Emx2 expression in the dorsal telencephalon. Development 129:3045-3054.
Toresson H, Potter SS, Campbell K (2000) Genetic control of dorsal-ventral identity in the telencephalon: opposing roles for Pax6 and Gsh2. Development 127:4361-4371.
Uylings HB, Groenewegen HJ, Kolb B (2003) Do rats have a prefrontal cortex? Behav Brain Res 146:3-17.
Xu J, Liu Z, Ornitz DM (2000) Temporal and spatial gradients of Fgf8 and Fgf17 regulate proliferation and differentiation of midline cerebellar structures. Development 127:1833-1843.
Xu J, Lawshe A, MacArthur CA, Ornitz DM (1999) Genomic structure, mapping, activity and expression of fibroblast growth factor 17. Mech Dev 83:165-178.
Zhang S, Lin Y, Itaranta P, Yagi A, Vainio S (2001) Expression of Sprouty genes 1, 2 and 4 during mouse organogenesis. Mech Dev 109:367-370.
Zhou C, Tsai SY, Tsai MJ (2001) COUP-TFI: an intrinsic factor for early regionalization of the neocortex. Genes Dev 15:2054-2059.
Zilles K, Wree A (1995) Cortex: areal and laminar structure. San Diego: Academic Press.

SUPPORTING FIGURES

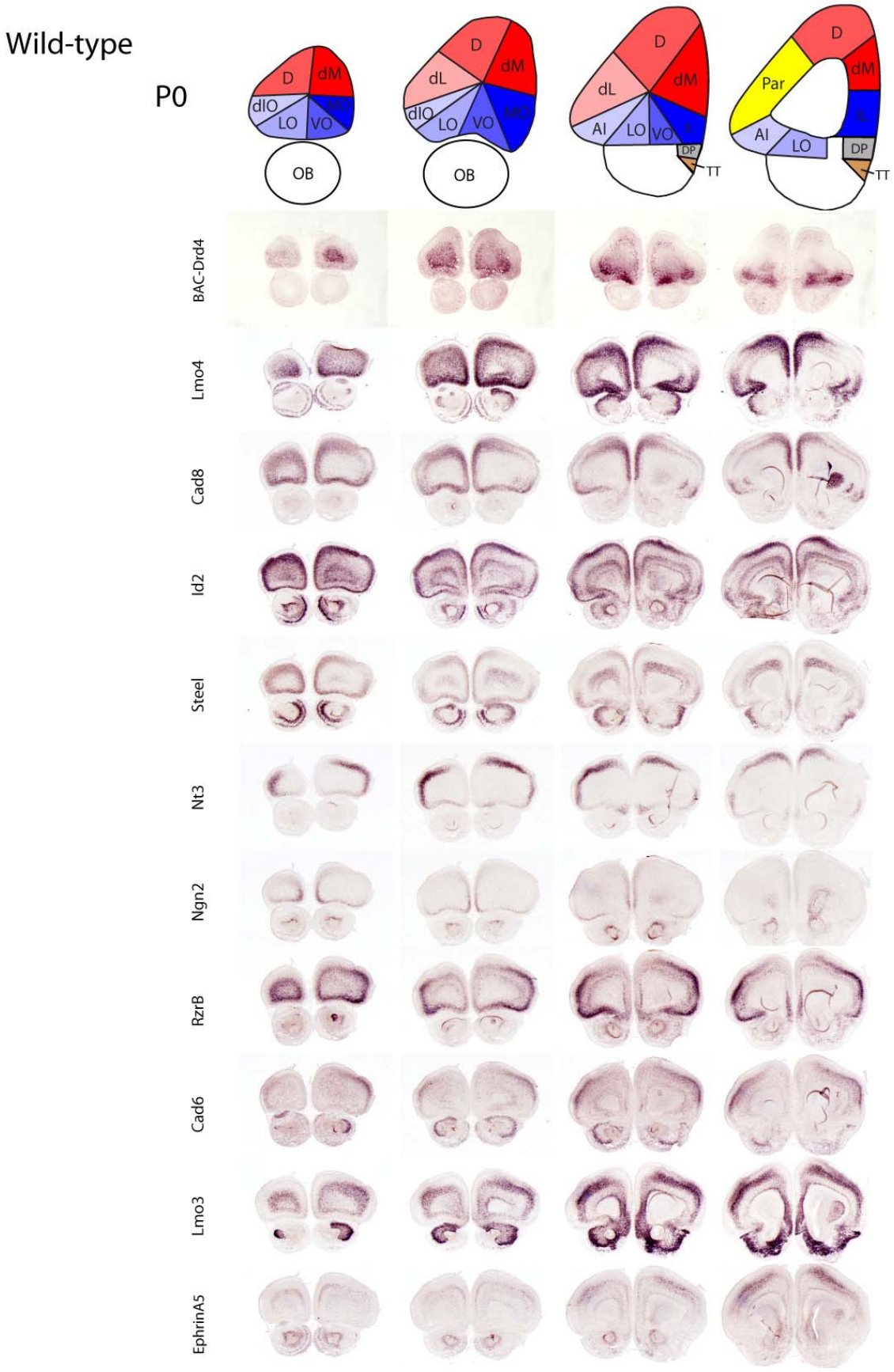
Wild-type
P0
D
dM
dIO
LO
VO
MO
OB
dL
AI
Par
DP
TT
BAC-Drd4
Lmo4
Cad8
Id2
Steel
Nt3
Ngn2
RzrB
Cad6
Lmo3
EphrinA5

Fig. S1. Gene expression map of wild-type newborn frontal cortex (FC). This figure and legend is reproduced from (Cholfin and Rubenstein, in press) and modified with permission. The top row displays a schema of gene expression-derived subdivisions at 4 rostral-caudal levels (left to right). Red and blue colors demarcate dorsal and ventral FC subdivisions, respectively. Parietal cortex is in yellow. The row labeled BAC-Drd4 is a rostral to caudal series of coronal sections from a P0 *Fgf17*$^{+/+}$;BAC-Drd4 GFP+ brain processed for anti-GFP immunohistochemistry. The rows below show rostral to caudal series of coronal sections from a representative P0 wild-type brain processed for *in situ* hybridization for *Lmo4*, *Cadherin-8* (*Cad8*), *Id2*, *Steel*, *Neurotrophin-3* (*Nt3*), *Neurogenin-2* (*Ngn2*), *Rzr-β*, *Cadherin-6* (*Cad6*), *Lmo3* and *EphrinA5*.

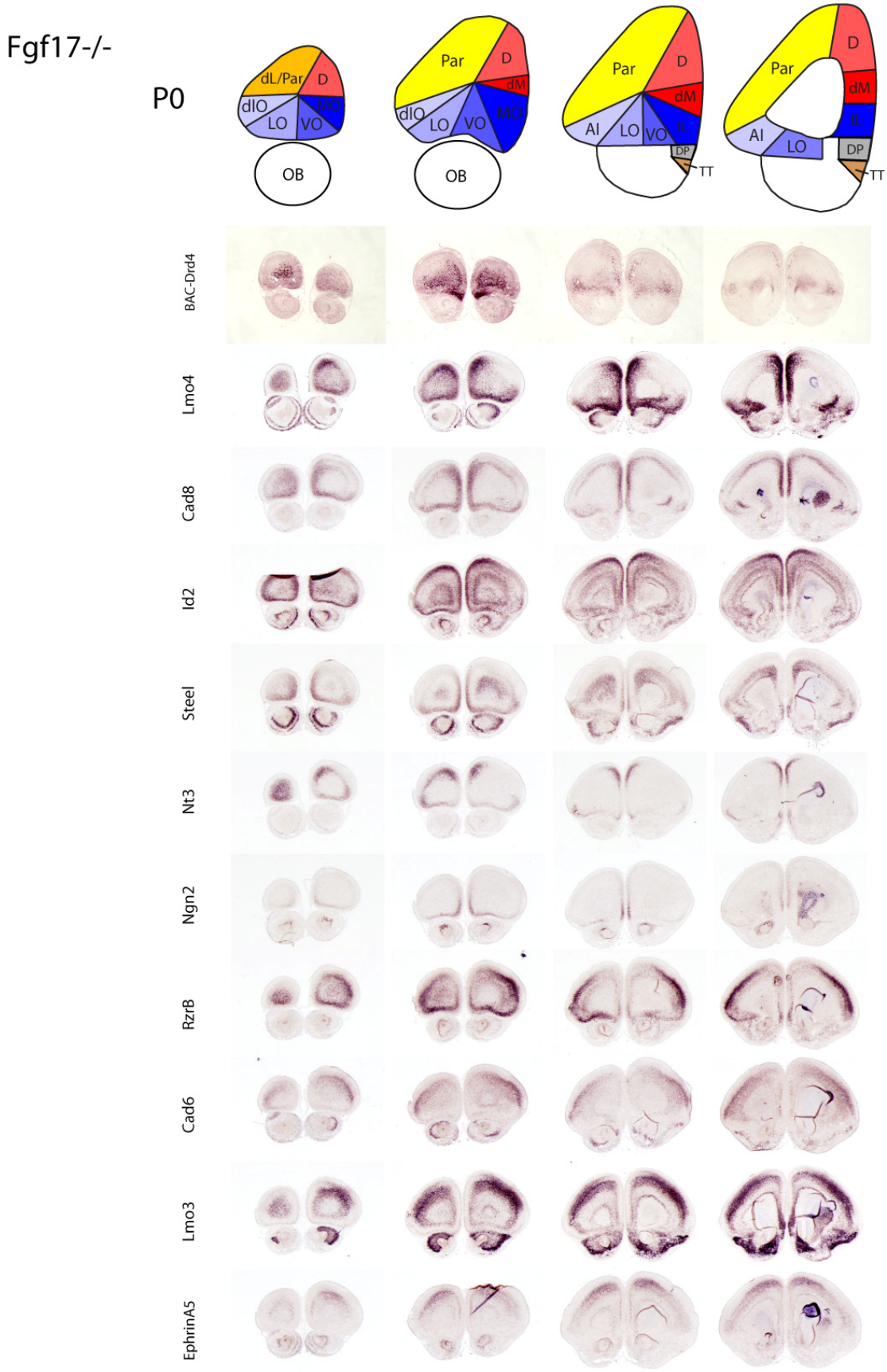
Fgf17-/-
P0
dL/Par
D
dlO
MO
LO
VO
OB
Par
D
dM
dlO
LO
VO
MO
OB
Par
D
dM
Al
LO
VO
lL
DP
TT
Par
D
dM
lL
Al
LO
DP
TT
BAC-Drd4
Lmo4
Cad8
Id2
Steel
Nt3
Ngn2
RzrB
Cad6
Lmo3
EphrinA5

Fig. S2. Changes in dorsal FC regionalization in a representative *Fgf17*$^{-/-}$ mutant brain. This figure and legend is reproduced from (Cholfin and Rubenstein, in press) and modified with permission. The schema (top row) displays a summary of the BAC-transgenic GFP and *in situ* hybridization data: contraction and medial shift of dorsal FC subdivisions (red), with a complementary rostromedial expansion of parietal cortex (yellow). Ventral FC regions are preserved (blue). The row labeled BAC-Drd4 is a rostral to caudal series of coronal sections from a P0 *Fgf17*$^{-/-}$;BAC-Drd4 GFP+ brain processed for anti-GFP immunohistochemistry. The rows below show rostral to caudal series of coronal sections from a representative P0 *Fgf17*$^{-/-}$ brain processed for *in situ* hybridization for *Lmo4*, *Cadherin-8* (*Cad8*), *Id2*, *Steel*, *Neurotrophin-3* (*Nt3*), *Neurogenin-2* (*Ngn2*), *Rzr-β*, *Cadherin-6* (*Cad6*), *Lmo3* and *EphrinA5*. Abbreviations are as defined in Fig. 1 and Table S1.

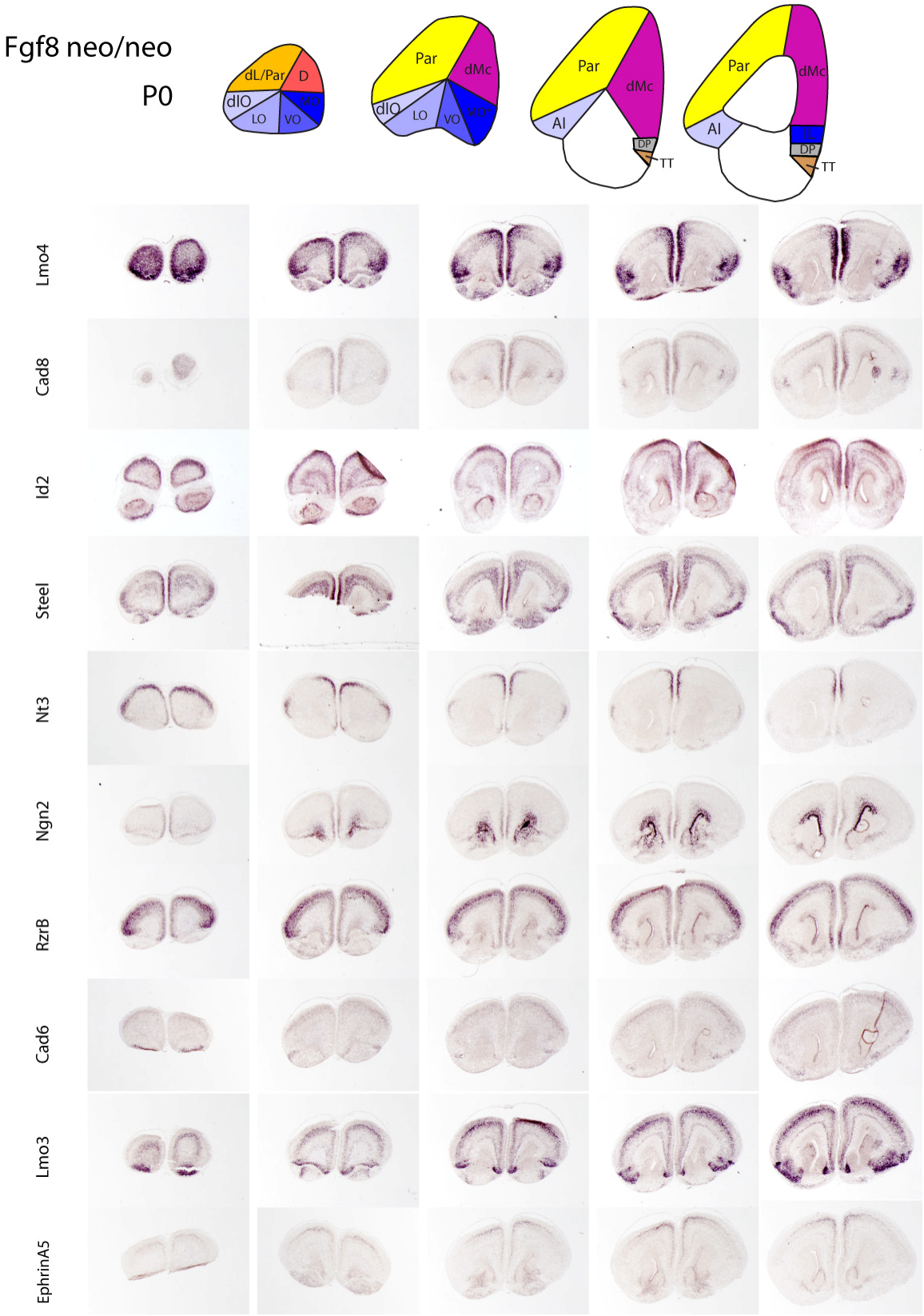

Fig. S3. Reduced dorsal and orbital FC in the *Fgf8*$^{n/n}$ mutant. Please refer to Fig. S1 legend for details.

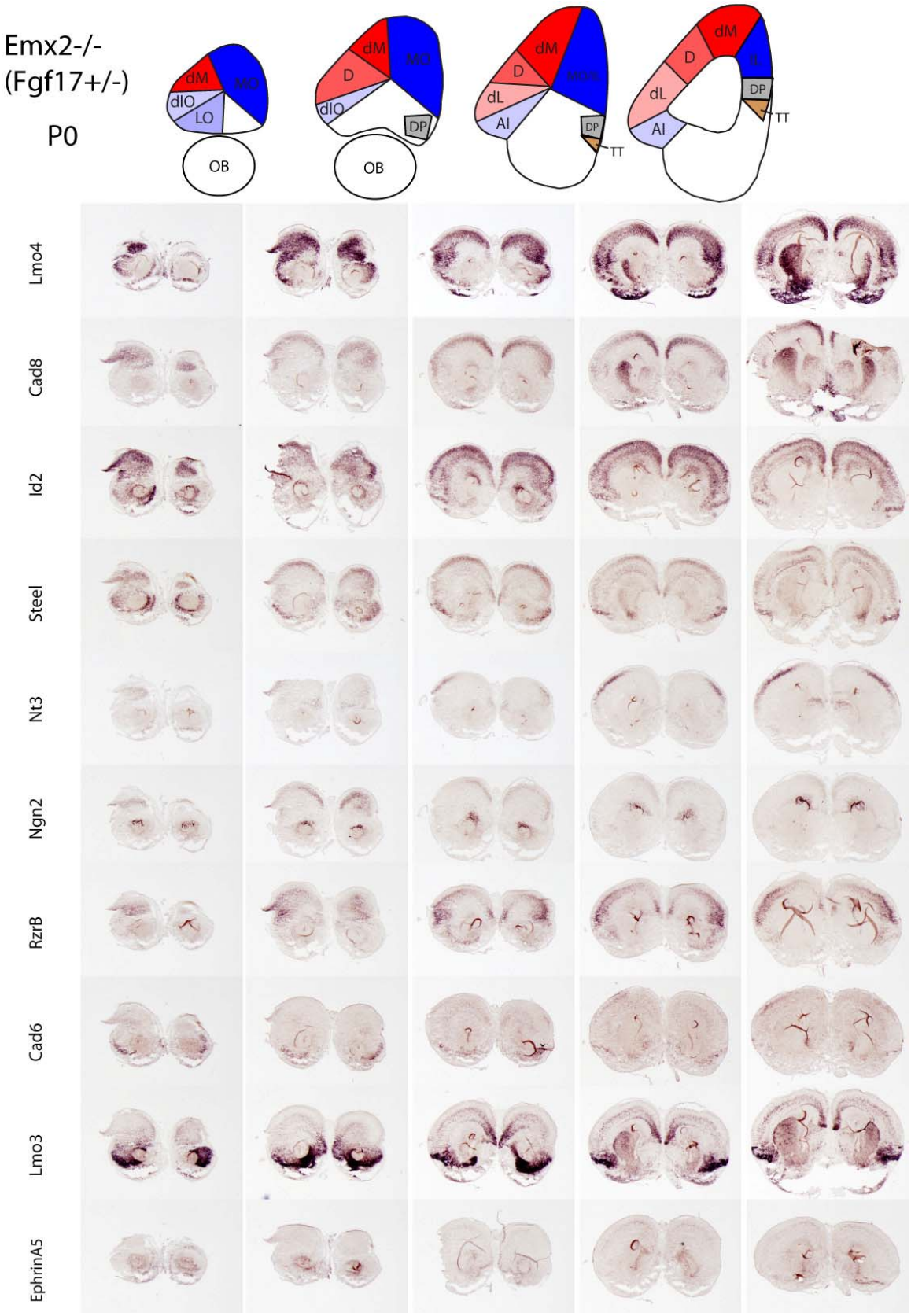
Emx2-/-
(Fgf17+/-)
P0
dM
MO
dlO
LO
OB
D
dM
MO
dlO
DP
OB
dL
AI
dM
D
MO
DP
TT
dL
AI
dM
D
DP
TT
Lmo4
Cad8
Id2
Steel
Nt3
Ngn2
RzrB
Cad6
Lmo3
EphrinA5

Fig. S4. Expansion of rostral cortical subdivisions in the *Emx2*$^{-/-}$ mutant. *Emx2*$^{-/-}$ and *Emx2*$^{-/-}$;*Fgf17*$^{+/-}$ mutants have comparable FC phenotypes; a *Emx2*$^{-/-}$;*Fgf17*$^{+/-}$ brain is shown. The neocortex and olfactory bulbs of *Emx2*$^{-/-}$ mutants were hypoplastic; ventrolateral pallial structures (anterior olfactory nuclei, olfactory tubercle, pyriform cortex) appear rostrally shifted. Please refer to Fig. S1 legend for details.

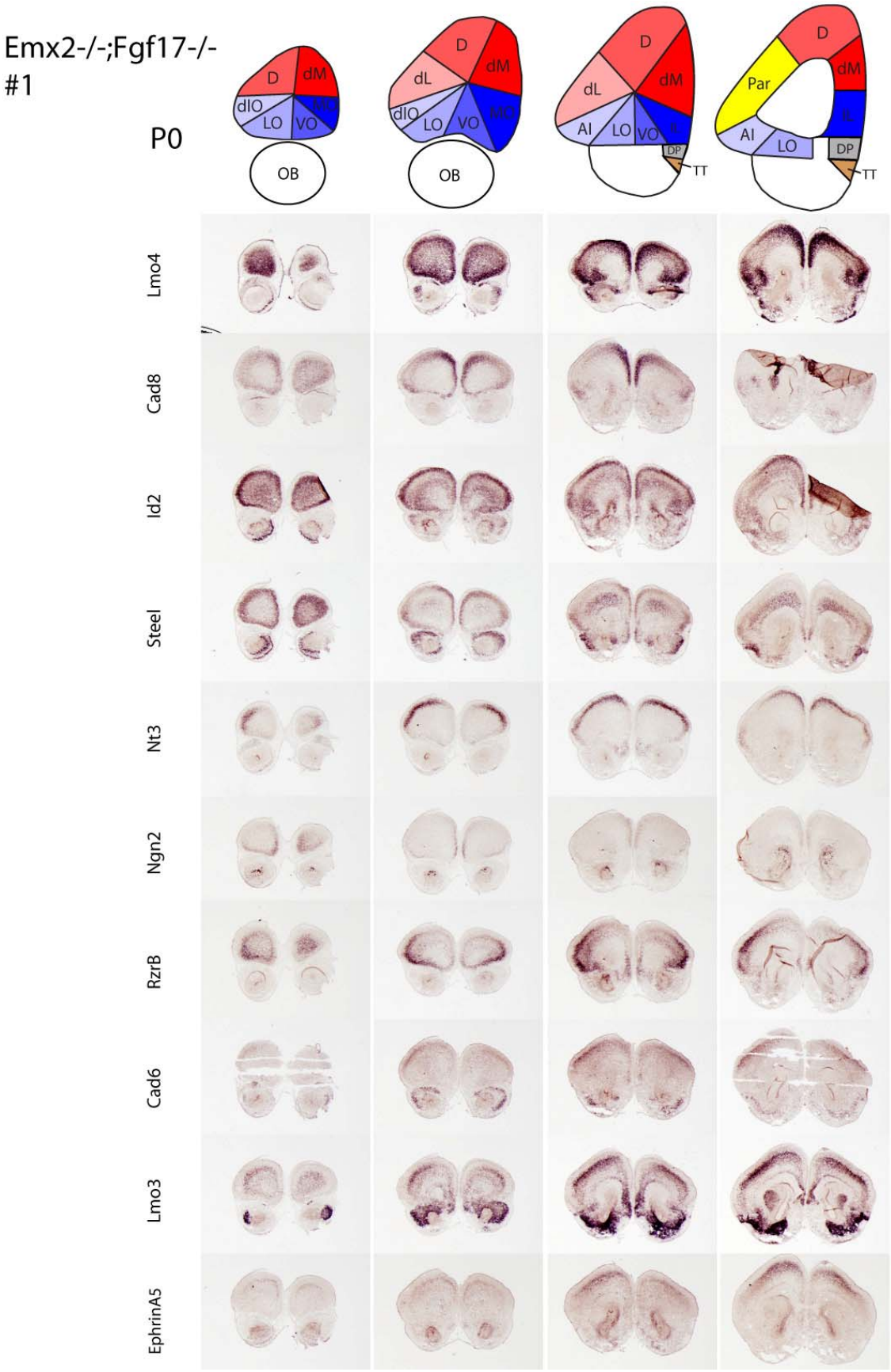
Emx2-/-;Fgf17-/-
#1
P0
D
dM
dlO
LO
VO
MO
OB
dL
Al
Par
DP
TT
Lmo4
Cad8
Id2
Steel
Nt3
Ngn2
RzrB
Cad6
Lmo3
EphrinA5

Fig. S5. Rescue of FC regionalization in a *Emx2*$^{-/-}$*;Fgf17*$^{-/-}$ double mutant (brain #1). Please refer to Fig. S1 legend for details.

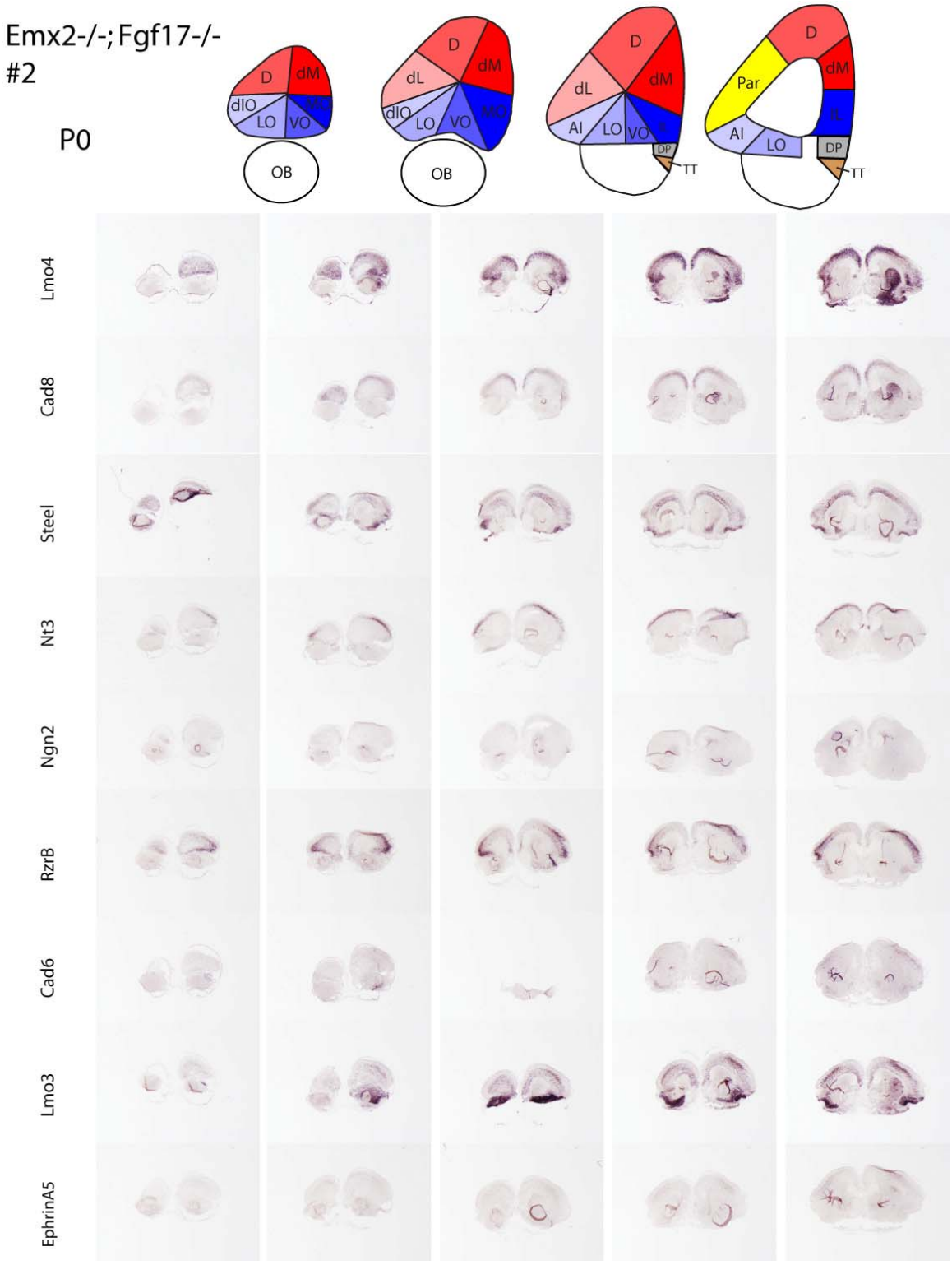

Fig. S6. Partial rescue of FC regionalization in a *Emx2*$^{-/-}$*;Fgf17*$^{-/-}$ mutant (brain #2). Please refer to Fig. S1 legend for details.

Fig. S7. Wild-type E12.5 coronal section gene expression

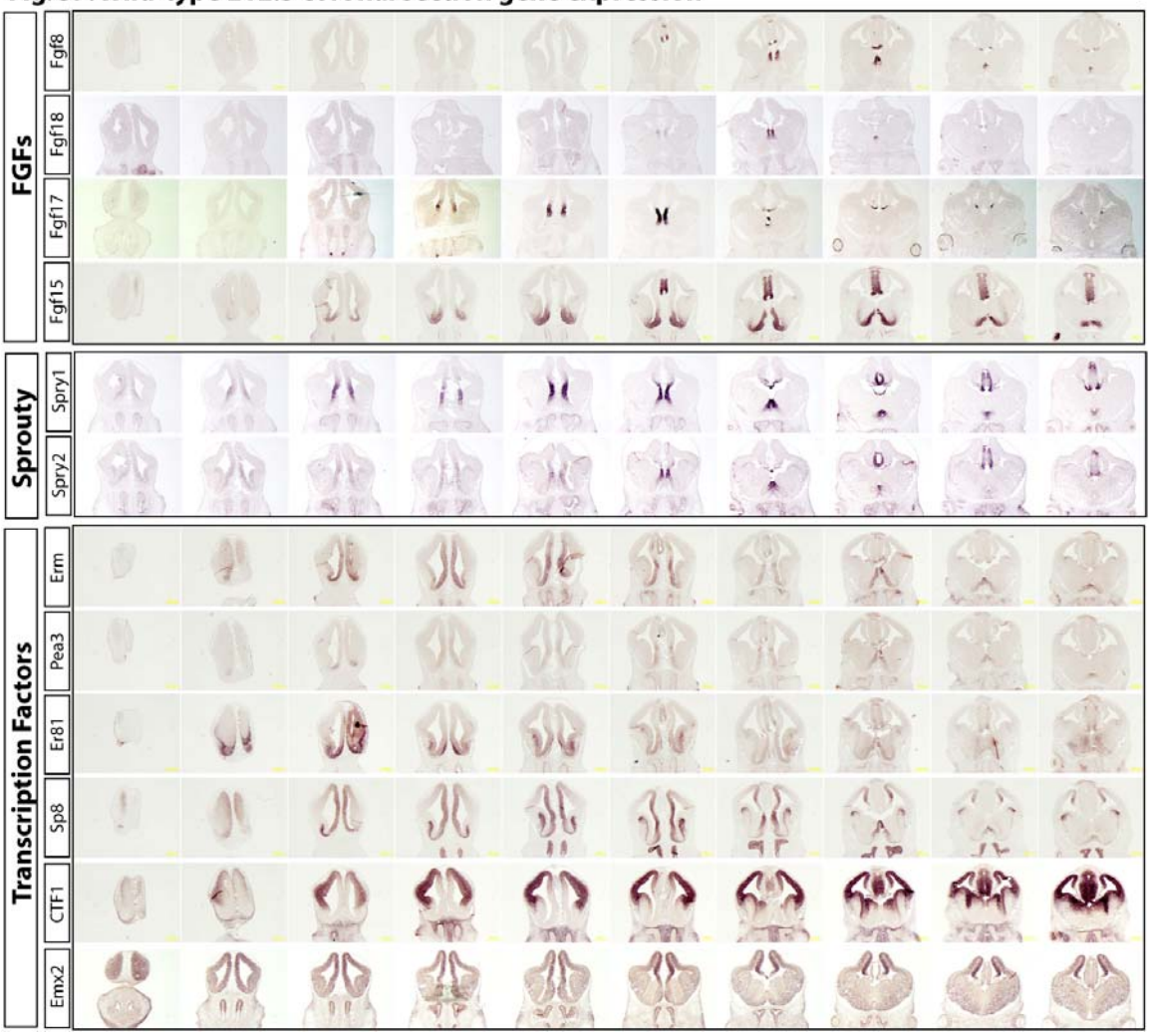

Fig. S7. In situ hybridization on E12.5 rostral to caudal (left to right) wild-type coronal section series for FGF genes (*Fgf8, Fgf18, Fgf17, Fgf15*), Sprouty genes (*Spry1, Spry2*), and transcription factors (*Erm, Pea3, Er81, Sp8, COUP-TF1, Emx2*).

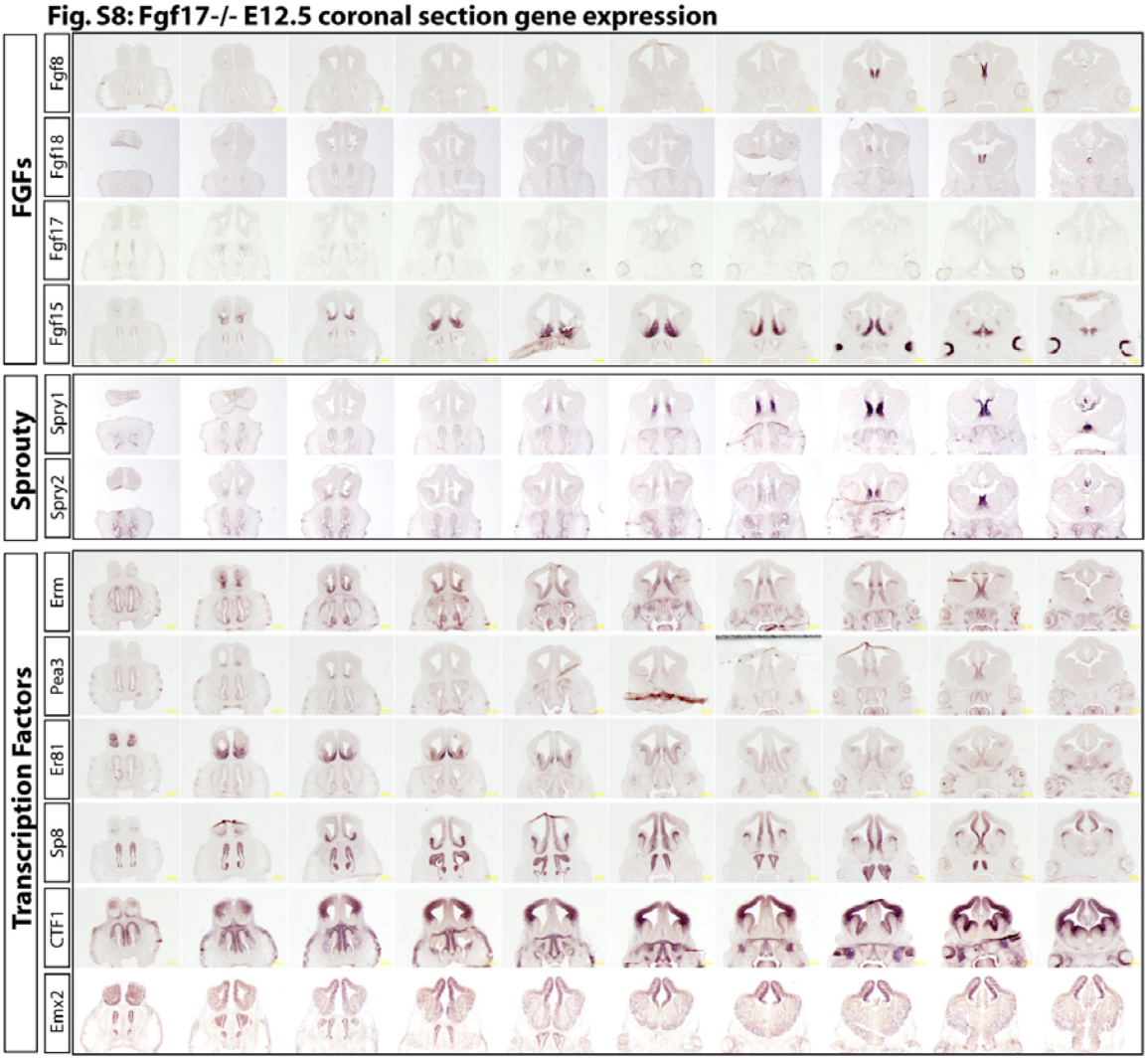

Fig. S8. In situ hybridization on E12.5 rostral to caudal (left to right) *Fgf17*$^{-/-}$ coronal section series for FGF genes (*Fgf8, Fgf18, Fgf17, Fgf15*), Sprouty genes (*Spry1, Spry2*), and transcription factors (*Erm, Pea3, Er81, Sp8, COUP-TF1, Emx2*).

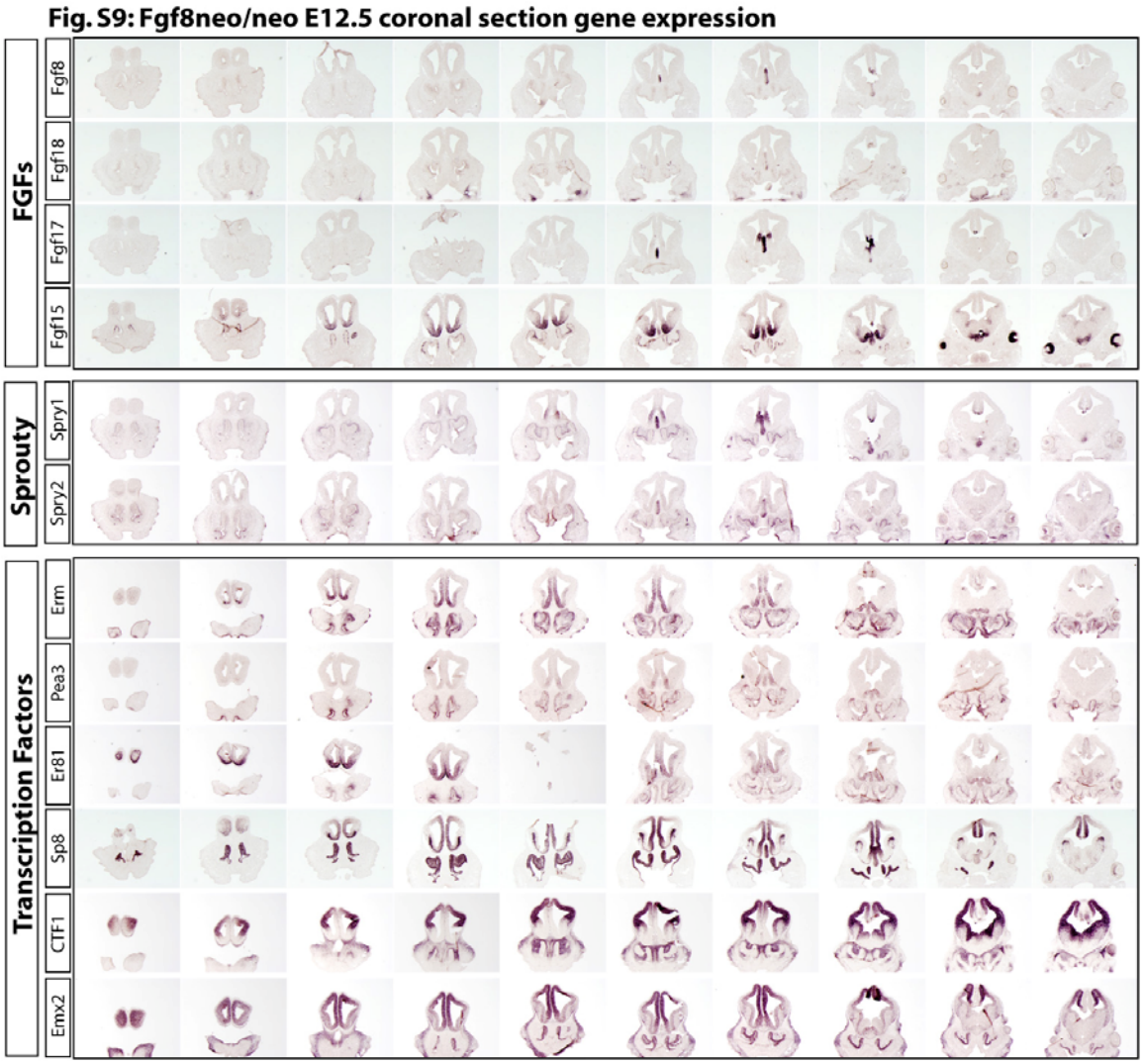

Fig. S9. In situ hybridization on E12.5 rostral to caudal (left to right) *Fgf8*$^{n/n}$ coronal section series for FGF genes (*Fgf8, Fgf18, Fgf17, Fgf15*), Sprouty genes (*Spry1, Spry2*), and transcription factors (*Erm, Pea3, Er81, Sp8, COUP-TF1, Emx2*).

Fig. S10: Emx2-/- E12.5 coronal section gene expression

Fig. S10. In situ hybridization on E12.5 rostral to caudal (left to right) *Emx2*$^{-/-}$ coronal section series for FGF genes (*Fgf8, Fgf17, Fgf15*), *Spry1* and transcription factors (*Erm, Pea3, Er81, Sp8, COUP-TF1*).

Fig. S11: Emx2-/-;Fgf17-/- E12.5 coronal section gene expression

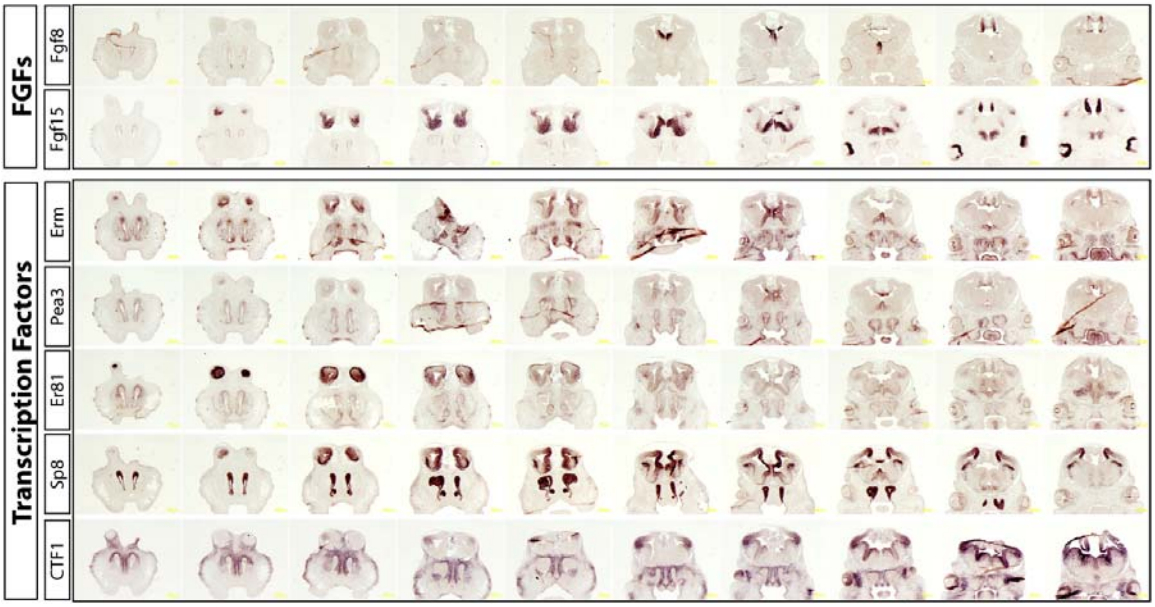

Fig. S11. In situ hybridization on E12.5 rostral to caudal (left to right) *Emx2*$^{-/-}$*;Fgf17*$^{-/-}$ coronal section series for FGF genes (*Fgf8, Fgf15*) and transcription factors (*Erm, Pea3, Er81, Sp8, COUP-TF1*).

Fig. S12 Comparison of FGF signaling in Fgf8n/n mutant

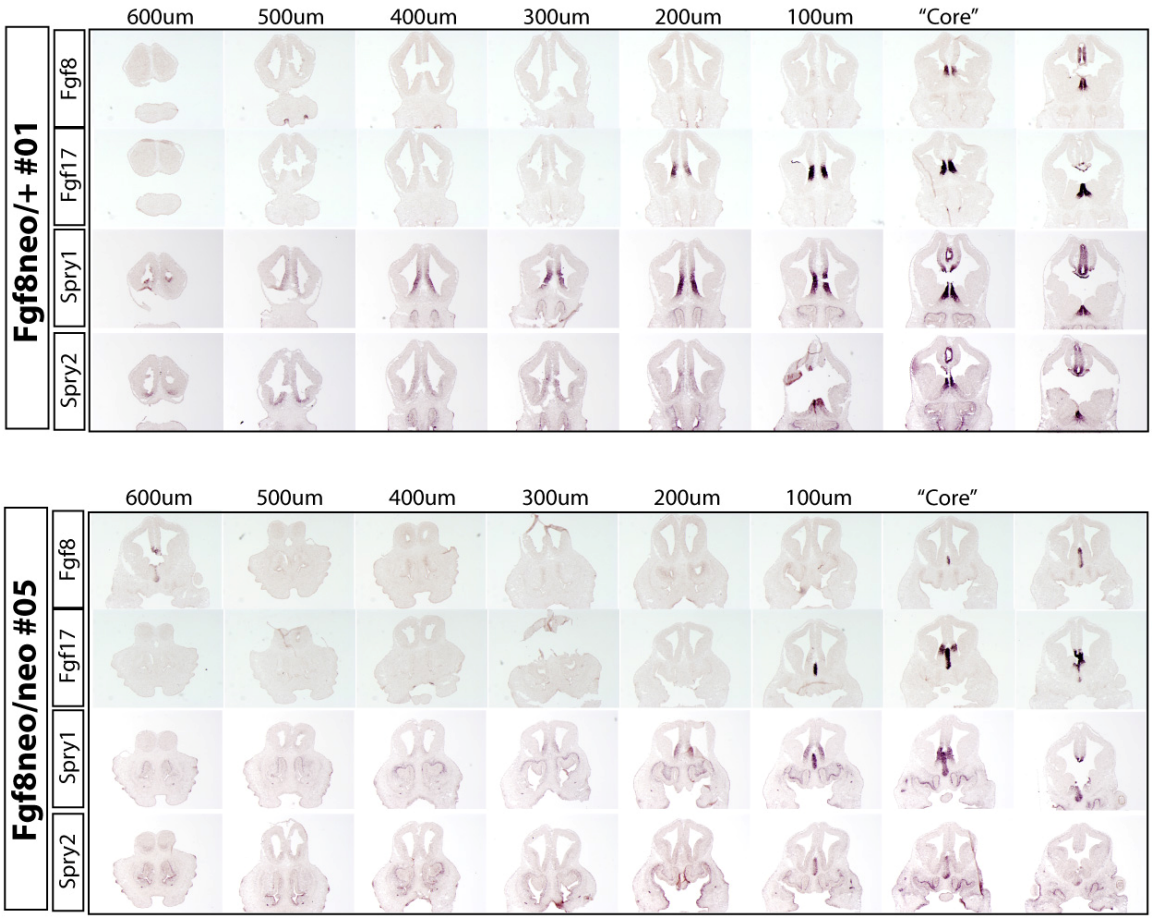

Fig. S12. Comparison of FGF signaling in the E12.5 *Fgf8*$^{n/n}$ mutant. Rostral-to-caudal coronal sections series from *Fgf8*$^{+/n}$ and *Fgf8*$^{n/n}$ brains processed for ISH to *Fgf8*, *Fgf17*, *Spry1* and *Spry2*. Sections were aligned from the right (caudally) starting at the "core" Fgf8 expression domain. Distance from the "core" is labeled above. Sections are 10 microns thick and each is spaced 100 microns from the next in the series.

Table S1: Frontal cortex subdivision definitions

	Anatomical areas	
Gene-defined region	**Zilles & Wree, 1995**	**Krettek & Price, 1977**
dorsolateral (dL)	Fr1, Fr3	PrCl
dorsal (D)	Fr1, Fr2	PrCl, PrCm
dorsomedial (dM)	Cg3	PL
dorsomedial caudal (dMc)	Cg1, Cg2	ACd, ACv
infralimbic (IL)	IL	IL
medial orbital (MO)	MO	MO
ventral orbital (VO)	VO	VO
lateral orbital (LO)	LO	LO
dorsolateral orbital (dlO)	DLO	DLO
agranular insular (AI)	AID/AIV	AId/AIv
parietal (Par)	Par1	S1

Chapter 4

Conclusions

While previous studies have yielded insight into the genetic mechanisms that govern cortical patterning and arealization with respect to large-scale territories (i.e. into frontal, parietal and occipital cortex), there has been relatively little attention paid to the patterning of subdivisions within these more general cortical regions. In comparison with primary cortical areas (i.e. motor, somatosensory, visual cortex), the development of higher-order cortical areas (i.e. PFC) has not been well-studied. The ability to study PFC development is predicated on having a set of markers that delineate regional subdivisions.

My studies of PFC regionalization using a new panel of gene expression markers have provided insight into the genetic mechanisms that govern the early patterning and regionalization of the PFC. In contrast to the more general role of *Fgf8* in patterning the overall neocortex through regulation of caudal transcription factors *Emx2* and *COUP-TF1*, *Fgf17* more selectively affects development of the rostral cortex. The unexpectedly selective role of *Fgf17* in dorsal PFC development may be explained by the maintenance of *Fgf8*, *Fgf18*, *Fgf15* expression in their normal spatial patterns, and the selective downregulation of transcription factors *Erm*, *Pea3* and *Er81* in the rostrodorsal ventricular zone. In addition, genetic interactions between *Emx2* and *Fgf17* appear to be particularly important for regionalization of the PFC, in that they reciprocally control expression of *Erm*, *Pea3* and *Er81* in the rostral cortical primordium.

These results highlight the importance of taking the spatial relationships of regulatory gene expression into account when determining the *in vivo* function of a gene during cortical development. Since *Erm*, *Pea3* and *Er81* are expressed in the medial PFC anlage and are regulated by *Fgf17*, they represent excellent candidates for regulating PFC development. These transcription factors may be involved directly in regional specification or may regulate the development of area-specific properties of the PFC such as its unique connectivity.

The finding of circumscribed social deficits with associated dorsal PFC hypoactivity (see Appendix) provides evidence that *Fgf17* mutant mice exhibit behavioral deficits related to PFC dysfunction. Although previous work has identified an important role for the PFC in regulating rodent social behavior, there is a relative paucity of data on distinct roles for dorsal and ventral PFC subdivisions. Therefore, I hypothesize that *Fgf17* mice will be useful in distinguishing functions of the dorsal and ventral PFC.

The human *FGF17* gene is located on chromosome 8p21, a region that is linked to schizophrenia, a disorder that involves profound social abnormalities and decreased PFC function. While a direct link between *FGF17* and neuropsychiatric disease remains to be tested, *Fgf17* mutant mice may nonetheless provide a valuable animal model for aspects of human disorders that involve both hypofrontality and altered social interactions.

Appendix: Behavioral and neural activation studies in *Fgf17*$^{-/-}$ mutants

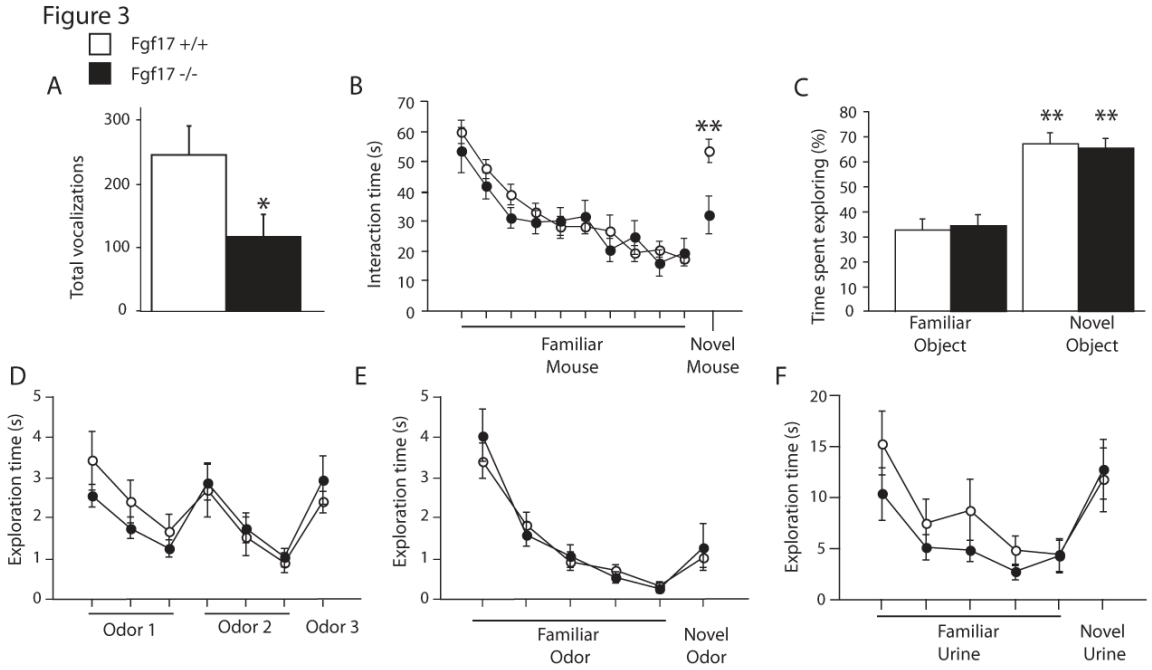

Fig. A1. Abnormal social behavior in *Fgf17*$^{-/-}$ mice (black bars and symbols).

(A) Total number of ultrasonic vocalizations elicited by isolation, brief maternal interaction, and isolation after maternal interaction is lower in *Fgf17*$^{-/-}$ mice than *Fgf17*$^{+/+}$ mice. [Student's t-test: significant genotype difference, t = 2.57, df = 19, * P < 0.05, n = 14 -/- and 7 +/+].

(B) Time spent interacting with a mouse decreases with repeated exposure to the same mouse in both *Fgf17*$^{+/+}$ and *Fgf17*$^{-/-}$ mice, but *Fgf17*$^{-/-}$ show a reduced response to a novel mouse. [Student's t-test: significant genotype difference on time spent interacting with novel mouse, t = 3.23, df = 27, ** P < 0.005, n = 13 -/- males and 16 +/+ males].

(C) *Fgf17*$^{-/-}$ mice show normal response to unscented novel objects. [Paired t-test: significantly more exploration of novel object vs. familiar object for both *Fgf17*$^{-/-}$ mice (t=-3.618, df = 20, ** P < 0.005, n = 21) and *Fgf17*$^{+/+}$ controls (t = -3.837, df = 17, ** P < 0.005, n = 18)].

(D, E) *Fgf17*$^{-/-}$ mice and wild-type littermates show similar habituation to a familiar odor followed by dishabituation to novel odors. D: 3-minute odor exposure, no intertrial interval, n = 7 +/+ and 14 -/-. E: 3-minute odor exposure, 3-minute intertrial interval, n = 19 +/+ and 23 -/-.

(F) *Fgf17*$^{-/-}$ mice and wild-type littermates show similar habituation and dishabituation to pheromone cues (urine samples from opposite-sex FVB/N mice). n = 14 +/+ and 21 -/-.

Figure 4

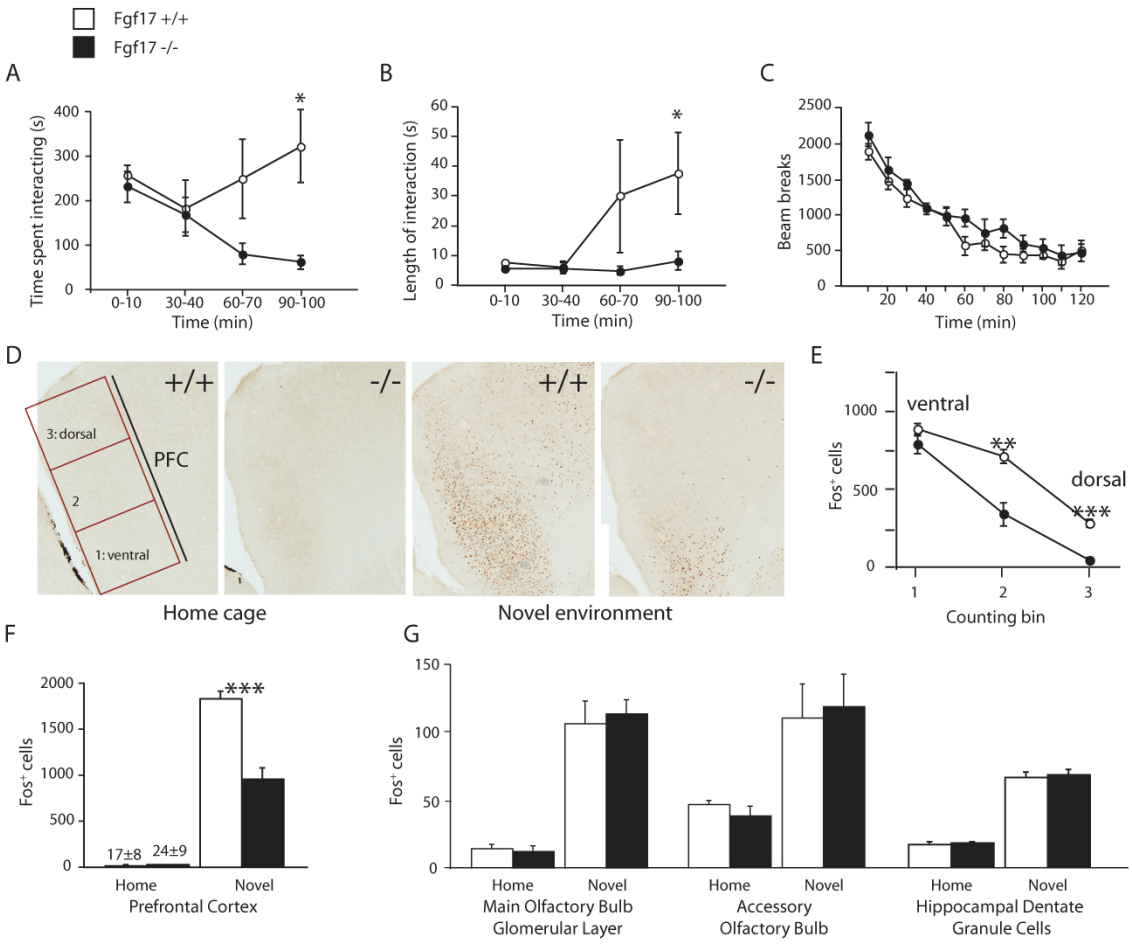

Fig. A2. Reduced social interaction and decreased dorsal frontal cortex activation during exploration of novel environment with new same-genotype cagemate.

(A) Decreased time interacting with same-genotype cagemates after spending 1 hour in a novel environment. [Repeated measures ANOVA: significant genotype x time interaction, $F_{(3.24)} = 3.61$, $P < 0.05$, significant genotype difference at 90-100 minute time point by post-hoc Scheffé, *$P < 0.05$, n = 5 -/- pairs and 5 +/+ pairs.]

(B) Average length of social interactions in novel environment. [Post-hoc Scheffé, *$P = 0.05$, n = 5 -/- pairs and 5 +/+ pairs.]

(C) No difference in activity in pairs of same-genotype mice exploring an open field.

(D) Photomicrographs showing sagittal sections of medial prefrontal cortex stained for Fos. Overlay shown on +/+ home cage section illustrates placement of bins used to count Fos^+ cells.

(E) Quantification of Fos^+ cells in most medial sagittal brain section. [Repeated measures ANOVA: significant effects of genotype, $F_{(1.8)} = 21.5$, $P < 0.005$; counting bin, $F_{(2.16)} = 182.3$, $P < 0.001$; and genotype x bin interaction, $F_{(2.16)} = 7.6$, $P < 0.005$. Significant genotype differences in bins 2 **$P<0.005$ and 3 *** $P < 0.0001$ by post-hoc Scheffé, n = 5 +/+ and 5 -/- brains].

(F) Total number of Fos^+ cells averaged across the two most medial sagittal brain sections. [ANOVA: significant genotype effect for novel environment only, $F_{(1.8)} = 37.0$, ***$P < 0.0005$, n = 5 +/+ and 5 -/- brains].

(G) Total number of Fos^+ cells counted in sagittal sections of olfactory bulb, accessory olfactory bulb and hippocampal dentate gyrus granule cells.

Figure S11

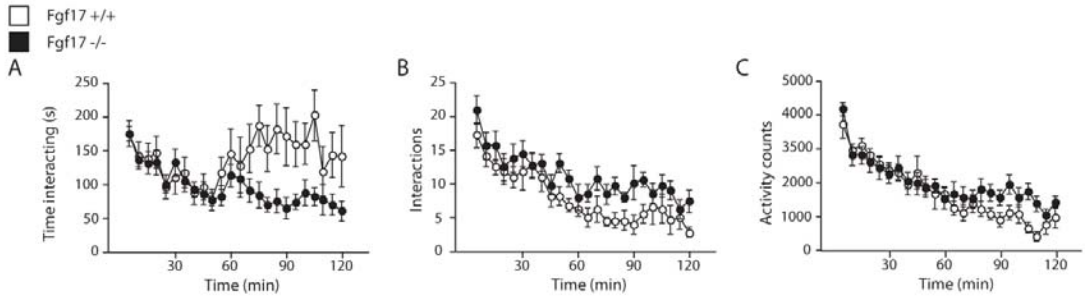

Fig. A3. Automated detection of reduced social interaction during exploration of home cage with new same-genotype female.

(A) Decreased time interacting with same-genotype partners after spending 1 hour together. [Repeated measures ANOVA: significant genotype difference, $F_{(1.14)} = 5.0$, $P < 0.05$, and a significant genotype by time interaction, $F_{(1.23)} = 2.6$, $P < 0.0001$, n = 7 +/+ and 8 -/- pairs]

(B) Total number of discrete social interactions is increased between *Fgf17*$^{-/-}$ mice. [Repeated measures ANOVA: significant genotype difference, $F_{(1.14)} = 9.3$, $P < 0.01$, n = 7 +/+ and 8 -/- pairs]

(C) No significant genotype difference in activity in pairs of same-genotype mice. [Repeated measures ANOVA, $P > 0.15$, n = 7 +/+ and 8 -/- pairs]

Fig. S13

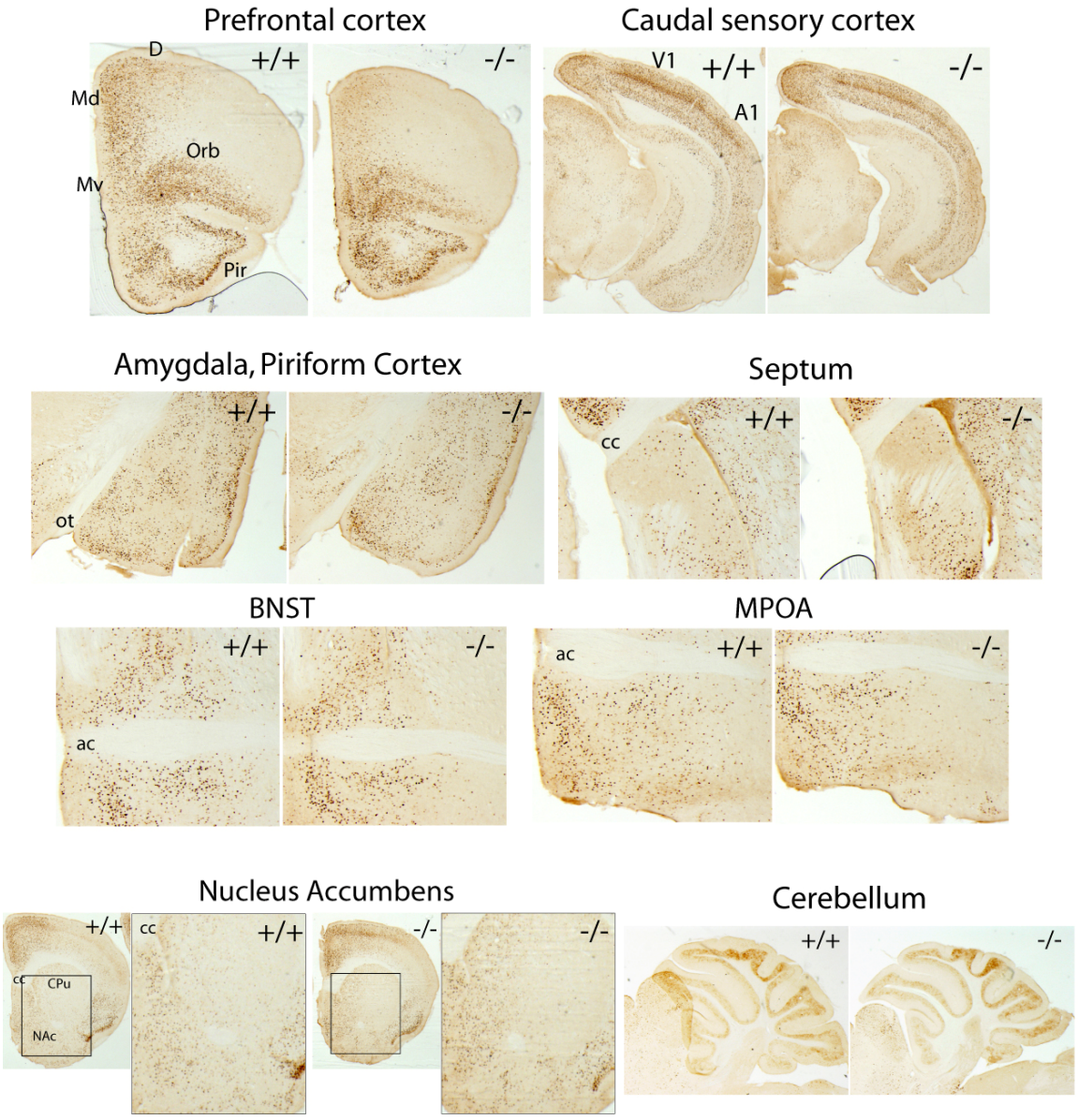

Fig. A4. Fos induction in the forebrain and cerebellum of *Fgf17*$^{+/+}$ and *Fgf17*$^{-/-}$ mice by social exploration of a novel environment. We observed a large and specific reduction of Fos protein induction in the dorsal/dorsomedial prefrontal cortex (regions D and Md) of *Fgf17*$^{-/-}$ mutants. In contrast, Fos induction was not obviously altered in the orbital FC or olfactory structures such as olfactory bulb, accessory olfactory bulb, anterior olfactory nuclei and piriform cortex. Additionally, we did not observe obvious genotype differences in Fos expression in any of the following brain structures: caudal sensory cortex, amygdala, septum, bed nucleus of the stria terminalis (BNST), medial preoptic area (MPOA), nucleus accumbens, and cerebellum. Wildtype sections (+/+) are on the left, while mutant (-/-) are on the right. For the nucleus accumbens, higher magnification images of the boxed areas are shown. Abbreviations: A1, primary auditory cortex; ac, anterior commisure; amgydala; cc, corpus callosum; CPu, caudate putamen; D, dorsal frontal cortex; Md, dorsomedial prefrontal cortex; Mv, ventromedial prefrontal

cortex; NAc, nucleus accumbens; Orb, orbital cortex; ot, optic tract; Pir, piriform cortex; V1, primary visual cortex.

Fig. S10

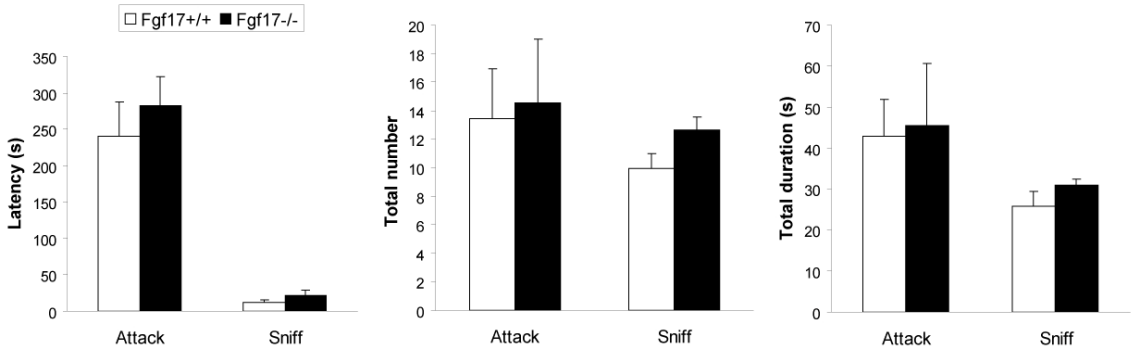

Fig. A5. No differences between *Fgf17*$^{+/+}$ and *Fgf17*$^{-/-}$ mice in aggressive behavior on the resident-intruder test, including latency, total number, and total duration of attacks. No genotype differences were observed in sniffing, tail rattles, grooming, mounting or chasing.

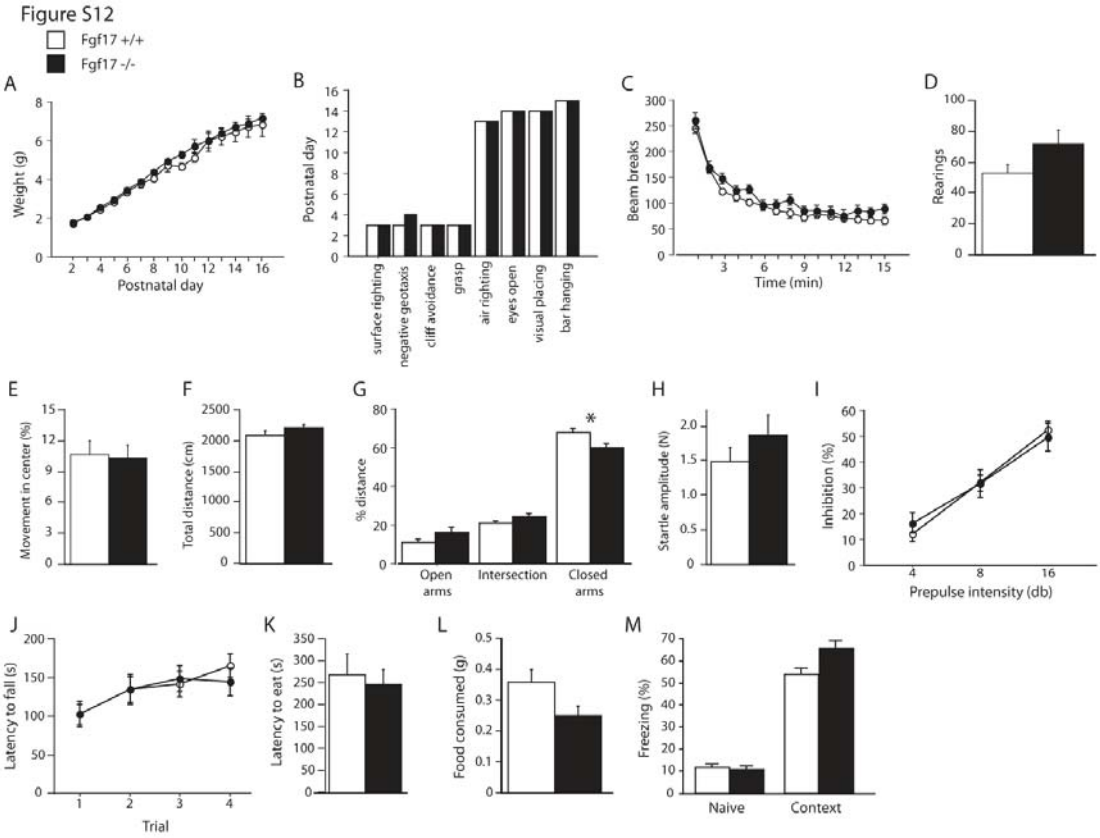

Fig. A6. Normal motor and sensory functions, anxiety and contextual fear learning in *Fgf17*$^{-/-}$ mice (black bars and symbols) relative to *Fgf17*$^{+/+}$ littermates (white bars and symbols).

(A) *Fgf17*$^{-/-}$ mice grow at the same rate as *Fgf17*$^{+/+}$ mice postnatally (n = 7 +/+ and 14 -/-pups).

(B) No significant differences were observed in the attainment of developmental milestones. Bars represent median day after birth for achievement of each behavior for 7 +/+ or 14 -/- pups.

(C-E) Open field behavior for 25 +/+ and 17 -/- mice. During 15 min in an open field, no genotype differences were detected in either (C) horizontal locomotor activity, (D) vertical rearings, or (E) percentage of movement occurring in the center portion of the field.

(F-G) Elevated plus maze behavior for 25 +/+ mice and 17 -/- mice. (F) No genotype difference in total distance moved on the maze. (G) A small but significant reduction in percentage of distance moved in the closed arms was detected for *Fgf17*$^{-/-}$ mice [ANOVA: genotype effect $F(1, 40) = 6.01$, * $P < 0.05$], but *Fgf17*$^{-/-}$ mice did not move significantly more distance in either the open arms or intersection area.

(H-I) No genotype differences in amplitude in whole body startle in response to 120 db stimulus (H) or in prepulse inhibition of startle when 120 db startle stimulus is preceded by prepulses of 4-16 db (I). n = 25 +/+ and 17 -/- mice.

(J) Normal motor behavior as shown by latency to fall off an accelerating rotorod over 4 trials, n = 25 +/+ and 17 -/- mice.

(K-L) Novelty-suppressed feeding test (n = 11 +/+ and 7 -/- mice) reveals no genotype effects on either latency to begin eating (K) or amount of food consumed immediately after test (L).

(M) No genotype differences in basal freezing or in freezing after contextual fear conditioning. n = 12 -/- males and 14 +/+ males.

MATERIALS AND METHODS

Subjects

All mice (*1*) were housed and handled in accordance with the National Institutes of Health's *Guide for the Care and Use of Laboratory Mice* and the Institutional Animal Care and Use Committee of the University of California, San Francisco. The first 24 hours after birth is considered P0. The *Fgf17* line was maintained on a mixed 129Sv/C57BL/6 background.

For behavioral analysis, $Fgf17^{+/-}$ males and females that had been backcrossed 1 generation to C57BL/6 were mated to generate $Fgf17^{+/+}$, $Fgf17^{+/-}$ and $Fgf17^{-/-}$ progeny. Pups were weaned at 21 days and group housed, with males and females separated. Ear hole punches were taken to mark individuals and 0.5 cm of tail clipped for genotyping.

Genotyping

Genotyping was performed on genomic DNA obtained from tail clippings using polymerase chain reaction (PCR). Standard reagents were used for all PCR reactions. *Fgf17* primers: (WT allele) 5'-GAAGTTTCTCCAGCGATGGG-3' and 5'-GACAGCAGAGAATCAATAGCTGC-3'; (Mutant allele- Cre) 5'-CCATGAGTGAACGAACCTGG-3' and 5'-TTGGCTTCTCTGGGACTCTAC-3'. Cycle program: 95°C for 10', followed by 35 cycles of 94°C for 45", 58°C for 45", 72°C for 1', then 72°C for 10'. GFP primers: 5'-CCTACGGCGTGCAGTGCTTCAGC-3' and 5'-CGGCGAGCTGCACGCTGCGTCCTC-3'. Cycle program: 95°C for 5', followed by

35 cycles of 95°C for 1', 60°C for 1', 72°C for 1', then 72°C for 10'. Amplified PCR products were electrophoresed on 1% agarose gels and visualized using UV fluorescence.

Tissue Preparation

Animals were deeply anesthetized with chlorohydrate and perfused with cold 1X PBS. Brains were removed, fixed in 4% PFA overnight, and stored in fresh PBS at 4 degrees. Tissue was cryoprotected before sectioning by transferring to 30% sucrose in PBS overnight. Section were cut on a freezing microtome at 30 microns.

Immunohistochemistry

Immunohistochemistry was performed using standard protocols with a rabbit anti-Fos, Ab-5 antibody (1:10,000, Calbiochem), and detected with goat anti-rabbit biotinylated secondary antibody (1:200-1:400; Vector Laboratories, Burlingame, CA) and ABC kit (Vector).

Fos analysis

Analysis was performed blind to genotype and experimental condition. The 2 most medial sagittal sections from each brain were photographed at high resolution using a microscope-mounted camera. Cell counting was performed using Photoshop (Adobe). For frontal cortex analysis, each image was overlaid with a standard 3-box grid using the rhinal sulcus and corpus callosum/striatum as landmarks. Number of Fos^+ cells in each bin was recorded. For main olfactory bulb, sagittal sections were photographed and aligned and Fos+ cells in the ventral side of the glomerular layer were counted and

averaged for 2 medial sections. For accessory olfactory bulb, all Fos^{+} cells in 2 sagittal sections in which the AOB was clearly defined were counted and averaged. For hippocampus, Fos^{+} cells in the granule cell layer of the dentate gyrus were counted and averaged for 5 sections. A separate series of coronal sections was also analyzed to confirm the sagittal section results.

Behavior

Mice were housed in a pathogen-free barrier facility on a 12-hour light-dark cycle. Food and water were freely available. All behavioral testing occurred between 8 AM and 5 PM, during the light cycle. Experimenter was always blind to mouse genotype during testing. Data is presented from several different adult cohorts. The first two cohorts went through the same tests in the same order: elevated plus maze, open field, social recognition, passive avoidance, prepulse inhibition of startle, olfactory recognition, Y maze, rotorod, novel object recognition, novelty suppressed feeding, fear conditioning, and social exploration of novel environment. The third cohort was used for more limited tests: novel object recognition, olfactory recognition, fear conditioning, urine habituation/dishabituation and videoanalysis of social interaction. A fourth independent cohort was used for the resident-intruder test.

Developmental assessment

Fgf17$^{+/-}$ males and females were mated, and plugged females were separated until the litters were weaned. Beginning on P2, pups were individually numbered (using non-toxic ink on their stomachs) and monitored daily. On days P2-P6, early milestones were

assessed. During testing, all pups were transferred to a cage filled with clean bedding placed over a heating pad to maintain the temperature at the surface of the bedding at 22-24°C. Individual pups were removed, checked for physical abnormalities and weighed. To assess surface righting, the pup was gently placed on its back and monitored for 60 s or until it successfully righted itself. To assess negative geotaxis, a sheet of textured plastic was placed at a 30° angle with the lower edge resting in soft bedding. The pup was placed on the inclined plane with head facing downward. Negative geotaxis was present if the mouse reoriented itself so its head and forelimbs were higher up the plane than its hindlimbs within 60 s. To assess cliff avoidance, the mouse was placed with its hindlimbs resting on a circular Styrofoam platform mounted on a 30-cm high stand. The pup was positioned so its forepaws and nose were suspended over the edge of the platform, but its weight rested fully on the platform. Successful cliff avoidance was scored if the pup moved away from the edge by backing up or turning sideways within 60 s. To assess grasp reflex, each forepaw was gently stroked with the wooden end of a swab. If the pup immediately curved its paw to grasp the swab, the grasp reflex was considered present. Late milestones were assessed on days P10-P18. Mice were physically inspected and the date when both eyes were open was recorded. Once eyes were open, visual placing was assessed by suspending the pup by its tail and gently lowering it toward the table top. If the pup raised its head and extended forelimbs toward the surface, visual placing was scored. To assess air righting reflex, the pup was held with its ventral side facing upward about 60 cm above a chamber filled with soft bedding. The pup was released, and air righting was considered present if the pup turned while falling so that it landed on its feet with its ventral side down. To assess bar hanging, the pup was

moved close to a small wire bar and allowed to grasp it. Then the pup was released so that it was hanging by its forelimbs above a bedding-filled chamber. Once the pup was able to hang suspended for 10 s, bar holding was scored as present. On day P21, mice were weaned, and tails were clipped for PCR genotyping.

Isolation-induced ultrasonic vocalization

On day P8, ultrasonic vocalizations (USV) were assessed in pups of *Fgf17*$^{+/-}$ mothers. The pups were removed from their home cage and placed in a cage filled with clean bedding on top of a heating pad. The mother was returned to the housing room. If the litter contained 6 or more pups, the pups were randomly divided into 2 groups that were assessed separately to minimize length of time away from mother. Pups were given 10 min to adjust to maternal separation. Then, a pup was removed from the litter, taken to a different room, and placed in a clean cage with no bedding. Its ultrasonic vocalizations were counted for 3 min using the UltraVox detector (Noldus Information Technology, The Netherlands). The detector was tuned to 65kHz. Before each testing session, a 3-min background reading was taken and the gain on the detector was adjusted to minimize false positive USV detections. After the 3-min isolation task, the mother was placed in the test chamber for 3 min and vocalizations from both mother and pup were recorded to assess contact quieting. Then, the mother was removed again and pup vocalizations were recorded for 3 min. The test chamber was cleaned with lukewarm water before testing the next pup. Genotype-dependent differences were apparent and similar in magnitude throughout all phases of testing. Therefore, the number of vocalizations during the two isolation periods were added together for analysis.

Social recognition

Male mice were singly housed at least 5 days prior to testing. The home cage was moved to the testing area and the lid and food hopper were removed and the mouse was allowed to habituate for 3 min. A novel ovariectomized C57BL/6 female (Jackson Labs, Bar Harbor, ME) was introduced into the cage and the two mice were allowed to interact freely. The use of an ovariectomized female allows social interaction with minimal aggression (expected against unfamiliar males) or mating behavior (expected toward intact females). The amount of time spent interacting was recorded. After 90 seconds, the female was returned to her home cage while the male mouse rested in his home cage for 3 min. Then the same female was reintroduced for another 90 s interaction interval. A series of 90 s interaction periods with 3-min intertrial intervals was repeated 10 times. On the 11^{th} and final trial, a different ovariectomized C57BL/6 female was introduced and the time spent interacting was recorded. We used 5 different females and rotated them among males, counterbalanced according to genotype.

Novel object recognition

Mice were habituated to the testing chamber during 3 different 15-min exposures to the chamber across 3 days. For training, mice were placed in the chamber with a single object (either a die or marble) for 10 min. The amount of time spent interacting with the object was recorded. Four hours later, the mouse was returned to the chamber and exposed to an exact duplicate of the first object and a novel object. The time spent exploring each object was recorded during the 10-min test. The choice of novel object

and the location of the novel object was varied for each trial and counterbalanced for each genotype. After testing each mouse, the chamber and objects were thoroughly cleaned with 70% EtOH to remove odors.

Olfactory habituation and dishabituation

Two different protocols were used to assess olfactory habituation and dishabituation. Protocol 1 was designed to mimic the time course and procedure of social recognition testing as closely as possible. Singly housed male mice were used for this protocol. The home cage was moved to the testing area and the lid and food hopper were removed and the mouse was allowed to habituate for 3 min. A cotton ball was soaked in a novel odorant and placed inside a perforated plastic tube. This tube was introduced to the animal's home cage and the time the mouse spent actively exploring the tube (touching, licking or sniffing from a distance of <1 cm) was recorded for 3 min. After 3 min, the tube was removed and the mouse rested for 3 min. Then, the odorant tube was reintroduced to the cage for another 3-min trial. This procedure was repeated for a total of 5 trials with 3-min intertrial intervals. On the 6^{th} and final trial, a new tube with a new smell was introduced. Cineole and limonene (Sigma Chemicals, St. Louis, MO) were used as odors. The novel odor was varied for each mouse and counterbalanced for each experimental group.

Protocol 2 was designed to increase dishabituation to novel odors. Pair-housed male mice were tested in their home cages. The cagemate was moved to a clean holding cage while each mouse underwent testing in his home cage. A cotton swab soaked in vehicle (mineral oil) was suspended from a wire top over the cage and the mouse was

allowed to habituate to this for 10 minutes. Then, the swab was replaced by a swab soaked in a novel odorant (cineole, limonene or isoamyl acetate) and the mouse was allowed to explore for 3 minutes while an observer scored the number and length of explorations (mouse bringing his nose within 1 cm of swab and sniffing). After 3 minutes, the swab was removed and immediately replaced by a swab soaked in the same odorant. This was repeated for a total of 3 presentations of the odor with no intertrial intervals. On the 4th trial, a new odor was introduced, and the sequence of 3 presentations was repeated. A third odor was introduced on the final trial. The order of odor presentations was counterbalanced across genotype.

Pheromone recognition

Urine from FVB/N mice was collected by allowing the mice to urinate on filter paper. The moist filter paper was then cut into 1 cm squares that were used as the stimuli for this test. Squares from each mouse were stored separately and discarded after 48 hours. Each mouse was tested in its home cage. The lid and food hopper were replaced by a wire mesh lid. A square of clean filter paper was suspended from the wire lid and the mouse was allowed to habituate for 3 min. Then, the clean paper was replaced by a urine-soaked square taken from an opposite-sex mouse. The time the mouse spent actively exploring the square (touching, licking or sniffing from a distance of <1 cm) was recorded for 3 min. After 3 min, the square was removed and the mouse rested for 3 min. Then, a new square soaked in urine from the same mouse was reintroduced to the cage for another 3-min trial. This procedure was repeated for a total of 5 trials with 3-min intertrial intervals.

On the 6th and final trial, a new square soaked in urine from a different opposite-sex mouse was introduced and exploration time was recorded.

Social exploration of a novel environment

We adapted the novel environment task previously described (*9*). Mice were assigned to same-genotype opposite-sex pairs and allowed to explore a novel environment for 2 hours prior to sacrifice. The environment was a standard housing cage containing a new bedding type, and novel olfactory, pheromone, tactile and visual stimuli. The mice were videotaped and subsequently scored by a genotype-blind observer for social interactions. Four discrete time intervals were scored: 0-10 min, 30-40 min, 60-70 min and 90-100 min after introduction to the environment. Social interactions included sniffing, grooming, chasing, mounting, aggression, and direct physical contact. The total time spent interacting was recorded, the number of interactions was counted. After novel environment exposure, mice were immediately sacrificed and their brains processed for Fos staining. Control mice remained singly housed and undisturbed in their home cages for 3 days prior to sacrifice.

Social interaction – videoanalysis

Male mice were tested in their home cages. The lids were removed and a novel, same-genotype female was introduced into the cage. A videoanalysis program (Social Scan, Clever Sys Inc., Reston VA) recorded digital video of the mice for 2 hours and determined the number and length of social interactions between the 2 mice. It also recorded activity counts over the 2 hours. For 2 of the pairs, manual scoring of social

interaction was also conducted to verify the fidelity and accuracy of the automated analysis.

Open field

Mice were placed in a novel open chamber (16" x 16") and allowed to explore it freely for 15 minutes. Activity was recorded by an array of infrared photocells interfaced with a computer (Photobeam Activity System, San Diego Instruments, San Diego, CA) that could detect and distinguish horizontal ambulatory movements, fine movements, and vertical movements (rearing). For analysis, the center of the field was defined as the central 4" x 4" square. After testing of each mouse, the open field was thoroughly cleaned to remove odors. In a separate experiment to control for novel environment exploration, pairs of mice were allowed to explore the field freely for 2 hours. The total activity for the pair of mice was monitored for the full 2 hours.

Elevated plus maze

Emotional and exploratory behaviors were assessed with an elevated, plus-shaped maze consisting of two open arms and two closed arms equipped with rows of infrared photocells interfaced with a computer (Hamilton-Kinder, Poway, CA). Mice were placed individually in the center of the maze and allowed free access for 10 min. The time spent and distance moved in each of the arms and the number of times the mice extended over the edges of the open arms were calculated from recorded beam breaks. After testing of each mouse, the equipment was thoroughly cleaned to remove odors.

Rotarod

Motor coordination and balance were assessed by placing mice on a rotating drum (Rota-Rod 5-station mouse treadmill, MED Associates, St. Albans, VT) 3.2 cm in diameter suspended 16.5 cm above a surface. We then measured the time each mouse was able to maintain its balance on the rod as it accelerated (fall latency). The speed of the rod was accelerated from 4–40 rpm over 5 min. Each mouse received 4 trials, with an intertrial interval of at least 1 h. The surface of the rod and the lanes beneath the rod were cleaned with 70% EtOH between each trial.

Startle reactivity and prepulse inhibition.

Acoustic startle reactivity was measured with two identical startle chambers (Hamilton-Kinder) containing a transparent nonrestrictive plastic box resting on a platform inside a sound-proof, ventilated box. A high-frequency speaker mounted 15 cm above the box produced all of the acoustic stimuli. Mouse movements were detected and transduced by a piezoelectric accelerometer mounted under each cylinder. Movements were digitized and stored by a computer and interface assembly. Movements were monitored for 100 ms after the onset of each stimulus, and the maximum amplitude response (Newton) was used to determine the startle response.

For testing, mice were placed inside the chamber and exposed to a background noise of 65 decibel (db). After a 5-min acclimation period, each session consisted of 80 trials of five types: 24 trials of a 40-ms 120-db startle stimulus alone (to measure maximum acoustic startle amplitude), 14 trials without startle stimulus (to measure baseline movements in the chamber), and 14 trials each of a 40-ms stimulus at 4-, 8-, or

16-db above background (prepulse), followed by a 100-ms interval, and then a 40-ms 120-db startle stimulus. In the first 5 and the last 5 trials of each session, the startle stimulus alone was presented to determine the degree of habituation to the startle stimulus. The other trials of startle stimulus alone and of prepulse plus startle stimulus were presented in pseudorandom order with an average intertrial interval of 15 s (range 7–23 s).

Percent prepulse inhibition of the startle response was calculated: 100 – [(average response to prepulse plus startle stimulus/average response to startle stimulus alone) x 100].

Novelty suppressed feeding

Mice were singly housed at least 5 days prior to testing. 18 hours before testing, food was removed from the cage. The next day, the mouse was placed in a brightly lit novel arena (16" x 16") that contained a small dish of food pellets at the center of the field. The mouse was allowed to explore the field freely for 10 min or until it began to eat the food. At the end of the test, the dish of food was placed with the mouse in its home cage and the mouse was allowed to eat for 5 min. To evaluate the amount of food consumed by each mouse the dish was weighed before beginning the test and again after the 5-min feeding period.

Fear conditioning

Mice were testing using a conventional fear conditioning protocol in the Freeze Monitor (San Diego Instruments, San Diego, CA).

Resident-intruder aggression test

Adult animals were housed under a reversed 12:12 hour light-dark cycle, with the lights switched on at 1 AM. Food and water were provided *ad libitum*. The wildtype (*Fgf17*$^{+/+}$) and mutant (*Fgf17*$^{-/-}$) males were group-housed by sex upon weaning, and then moved to individual housing at 7-9 weeks after birth. All mice were sexually naïve. Behavioral testing commenced 7-10 days after the animals had been singly housed. The intruder was an 8-12 week old gonadally intact 129SvEv wildtype male, group-housed since weaning. The intruder was placed in the home cage of the resident, and the interactions were recorded for 15 minutes in the dark, using a Sony camcorder capable of recording under low infrared illumination. Each of the 7 mutant and 11 wildtype males used as residents were tested 3 times in this assay. No animal was tested on consecutive days, nor were individuals tested more than twice a week. Each resident was tested with a different intruder for each assay. The assays were scored for ano-genital chemoinvestigation (sniffing), grooming, attacking, chasing, mounting, and tail rattles displayed by either the resident or the intruder. An episode of attack includes one or more instances of biting, tumbling, or wrestling. The experimenter was blind to the genotypes while setting up and scoring the assay. The behaviors were scored using customizable settings in Observer, a behavioral analysis software suite (Noldus).

Publishing Agreement

It is the policy of the University to encourage the distribution of all theses and dissertations. Copies of all UCSF theses and dissertations will be routed to the library via the Graduate Division. The library will make all theses and dissertations accessible to the public and will preserve these to the best of their abilities, in perpetuity.

Please sign the following statement:

I hereby grant permission to the Graduate Division of the University of California, San Francisco to release copies of my thesis or dissertation to the Campus Library to provide access and preservation, in whole or in part, in perpetuity.

Author Signature Date